

Copyright
by
Claudine D'Annunzio
2009

The Dissertation Committee for Claudine D'Annunzio
certifies that this is the approved version of the following dissertation:

**Generation Adequacy Assessment of Power Systems
with Significant Wind Generation:
A System Planning and Operations Perspective**

Committee:

Surya Santoso, Supervisor

Ross Baldick

Mircea D. Driga

W. Mack Grady

Gary C. Vliet

**Generation Adequacy Assessment of Power Systems
with Significant Wind Generation:
A System Planning and Operations Perspective**

by

Claudine D'Annunzio, B.S., M.S.E.

DISSERTATION

Presented to the Faculty of the Graduate School of
The University of Texas at Austin
in Partial Fulfillment
of the Requirements
for the Degree of

DOCTOR OF PHILOSOPHY

THE UNIVERSITY OF TEXAS AT AUSTIN

May 2009

To my family and friends

Acknowledgments

Foremost, I would like to thank my dissertation supervisor, Dr. Surya Santoso. Each time I met with Dr. Santoso to discuss about my research, I *always* felt better coming out of the meeting. I don't know many graduate students who can say the same! He would always give me useful and constructive feedback, and he always had a positive attitude. I am very grateful for his guidance. I thank the National Science Foundation for supporting me as a research assistant. I would also like to thank the members of my dissertation committee for their valuable feedback on this work and also my editor, Roger Gathman, for all his hard work.

Having been a student at UT since undergraduate school, I got to know many people working in the Department. Thank you all for your smiling faces and encouragements: Tony Ambler, Carole Bearden, Melanie Gulick, Kathleen Rice, Trudie Redding, Michelle Belisle, Melody Singleton, Mona Venegas, Perry Durkee, Daryl Goodnight and Merydith Turner.

Without the support of my mom during the last stages of this dissertation, I doubt I would have been able to complete the work. “Mom, tu ne peux pas savoir comment j'apprecie que tu sois venue m'aider”. I can't forget my dad, who was always there to listen and give me reassuring words. I would also like to thank Patrick, Oksana, Marc and Julie for encouraging me in difficult

times. Thank you to my dear friends for being so wonderful: Janine Mauze-
roll et Steen Schougaard, Virat Kapur, Zezette Ouimet, Lisa Accurso, Sanem
Kabadayi, Sabine and Joe Bowen, Deidre Kateri Aragon and Marshall Ryan
Maresca, Rachel Swieczkowski, Emmanouil Kalaitzakis, Miltis Papamiltiades,
Kashia Thuerwachter, Fred and Fanny Huang.

I would also like to thank the operations planning people at ERCOT,
for making it such a wonderful working environment. And, I can't forget to
mention the supplier of my favorite fuel: "Thank you Banzai Restaurant for
my Green Tea Bubble Teas with Extra Bubbles!".

Belle, bonne et capable!

CLAUDINE D'ANNUNZIO

May 2009

The University of Texas at Austin

P.S. And of course: Thank you Miss Mousse Mousse for being the loveliest
kitty in the world!

Statement of Originality and Academic Integrity

Finally, I certify that I have completed the online ethics training modules, particularly the Academic Integrity Module [1-2], of the University of Texas at Austin - Graduate School. I fully understand, and I am familiar with the University policies and regulations relating to Academic Integrity, and the Academic Policies and Procedures [3]. I also attest that this dissertation is the result of my own original work and efforts. Any ideas of other authors, whether or not they have been published or otherwise disclosed, are fully acknowledged and properly referenced. I also acknowledge the thoughts, direction, and supervision of my research advisor, Prof. S. Santoso.

[1] The University of Texas at Austin - Graduate Schools online ethics training modules, <http://www.utexas.edu/ogs/ethics/>

[2] The University of Texas at Austin - Graduate Schools online ethics training on academic integrity, <http://www.utexas.edu/ogs/ethics/transcripts/academic.html>

[3] The University of Texas at Austin, General Information, 2006-2007, Chapter 11, Sec. 11 101, <http://www.utexas.edu/student/registrar/catalogs/gi06-07/app/appc11.html>

**Generation Adequacy Assessment of Power Systems
with Significant Wind Generation:
A System Planning and Operations Perspective**

Publication No. _____

Claudine D'Annunzio, Ph.D.
The University of Texas at Austin, 2009

Supervisor: Surya Santoso

One of the great challenges to increasing the use of wind generation is the need to ensure generation adequacy. In this dissertation, we address that need by investigating and assessing the planning and operational generation adequacy of power systems with significant wind generation.

At the onset of this dissertation, key metrics are presented for determining a power system's generation adequacy assessment based on loss-of-load analytical methods. With these key metrics understood, a detailed methodology is put forward on how to integrate wind plants in the assessment's framework. Then, through the examination of a case study, we demonstrate that wind generation does contribute capacity to the system generation adequacy. Indeed, results indicates that at wind penetration levels of less than 5%, a wind plant's reliability impact is comparable to an energy equivalent conventional unit. We

then show how to quantify a wind plant's capacity contribution by using the effective load carrying capability metric (ELCC), providing a detailed description of how to implement this metric in the context of wind generation. However, as certain computational setbacks are inherent to the metric, a novel non-iterative approximation is proposed and applied to various case studies. The accuracy of the proposed approximation is evaluated in a comparative study by contrasting the resulting estimates to conventionally-computed ELCC values and the wind plant's capacity factor. The non-iterative method is shown to yield accurate ELCC estimates with relative errors averaging around 2%. Case study findings also suggest the importance of period-specific ELCC calculations to better evaluate the variable capacity contribution of wind plants.

Even when considering a well-planned system in which wind generation has been appropriately integrated in the adequacy assessment, wind plants do create significant challenges in maintaining generation adequacy on an operational level. To address these challenges, a novel operational reliability assessment tool is proposed to quantitatively evaluate the system's operational generation adequacy given potential generator forced outages, load and wind power forecasts, and forecasting deviations.

Table of Contents

Acknowledgments	v
Abstract	viii
List of Tables	xiv
List of Figures	xvii
Chapter 1. Introduction	1
Chapter 2. Generation Adequacy Assessment in System Planning using Loss-of-Load Analysis: An overview of key concepts	7
2.1 Loss-of-Load Probabilistic Metrics	8
2.1.1 Capacity Outage Probability Table	9
2.1.2 Loss-of-Load Probability	14
2.1.3 Loss-of-Load Expectation	15
2.1.4 Case Study: Daily Peak LOLE versus Hourly LOLE . .	20
2.2 Generating Unit Unavailability	21
2.2.1 Unavailability of Conventional Generating Units	22
2.2.1.1 Two-State Markov Model: Units with long operating cycles	23
2.2.1.2 Four-State Markov Model: Units with short operating cycles	24
2.3 Concluding Remarks	26
Chapter 3. Wind Plants and Generation Adequacy Assessment in System Planning	28
3.1 Integrating Wind Plants in Loss-of-Load Calculations	29
3.1.1 Multi-State Approach	29

3.1.2	Negative Load Adjustment Approach	30
3.1.3	Concerns about Wind Integration in Loss-of-Load Calculations	32
3.1.3.1	Wind/Load Correlation	32
3.1.3.2	Statistical Dependence of Wind Plants	34
3.2	Case Study: Wind Plant Contribution to Planning Generation Adequacy	36
3.2.1	Generation System Reliability Model	37
3.2.2	Wind Plant Multi-State Representation	38
3.2.3	Load Model	39
3.2.4	Analytical Approach	40
3.2.5	Case Study Results and Discussion	42
3.2.5.1	Base Case Scenario Results	42
3.2.5.2	Comparing LOLE Results	43
3.3	Concluding Remarks	46
Chapter 4. Effective Load Carrying Capability of a Wind Plant		48
4.1	ELCC Concept Overview	49
4.2	Classical Computing Method using Multi-State Representation	51
4.3	Classical Computing Method using Negative Load Adjustment	53
4.4	Discussion on Computing Methods	54
4.5	Non-Iterative ELCC Approximation	56
4.5.1	Basis	57
4.5.2	Graphical Parameter of the Existing Power System	58
4.5.3	Mathematical Derivation of the Estimating Function	59
4.5.4	Essential Steps of the Non-iterative Approximation	64
4.6	Case Studies and Discussion	65
4.6.1	Case Study I: ELCC and Wind Plant Penetration	66
4.6.1.1	Choosing the Evaluation Period	68
4.6.1.2	Building the Wind Plant's Reliability Model	68
4.6.1.3	Building the COPT of System 1	70
4.6.1.4	Determining the m parameter of System 1	71
4.6.1.5	Results	74

4.6.1.6	Discussion	75
4.6.2	Case Studies II and III: Period-specific ELCCs	77
4.6.2.1	Choosing the Evaluation Period	79
4.6.2.2	Building the Wind Plant's Reliability Model	82
4.6.2.3	Building the COPT of System 2 and System 3	83
4.6.2.4	Determining the m Parameter of System 2 and System 3	84
4.6.2.5	Results	87
4.6.2.6	Discussion	88
4.7	Concluding Remarks	92

Chapter 5. Operational Generation Adequacy Assessment for Power Systems with Wind Generation 94

5.1	Concept Description	95
5.2	Conventional Unit and Combined-cycle Plant Reliability Model	97
5.3	Proposed Operational Load Reliability Model	98
5.4	Proposed Operational Wind Plant Reliability Model	100
5.4.1	Integrating Wind Plant as Generation	101
5.4.2	Wind Plants Integrated as Negative Load	104
5.5	Operational LOLP Calculations	104
5.5.1	Operational LOLP Risk Criterion	107
5.6	Feasibility Study	108
5.6.1	Test System	109
5.6.2	Creating Hourly Generation Schedules	112
5.6.3	Step-by-step Application of the Operational Assessment	113
5.6.3.1	Step 1: Build the wind plant's operational reliability model	114
5.6.3.2	Step 2: Build the system's hourly COPT	116
5.6.3.3	Step 3: Determine the operational load model	116
5.6.3.4	Step 4: Compute the hourly operational LOLP	118
5.6.3.5	Step 5: Compare hourly LOLP to the criterion	119
5.6.3.6	Step 6: Consider demand response and fast start units	120
5.6.4	Case Study Results	125

5.6.5	Discussion	125
5.6.5.1	Effect of Demand Response and Fast Start Units on LOLP	130
5.6.5.2	Comparing Hour-ahead vs. Day-ahead Results .	133
5.6.5.3	Effect of Wind Penetration Level on Hourly LOLP	138
5.6.5.4	Effect of Capacity Margin on Hourly LOLP . .	139
5.6.5.5	Effect of Large Units on the LOLP	141
5.6.6	Concluding Remarks	143
Chapter 6.	Summary and Conclusion	145
Appendices		149
Appendix A.	Combined-Cycle Plant Reliability Modeling	150
A.1	Combined-Cycle Plants	150
A.2	Plant-Specific Dispatch Model	152
A.3	Generic Dispatch Model	154
A.4	Concluding Remarks	157
Bibliography		159
Vita		166

List of Tables

2.1	Example: Simple power system	11
2.2	Example: Simple system COPT	14
2.3	Example: Daily peak LOLE versus hourly LOLE	20
2.4	Example of the unavailability probability of generating units using the two-state (TS) and four-state (FS) Markov models	26
3.1	Example: Multi-state model of a 20-MW wind plant given a 2-MW resolution	31
3.2	Generating units for the 2,728-MW base case power system	38
3.3	Wind plants' energy equivalent conventional units	41
4.1	Case Study I: Generating units data of System 1	67
4.2	Case Study I: Multi-state representation of a 55-MW wind plant using WP-1 power output data and a resolution of 1-MW	70
4.3	Case Study I: COPT for a 2,783-MW power system including a 55-MW wind plant using WP-1 power output data	72
4.4	Case Study I: System 1's LOLE for various load data time-series	73
4.5	Comparison of ELCC results for Case Study I	76
4.6	Case Study II: IEEE-RTS Generating units reliability data	77
4.7	Case Study II: Multi-state representation for the 150-MW wind plant using a resolution of 1-MW and an evaluation period of a year	84
4.8	Case Study II: LOLE for various load data time-series during August for System 2	85
4.9	Case Study II: Comparison of ELCC results obtained for 150-MW wind plant (Percent relative errors in parenthesis)	89
4.10	Case Study III: Comparison of ELCC results for 114-MW wind plant (Percent relative errors in parenthesis)	90
5.1	Example: Simple history of forecasts and actual load demands for estimating forecasting deviations (Note that the load history is specific to the period of interest.)	99

5.2	Example: Estimated load forecasting deviations distribution by load forecast	100
5.3	Example: Forecasting deviations distribution associated with a 70-MW forecast of a 100-MW wind plant	102
5.4	Example: Operational multi-state representation of a 100-MW wind plant given a 70-MW forecast	103
5.5	Feasibility Study: Conventional generating units data	110
5.6	Feasibility Study: Two days of 24 hourly load forecasts (L_f) and wind plant power output forecasts (W_f)	111
5.7	Discrete seven-step approximation of the normal distribution	112
5.8	Hour-ahead wind power forecasting deviations for a 200-MW forecast using the discrete seven-step approximation of the normal distribution	112
5.9	Summer Day at 11PM: Conventional generators scheduled given a 120-MW wind power forecast and a 1330-MW load forecast	114
5.10	Summer Day at 11PM: Day-ahead wind power forecasting deviations for a 120-MW forecast	115
5.11	Summer Day at 11PM: Day-ahead wind plant operational multi-state representation for a 120-MW forecast	116
5.12	Summer Day at 11PM: Day-ahead hourly COPT	117
5.13	Summer Day at 11PM: Day-ahead load reliability model for 1330-MW forecast	117
5.14	Summer Day at 11PM: Day-ahead available fast start generators	122
5.15	Summer Day at 11PM: Day-ahead COPT including additional fast start unit	123
5.16	Summer Day at 11PM: Hour-ahead wind power forecasting deviations for a 120-MW forecast	134
5.17	Summer Day at 11PM: Hour-ahead wind plant multi-state representation for a 120-MW forecast (Note that the capacity outage state of 192-MW has no impact on the whole system's COPT. However, it must be considered in the maximum possible capacity of the system C_s when computing the LOLP.)	134
5.18	Summer Day at 11PM: Hour-ahead hourly COPT	135
5.19	Summer Day at 11PM: Hour-ahead load reliability model for 1330-MW forecast	136
A.1	Example: Combined-cycle units unavailability	151

A.2	Example: Initial combined-cycle plant availability matrix . . .	153
A.3	Example: Plant-specific dispatch patterns for the 3GT-1ST combined-cycle plant	154
A.4	Example: Complete combined-cycle availability matrix (The symbol * indicates when the minimum requirement of 2 GT is not met) . . .	155
A.5	Example: Combined-cycle plant multi-state representation using the plant-specific dispatch model	155
A.6	Example: Generic dispatch patterns for the 3GT-1ST combined-cycle plant	156
A.7	Example: Combined-cycle plant multi-state representation using the generic dispatch model	157
A.8	Example: Combined-cycle plant multi-state representation considering independent units	157

List of Figures

2.1	Two-state Markov model	23
2.2	Four-state Markov model	24
3.1	Monthly LOLE: Base case scenario	43
3.2	Monthly LOLE: Wind plants of various penetration levels . . .	44
3.3	Monthly LOLE: Capacity equivalent conventional units	44
3.4	Monthly LOLE: Energy equivalent conventional units	45
3.5	Yearly LOLE of wind plants, equivalent energy conventional units and equivalent capacity conventional units	46
4.1	Case Study I: Exponential relationship between the existing system's LOLE and a shifted increase or decrease in the typical load demand.	74
4.2	Case Study I: Comparing ELCC results from the conventional calculations, non-iterative approximation and capacity factor approximation for: (a) wind plants created from WP-1 source data, and (b) wind plants created from WP-2 source data . . .	75
4.3	Case Study II: Hourly load data time-series for System 2 over a year long evaluation period	78
4.4	Case Study II: Power output for the 150-MW wind plant over a year long evaluation period (Note the interannual variability of the wind generation.)	78
4.5	Case Study III: Power output for the 114-MW wind plant over the year long evaluation period (Note the interannual variability of the wind generation.)	79
4.6	Case Study II: Hourly load data time-series for August	80
4.7	Case Study II: Power output for the 150-MW wind plant during August	81
4.8	Case Study II: Superimposed load and wind power output time-series for August	82
4.9	Case Study II: Correlation graph between load demand and wind power output time-series for August	82

4.10	Case Study II: Exponential relationship between the existing system's LOLE and a shifted increase or decrease in the typical load demand during August	86
4.11	Case Study II: Comparing ELCC results obtained from the non-iterative approximation (NI), the conventional method and capacity factor approximation(CF)	87
4.12	Case Study III: Comparing ELCC results obtained from the non-iterative approximation (NI), the conventional method and capacity factor approximation(CF)	88
5.1	Conceptual diagram of the operational reliability assessment tool reflecting hourly operational LOLP calculations	96
5.2	Summer Day: Day-ahead assessment results	126
5.3	Summer Day: Hour-ahead assessment results	127
5.4	Winter Day: Day-ahead assessment results	128
5.5	Winter Day: Hour-ahead assessment results	129
5.6	Summer Day Day-ahead Assessment: Effects of demand response (DR) and fast start units (FS) on LOLP	131
5.7	Summer Day Hour-ahead Assessment: Effects of demand response (DR) and fast start units (FS) on LOLP	131
5.8	Winter Day Day-ahead Assessment: Effects of demand response (DR) and fast start units (FS) on LOLP	132
5.9	Winter Day Hour-ahead Assessment: Effects of demand response (DR) and fast start units (FS) on LOLP	132
5.10	Summer Day: Day-ahead against hour-ahead hourly LOLP results	139
5.11	Winter Day: Day-ahead against hour-ahead hourly LOLP results	140
5.12	Effect of wind penetration on hourly LOLP	141
5.13	Effect of capacity margin on hourly LOLP	142
5.14	Summer Day Day-ahead Assessment: Effect of large units on LOLP	143

Chapter 1

Introduction

Wind power represents the worldwide fastest growing component of electric generation portfolios. In the U.S. alone, the total wind generation capacity has expanded by 45% in a single calendar year going from 11,603-MW in 2006 to 16,818-MW in 2007 [1]. Wind capacity in the U.S. and in Europe has seen growth rates of 20% to 30% over the past decade [2]. Based on this trend, wind power should continue along this growth pattern and become an even more significant portion of future generation portfolios. Major growth drivers include advances in wind energy conversion technologies, the need to lessen our dependence on fossil fuel, climate change, environmental sustainability, and various federal and state policies to promote the use and development of renewable energy sources. A recent report by the U.S. Department of Energy has investigated scenarios where wind energy could provide 20% of the U.S. Electricity needs by 2030 [3]. As of 2007, 25 U.S states and the District of Columbia have adopted Renewable Portfolio Standards¹ ranging from 2% to 40% of the electricity supply which are expected to be reached in the next two

¹“A renewable portfolio standard (RPS) is a state policy that requires electricity retailers to provide a minimum percentage or quantity of their electricity supplies from renewable energy sources [4].”

decades [4]. Since wind power possesses unique characteristics and attributes which differentiate it from conventional fossil-based electric power, an increase in wind penetration level commands attention. From a plant terminal point of view, new wind plants are behaving more and more like conventional generation by providing low-voltage ride-through, voltage support and dynamic reactive capabilities [5]. However, unlike fossil-based power where the rate of energy throughput is controllable, wind power is variable, uncertain and therefore non-dispatchable. Indeed, wind generation could vary according to diurnal heating and cooling pattern or suddenly increase with a storm front. Without any form of storage, the wind energy being converted into electric power has to be consumed immediately. When wind generation was an insignificant portion of generation portfolios, existing system capabilities and operations processes were enough to handle its variable and uncertain nature. However, as wind penetration is increasing, it is creating new challenges for both system planners and operators. Among these challenges has been the need to ensure capacity adequacy from both a system planning and operations perspective.

From a system planning perspective, generation adequacy assessment studies must be performed to determine the adequate planning reserve margins which will ensure desired levels of reliability. Initially, wind plants were considered as providing no capacity to the generation adequacy of power systems. Although studies from the late 1970s and early 1980s [6–8] suggested that wind plants could have some reliability contribution, it is only in the

new millennium that utilities started recognizing the capacity contribution² of wind plants [9]. Methods of quantifying the wind plant capacity contribution has evolved over the years and the electric community has still to reach a firm consensus on the most adequate computing method [10–13]. Appropriately integrating wind plants into planning adequacy assessment is essential to determine the right amount of planning reserve margins and meet projected load demands.

Assuming wind plants are appropriately integrated in planning generation adequacy studies and resultant power systems are well-planned, the variable and uncertain nature of wind generation is still creating challenges from an system operations perspective. System operators are responsible for maintaining adequate system reliability, while constantly monitoring and matching the system generation to the load demand. Ancillary services are procured to maintain security and reliability during system disturbances and to account for load forecasting deviations. Several wind integration studies have investigated the prospective impact of increasing wind penetration on ancillary services requirements [14–19]. Currently, adequate monthly or annual ancillary service requirements are usually determined based on engineering judgment and a system’s historical performance. Since these requirements may or may not capture wind generation’s uncertainty in operational time frames, being able to assess the operational system reliability status would be very beneficial for system operators. Utilities seem to be progressively incorporating wind power

²Capacity contribution may also be known as capacity credit or value.

forecasting tools in their system operations. Developing an operational reliability assessment tool which would incorporate wind forecast and potential forecasting deviations would be an important step in ensuring operational generation adequacy for systems with significant wind generation. Based on the aforementioned reasons, the objective of this dissertation focuses on investigating and assessing the generation adequacy of power systems with significant wind generation, both from a system planning and operations perspective, while offering the following incremental and key contributions.

From a system planning perspective:

- *Provide a detailed methodology for appropriately integrating wind plants in planning generation adequacy assessment based on analytical loss-of-load methods.* (Chapter 2 and 3)
- *Recognize the wind plant's reliability contribution through the reduction in system loss-of-load expectation and compare it to contribution of capacity and energy equivalent conventional units.* These findings were published in [20]. (Chapter 3)
- *Provide a detailed and clear methodology for quantifying the capacity contribution of wind plants using the ELCC concepts.* Our insights and observations on the classical ELCC computing methodologies were shared in a collaborative work on the capacity contribution of wind plants [21]. (Chapter 4)

- *Propose a novel non-iterative method of approximating the capacity contribution of a wind plant.* As a key contribution, the proposed method was published in [22,23] and cited in [21]. By using a simple estimating function, the non-iterative approximation is shown to give accurate ELCC estimates (with an averaged errors of 2%) while being a less computationally-intensive method that requires minimal reliability modeling. (Chapter 4)

From a system operations perspective:

- *Propose a novel operational reliability assessment tool to ensure adequate operational risk levels.* The proposed concept was presented in [24] and represent a key contribution. The operational tool computes hourly operational loss-of-load probabilities for both day-ahead and hour-ahead time horizons, while considers possible generator forced outages, wind plant power output and load forecasts, and corresponding forecasting deviations. Given an acceptable hourly risk criterion, high risk periods can be identified and appropriate measures can be taken to reduce the hourly risk, such as considering demand response or scheduling additional fast start units. (Chapter 5)

Again, parts of this dissertation have been published in IEEE journal and conference papers [20, 22–24].

The work presented in this dissertation is organized as follows. Chapter 2 will present the key concepts of planning generation adequacy assessment us-

ing loss-of-load analytical methods. Chapter 3 will provide a detailed methodology on how wind plants can be integrated in the adequacy assessment and how they can contribute to the system planning generation adequacy. In Chapter 4, a wind plant's capacity contribution will be quantified using the concept of effective load carrying capability while also proposing a novel non-iterative ELCC approximation. Then, from an operational perspective, Chapter 5 will propose a novel operational reliability assessment tool. Finally, a conclusion chapter will summarize the work and the key contributions.

Chapter 2

Generation Adequacy Assessment in System Planning using Loss-of-Load Analysis: An overview of key concepts

Obviously, when it comes to maintaining power system reliability, the goal must be to avoid falling short of generating capacity. Power system planning groups perform generation adequacy assessment studies to ensure that enough capacity is available in the system to meet projected load demands. This static capacity evaluation relates to long-term overall system requirements in planning reserve margins and has been tested using such various methods¹ as:

1. Fixed criteria determined by *loss of the largest unit reserve* or *percentage reserve*;
2. Analysis of the system using *loss-of-load calculations*, *expected energy not supplied* or other assessment formulas; and
3. Simulation methods such as *Monte Carlo simulations*.

¹Methods are summarized in [25]

Choosing the appropriate method depends on the system under investigation and data availability. Although times are changing with the increase of computational power, analytical methods are usually preferred for assessing generation adequacy; simulations methods generally require lengthy computational times while fixed criteria can be inconsistent. Analytical methods, on the other hand, can provide system planners with reasonably accurate results with which to make objective decisions in fairly short computational times [25].

Chapter 2 reviews the key metrics determining a power system's generation adequacy assessment based on loss-of-load analytical methods. The concepts of loss-of-load probability (LOLP), loss-of-load expectation (LOLE), and the capacity outage probability table (COPT), along with generating units reliability modeling are presented to obtain a basic understanding of how generation adequacy is assessed [25–27]. With these key metrics understood, the next chapter will describe how to integrate wind plants in terms of these assessments methods, which will allow us to show through an examination of some case studies, that wind generation can indeed contribute to the generation adequacy of power systems.

2.1 Loss-of-Load Probabilistic Metrics

The metrics obtained from loss-of-load probability (LOLP) and loss-of-load expectation (LOLE) calculations are the most widely used probabilistic benchmarks for evaluating the generation adequacy of power systems [25].

Both of these calculations rely on a generation model and a load model to ultimately obtain a risk metric. Transmission system reliability or constraints are not usually factored into these methods ². The generation model used in loss-of-load calculations is the capacity outage probability table (COPT).

2.1.1 Capacity Outage Probability Table

The COPT represents the cumulative probability $P(X \geq x)$ of having a system capacity outage X greater than or equal to x . The discrete random variable X represents the possible capacity outage states of the system. The COPT is built using a recursive algorithm in which units are added sequentially to produce a table representing all the possible capacity outage states of the system, with their corresponding cumulative probability. Each generating unit can be incorporated in the COPT as either a two-state or a more general multi-state unit. In the two-state model, units are represented as being either fully on or fully off, while the multi-state model also includes one or more partial capacity outage states. The latter can be used for units with possible derated states. The probability that a unit be on forced outage and therefore unavailable can be obtained using Markov process theory and long-term unavailability statistics. Once modeled, each unit is added sequentially using basic probability to create the final model of the system. The unavailabilities of the units are considered random events and are therefore independent

²Since wind plants are usually located remotely from demand centers, they are more likely to be subject to possible transmission constraints. Further analysis to include these constraints in the generation adequacy assessment is part of future work.

of each other. The recursive algorithm is mathematically represented by the following equations.

The cumulative probability $P(X \geq x)$ of having a system capacity outage greater than or equal to x after adding a two-state unit of generating capacity C and unavailability probability p_{down} can be calculated as follows:

$$P(X_{After} \geq x) = (1 - p_{down})P(X_{Before} \geq x) + (p_{down})P(X_{Before} \geq x - C) \quad (2.1)$$

where X_{Before} and X_{After} are discrete random variables representing the possible capacity outage states of the system before and after the addition of the new two-state unit.

Equation (2.1) thus gives us the sum of two components corresponding to the two possible states of the new unit. In the first component, the unit is available with probability $(1 - p_{down})$; therefore, for a system capacity outage X_{After} of x or greater to occur, it needs to happen in the previous system, hence $P(X_{Before} \geq x)$. In the second component, the unit is assumed to be unavailable; therefore, to have a system capacity outage X_{After} of x or greater, only a system capacity outage of $x - C$ or greater needs to occur in the previous system, hence $P(X_{Before} \geq x - C)$. Similarly, a generalized equation can be extended to include multi-state units. A multi-state unit which can exist in k partial capacity outage states C_j of individual probability p_j can be added to the power system reliability model using the following equation:

$$P(X_{After} \geq x) = \sum_{j=1}^k p_j \times P(X_{Before} \geq x - C_j) \quad (2.2)$$

Equations (2.1) and (2.2) are initialized by setting $P(X_{Before} \geq x)$ equal to 1 when x or $x - C$ are smaller or equal to zero.

The following example ³ will illustrate how the recursive algorithm is applied to build the COPT of a simple power system. The generating units' capacity and unavailability probabilities are presented in Table 2.1. The simple system consists of two 25-MW units, represented with a two-state model, and one 50-MW unit represented with a multi-state model (since it can exist in one partial capacity outage state).

Table 2.1 Example: Simple power system

Two-state units	
Capacity C [MW]	Unavailability prob. p_{down}
25	0.02
25	0.02
Multi-state unit	
Capacity outage states C_j [MW]	Individual prob. p_j
0	0.960
20	0.033
50	0.007

The recursive algorithm in (2.2) is applied to the simple system by sequentially adding one unit at a time. The order in which the units are added is of no consequence to the final COPT; however, adding multi-state units last may

³This example was taken from [25].

speed up computational times. Step 1. add the first 25-MW unit:

$$P(X_{Af} \geq 0) = (0.98)P(X_{Bf} \geq 0) + (0.02)P(X_{Bf} \geq -25)$$

$$\mathbf{P}(\mathbf{X}_{Af} \geq \mathbf{0}) = (0.98)(1.0) + (0.02)(1.0) = \mathbf{1.0}$$

$$P(X_{Af} \geq 25) = (0.98)P(X_{Bf} \geq 25) + (0.02)P(X_{Bf} \geq 0)$$

$$\mathbf{P}(\mathbf{X}_{Af} \geq \mathbf{25}) = (0.98)(0) + (0.02)(1.0) = \mathbf{0.02}$$

Step 2. add the second 25-MW unit:

$$P(X_{Af} \geq 0) = (0.98)P(X_{Bf} \geq 0) + (0.02)P(X_{Bf} \geq -25)$$

$$\mathbf{P}(\mathbf{X}_{Af} \geq \mathbf{0}) = (0.98)(1.0) + (0.02)(1.0) = \mathbf{1.0}$$

$$P(X_{Af} \geq 25) = (0.98)P(X_{Bf} \geq 25) + (0.02)P(X_{Bf} \geq 0)$$

$$\mathbf{P}(\mathbf{X}_{Af} \geq \mathbf{25}) = (0.98)(0.02) + (0.02)(1.0) = \mathbf{0.00396}$$

$$P(X_{Af} \geq 50) = (0.98)P(X_{Bf} \geq 50) + (0.02)P(X_{Bf} \geq 25)$$

$$\mathbf{P}(\mathbf{X}_{Af} \geq \mathbf{50}) = (0.98)(0) + (0.02)(0.02) = \mathbf{0.0004}$$

Step 3. add the third 50-MW multi-state unit:

$$P(X_{Af} \geq 0) = (0.96)P(X_{Bf} \geq 0) + (0.033)P(X_{Bf} \geq -20) + (0.007)P(X_{Bf} \geq -50)$$

$$\mathbf{P(X_{Af} \geq 0)} = (0.96)(1.0) + (0.033)(1.0) + (0.007)(1.0) = \mathbf{1.0}$$

$$P(X_{Af} \geq 20) = (0.96)P(X_{Bf} \geq 20) + (0.033)P(X_{Bf} \geq 0) + (0.007)P(X_{Bf} \geq -30)$$

$$\mathbf{P(X_{Af} \geq 20)} = (0.96)(0.00396) + (0.033)(1.0) + (0.007)(1.0) = \mathbf{0.078016}$$

$$P(X_{Af} \geq 25) = (0.96)P(X_{Bf} \geq 25) + (0.033)P(X_{Bf} \geq 5) + (0.007)P(X_{Bf} \geq -25)$$

$$\mathbf{P(X_{Af} \geq 25)} = (0.96)(0.00396) + (0.033)(0.00396) + (0.007)(1.0) = \mathbf{0.0463228}$$

$$P(X_{Af} \geq 45) = (0.96)P(X_{Bf} \geq 45) + (0.033)P(X_{Bf} \geq 25) + (0.007)P(X_{Bf} \geq -5)$$

$$\mathbf{P(X_{Af} \geq 45)} = (0.96)(0.0004) + (0.033)(0.00396) + (0.007)(1.0) = \mathbf{0.0086908}$$

$$P(X_{Af} \geq 50) = (0.96)P(X_{Bf} \geq 50) + (0.033)P(X_{Bf} \geq 30) + (0.007)P(X_{Bf} \geq 0)$$

$$\mathbf{P(X_{Af} \geq 50)} = (0.96)(0.0004) + (0.033)(0.0004) + (0.007)(1.0) = \mathbf{0.0073972}$$

$$P(X_{Af} \geq 70) = (0.96)P(X_{Bf} \geq 70) + (0.033)P(X_{Bf} \geq 50) + (0.007)P(X_{Bf} \geq 20)$$

$$\mathbf{P(X_{Af} \geq 70)} = (0.96)(0) + (0.033)(0.0004) + (0.007)(0.00396) = \mathbf{0.0002904}$$

$$P(X_{Af} \geq 75) = (0.96)P(X_{Bf} \geq 75) + (0.033)P(X_{Bf} \geq 55) + (0.007)P(X_{Bf} \geq 25)$$

$$\mathbf{P(X_{Af} \geq 75)} = (0.96)(0) + (0.033)(0) + (0.007)(0.00396) = \mathbf{0.0002772}$$

$$P(X_{Af} \geq 100) = (0.96)P(X_{Bf} \geq 100) + (0.033)P(X_{Bf} \geq 80) + (0.007)P(X_{Bf} \geq 50)$$

$$\mathbf{P(X_{Af} \geq 100)} = (0.96)(0) + (0.033)(0) + (0.007)(0.0004) = \mathbf{0.0000028}$$

As seen in the above example, a capacity outage state of $x - C_j$ might not have been a possible state X_{Bf} in the previous system. Indeed, the value of $x - C_j$ might fall between two states. Since we are concerned with the

cumulative probability, the highest capacity outage state and its corresponding cumulative probability must be chosen. For example, in the third step, $P(X_{Bf} \geq 30)$ will correspond to $P(X_{Bf} \geq 50)$ and a probability of 0.0004, since only the capacity outages of 0, 25 and 50-MW exist. Furthermore, when $x - C_j$ is less than zero, $P(X_{Bf} \geq 0)$ is used. On the other hand, when $x - C_j$ is greater than the last possible capacity outage state X_{Bf} , then a probability of zero is assigned. The final COPT of the example system is represented in Table 2.2.

Table 2.2 Example: Simple system COPT

Capacity outage states x [MW]	Cumulative prob. $P(X \geq x)$
0	1.0
20	0.078016
25	0.0463228
45	0.0086908
50	0.0073972
70	0.0002904
75	0.0002772
100	0.0000028

Our next step is to use the COPT of the power system with a determined load model to compute the LOLP and LOLE reliability metrics.

2.1.2 Loss-of-Load Probability

The loss-of-load probability (LOLP) represents the probability of not having enough capacity available to meet a given load demand. The LOLP is

usually represented by the following equation:

$$LOLP = P(X > C_s - L) \quad (2.3)$$

where L is a given load demand, C_s is the system capacity available and $P(X > C_s - L)$ is the probability of having a capacity outage greater than the margin $C_s - L$, which represents the parameter determining when a loss of load would occur in the system. The cumulative probability $P(X > x)$ can be obtained from the systems COPT ⁴. The uncertainty in a load demand can be included in the LOLP calculation by using conditional probability and the law of total probability. It is worth mentioning that there are *no* units attached to the LOLP. Indeed, the LOLP is simply a probability that measures the likelihood of a loss-of-load event, or describes the risk of not meeting the load for a particular combination of load and system conditions. On the other hand, the calculation of the loss-of-load expectation (LOLE) can provide the compounded risk or the number of loss-of-load *events* that can be expected during a chosen evaluation period.

2.1.3 Loss-of-Load Expectation

The loss-of-load expectation is a risk metric that has been used in planning generation adequacy studies to determine acceptable level of planning reserves. Planning reserves are important to ensure that enough total system

⁴Notice that the loss of load is defined when the capacity outage is *greater than* the margin while the COPT represents cumulative probabilities for capacity outage *greater than or equal to* a particular value.

capacity is available to reliably meet expected load demands. The LOLE is usually described as the expected number of days or hours during a certain period when a loss-of-load would occur [25]. This metric is usually represented by one of the following equations:

$$LOLE = \sum_{i=1}^{365} P_i(X > C_{s,i} - L_i) \times \frac{days}{year} \quad (2.4)$$

$$LOLE = \sum_{i=1}^{8760} P_i(X > C_{s,i} - L_i) \times \frac{hours}{year} \quad (2.5)$$

Although the LOLE is a standard metric and these equations are commonly used and referenced, their mathematical derivation may not be commonly understood. Let us consider an evaluation period represented by n equal time durations where i represents the i^{th} time duration. For example, if the time duration is a day and the chosen evaluation period is a year, then n will be equal to 365. During a particular time duration, the load conditions L_i and available system capacity $C_{s,i}$ are considered *constant*. The available capacity of the system $C_{s,i}$ and its COPT can vary from one time duration to the next, depending on the maintenance schedules of the units⁵. For the i_{th} time duration and the corresponding load and system conditions, a discrete random variable I_i can be defined to indicate the system's loss-of-load state:

$$I_i = \begin{cases} 1, & \text{if a loss of load occurs (Event);} \\ 0, & \text{otherwise (No event);} \end{cases}$$

⁵Reference [25] presents various methods to consider the units' maintenance schedule in the COPT. The case studies included in this dissertation will not consider maintenance schedules.

Using the basic definition of the expectation of a random variable, the expectation of the indicator I_i can be shown as

$$\begin{aligned} E(I_i) &= 1 \times P(I_i = 1) + 0 \times P(I_i = 0) \\ E(I_i) &= P(I_i = 1) \end{aligned} \tag{2.6}$$

The probability of a loss of load occurring during the i_{th} time duration, or $P(I_i = 1)$, is equivalent to the probability there won't be enough generation available to meet the load. This probability is simply the LOLP defined in (2.3); the probability of a capacity outage greater than the margin between the available capacity $C_{s,i}$ and the load L_i .

$$E(I_i) = P(I_i = 1) = P_i(X > C_{s,i} - L_i) \tag{2.7}$$

The total number of *time durations* when a loss of load would occur during the chosen evaluation period can be defined as the sum Y of the random indicator variables I_i .

$$Y = I_1 + I_2 + \dots I_n \tag{2.8}$$

Therefore, the *expected number of time durations* when a loss of load would occur during an evaluation period of interest is defined as

$$E(Y) = E(I_1 + I_2 + \dots I_n). \tag{2.9}$$

Using the rule on the expectation of a sum of random variables and replacing the $E(I_i)$ s by (2.7), (2.9) becomes

$$\begin{aligned}
 E(Y) &= E(I_1) + E(I_2) + \dots E(I_n) \\
 E(Y) &= \sum_{i=1}^n P_i(X > C_{s,i} - L_i)
 \end{aligned}
 \tag{2.10}$$

where $E(Y)$ encompasses units of time durations over the entire period and consequently represents the concept of loss-of-load expectation found in (2.4) and (2.5). The generalized LOLE equation for any time duration and evaluation period would be

$$LOLE = \sum_{i=1}^n P_i(X > C_{s,i} - L_i) \times \frac{\text{time durations or (events)}}{\text{evaluation period}}.
 \tag{2.11}$$

It can be seen from the derivation that the chosen *time duration*, whether it is a day or an hour, will result in two LOLEs which are *not* equivalent by unit conversion. Indeed, calculating the yearly LOLE of a system using 365 daily peak loads versus 8760 hourly loads would result in two different LOLEs and planning reserve margins. The only way (2.5) and (2.4) could be equated by unit conversion is if the following unrealistic condition was met: for each day, *all* 24 hourly loads were equal and available capacities were equal. Consequently, the LOLE calculating method should always be clearly stated to avoid any confusion.

In generation adequacy planning studies, the industry standard of “1 day in 10 years” has been widely used to determine adequate planning reserve margins that qualify a well-planned and reliable system. This standard dates

back to literature from the late 1940s and 1950s, when 365 daily peak loads and total installed capacity were used in LOLE calculations [28–32]. However, “the question of what degree of service reliability must be provided in a particular situation depends entirely on local conditions and personal judgment” [29]. This standard was proposed while keeping in mind that “an acceptable risk level is best determined by reviewing past designs that were judged to be acceptable systems” [33]. Consequently, the “1 day in 10 years” criterion was proposed as a guideline rather than an absolute criterion. A system specific criterion should be based on what has historically been an acceptable risk level. Ideally, consumers expectation and economic factors would also be considered in determining the acceptable risk criterion.

The industry still references the “1 day in 10 years” criterion, although the analytical computing methods of the LOLE are moving from the daily peak approach to the hourly approach. As mentioned earlier, “1 day in 10 years” using the daily peak load approach is not equivalent to 24 hours in 10 years using the hourly load approach. If computing methods are changing, standards should also be revised. The following section presents a case study in which the LOLE of a system is calculated by using both the daily peak load and hourly load approach to highlight the difference in the resulting planning reserve margins.

2.1.4 Case Study: Daily Peak LOLE versus Hourly LOLE

In this case study, it will be shown that the planning reserve margin determined with the “1 day in 10 years” criterion is not the same as the “24 hours in 10 years” criterion. Only one year of load data will be used. Therefore, assuming that all ten years are equivalent, the criterion for the year will be 0.1 days per year or 2.4 hours per year. The test system used in this case study is the IEEE-RTS system [34]. This system consists of 32 generating units amounting to 3405-MW of capacity. All generating units were modeled as two-state units and the system COPT was built following the approach in Section 2.1.1. The load model described in [34] was used in the LOLE calculations. In [34], the system’s original annual peak load L_{pk} was set to 2850-MW. However, since this annual peak load results in a daily peak LOLE of 1.368 days/year, it was reduced to 2484-MW to obtain a daily peak LOLE of 0.1 days per year. The load demand was then adjusted again to obtain an hourly LOLE of 2.4 hours per year. Both LOLE calculation methods were applied for each load demand. The planning reserve margin results are presented in Table 2.3.

Table 2.3 Example: Daily peak LOLE versus hourly LOLE

LOLE Calculation method	$L_{pk}=2484$ -MW Margin 921-MW	$L_{pk}=2653$ -MW Margin 752-MW
Daily peak loads (2.4)	0.100 days/year	0.363 days/year
Hourly loads (2.5)	0.642 hrs/year	2.40 hrs/year

If the daily peak load calculation method was used to meet the 0.1 days per year criterion, the power system would only be able to reliably serve a load demand of 2484-MW annual peak load with a planning reserve margin of 921-MW. On the other hand, if the hourly calculation method was used to meet a 2.4 hrs per year criterion, the power system would be able to reliably serve an additional 173-MW, reducing the planning reserve to 752-MW. By shifting criteria from the daily peak calculations to the hourly calculation without redefining the acceptable LOLE levels, system planners may create unreliable systems.

2.2 Generating Unit Unavailability

As mentioned previously, each generating unit can be incorporated in the COPT as either a two-state unit or a more general multi-state unit. In this work, conventional generating units will be represented with a two-state model, bracketing possible derated states. The next section will describe how to create the two-state reliability model using Markov process theory and a generating unit's long-term unavailability statistics. The generating units of a combined-cycle plant can be modeled as separate two-state units or with a more refined model as proposed in [35]. The general outline of our proposed combined-cycle reliability modeling is given in Appendix A.

2.2.1 Unavailability of Conventional Generating Units

The unavailability probability or unplanned outage risk of a conventional unit can be calculated using Markov process theory and the unit's long term unavailability statistics. Given the two-state reliability representation, units with short operating cycles are modeled using a four-state Markov process, while units with long operating cycles are modeled with the simplified two-state Markov process. There is often some confusion between the two-state reliability model and the two-state Markov process. A unit can be represented with p_{up} and p_{down} , i.e. within the two-state reliability model, while using *either* a two-state Markov process *or* a four-state Markov process [36]. The four-state Markov process will consider the time when short-cycle units are on reserve shutdown and compute the probability of being unavailable *only* when the unit is needed. Using a two-state Markov process for peaking or cycling units would return abnormally high unplanned outage risks. Long term statistics are used to establish a probability for the unavailability of conventional units. If unit specific statistics are unavailable, the NERC GADS database can provide the necessary information to compute a probability for the units unavailability given its type and size [37].

The essential equations for the two different Markov models will be presented in the next subsections using the NERC GADS variable names. The presented equations will allow the reader to easily compute a two-state unit's unavailability p_{down} . Reference [36] includes the details of the mathematical derivations.

2.2.1.1 Two-State Markov Model: Units with long operating cycles

Units with long operating cycles can be represented with the two-state Markov model presented in Figure 2.1.

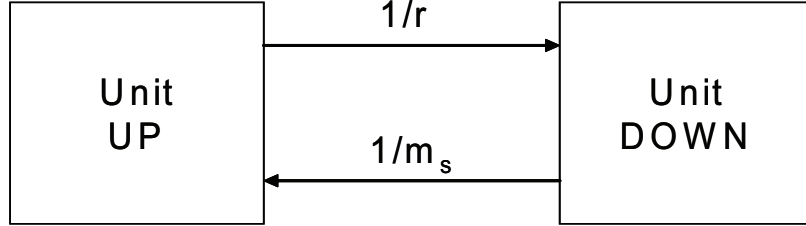


Figure 2.1 Two-state Markov model

The steady state unavailability probability p_{down} of a unit using the two-state Markov model can be calculated with the following formula:

$$p_{down} = \frac{r}{m_s + r} \quad (2.12)$$

where r is the mean forced outage time per forced outage and m_s is the mean service time per forced outage. These two quantities can be estimated using the following NERC GADS long term statistics: unplanned (forced) outage hours (FOH), service hours (SH) and number of occurrences of a forced outage (N).

$$\begin{aligned} r &\approx \frac{FOH}{N} \\ m_s &\approx \frac{SH}{N} \end{aligned} \quad (2.13)$$

The unavailability probability can then be estimated as

$$p_{down} = \frac{FOH}{SH + FOH} \quad (2.14)$$

The unavailability probability estimated by using the two-state Markov model is known as the forced outage rate (FOR).

2.2.1.2 Four-State Markov Model: Units with short operating cycles

Peaking and cycling units require a more detailed model to account for the reserve shutdown hours. In 1970, the IEEE Application of Probability Subcommittee developed a four-state Markov model which could accurately represent units with short operating cycles [36]. Figure 2.2 illustrates the

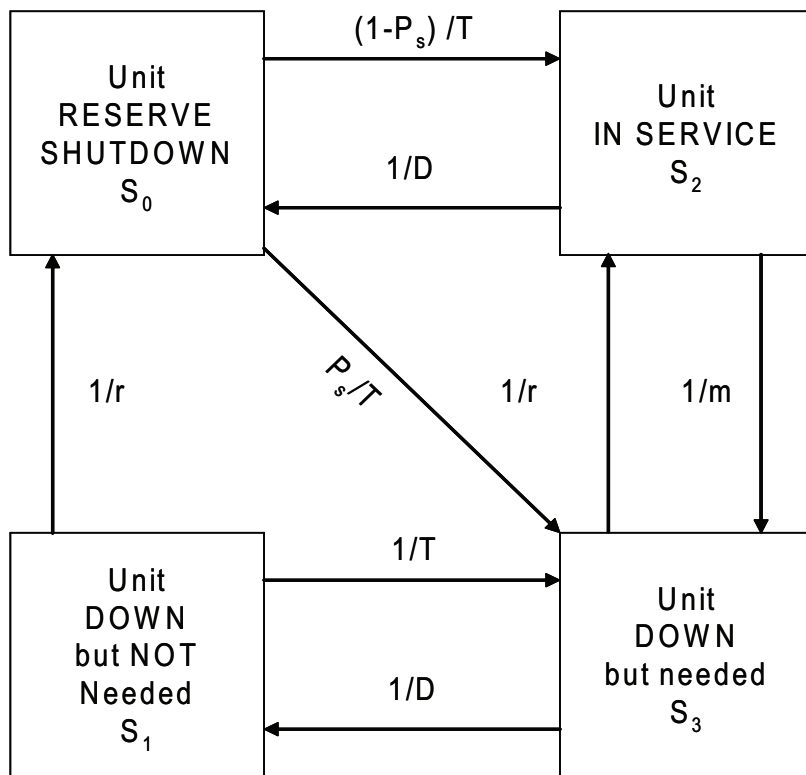


Figure 2.2 Four-state Markov model

IEEE model. In this case, the unavailability probability of a peaking or cycling unit should be the probability that the unit will be unavailable when it is actually needed to serve some demand. Therefore, p_{down} is computed by

$$p_{down} = \frac{P_3}{P_2 + P_3} \quad (2.15)$$

where P_3 is the unit's steady-state probability of being in state "3" or "unit down when needed" and P_2 is the steady-state probability of its being in state "2" or "in service". When the Markov problem is solved, p_{down} can be estimated as

$$p_{down} = \frac{\left(\frac{1}{r} + \frac{1}{T}\right) \left(\frac{D}{m} + P_s\right)}{\frac{1}{r} \left[D \left(\frac{1}{r} + \frac{1}{T}\right) + 1 \right] + \frac{D}{m} \left(\frac{1}{r} + \frac{1}{T}\right) + \frac{P_s}{T}} \quad (2.16)$$

where T is the average shutdown time between periods of need (excluding maintenance or other planned down time), D is its average in service time when needed, m is the average in-service time between forced outages (excluding forced outages due to failure to start), r is the average repair time per forced outages and P_s is the probability of a starting failure such that it is not able to serve the load during all or part of the demand period. As with the two-state Markov model, NERC GADS long term statistics can be used to estimate

these quantities.

$$\begin{aligned}
 r &\approx \frac{FOH}{N} \\
 m &\approx \frac{SH}{N} \\
 D &\approx \frac{SH}{NS} \text{ where NS is the number of actual starts} \\
 D + T &\approx \frac{SH + RSH}{NS} \text{ where RSH are the reserve shutdown hours} \\
 P_s &\approx \frac{NAS - NS}{NAS} \text{ where NAS is the number of attempted starts} \quad (2.17)
 \end{aligned}$$

Table 2.4 compares the unavailability probability of various units estimated by each Markov model. The commonly known forced outage rate or FOR is only an accurate method for baseload units, since it can overestimate the unavailability p_{down} of peaking and cycling units.

Table 2.4 Example of the unavailability probability of generating units using the two-state (TS) and four-state (FS) Markov models

Generation type in NERC GADS	FS p_{down} [%]	TS FOR [%]
GAS TURBINE 50 Plus MW	8.64	26.02
FOSSIL Coal Primary 600-799 MW	4.93	4.66
NUCLEAR PWR 1000 Plus MW	2.33	2.29

2.3 Concluding Remarks

In this chapter, we reviewed key concepts such as the loss-of-load probability (LOLP), loss-of-load expectation (LOLE) and the capacity outage probability table (COPT) in order to provide a basic understanding of planning

generation adequacy assessment. Methods of determining a generating unit's unavailability for conventional generation were also presented. The following chapters will investigate how wind generation can be integrated within this assessment framework, with an emphasis on how it can contribute to the generation adequacy of power systems.

Chapter 3

Wind Plants and Generation Adequacy Assessment in System Planning

In 2003, PJM Interconnection became one of the first system operators to adopt a rule that would recognize wind plant contributions to the generation adequacy of power systems [9]. As other system operators followed suit, wind plants quickly achieved universal recognition for contributing some capacity to generation adequacy [11]. This recent achievement stands at the end of a long, fraught history, in which system operators showed themselves to be reluctant to recognize *any* reliability contribution deriving from wind sources due to the perception that wind plants' power output was too variable, a perception that was abetted by the lack of studies on the subject. The first serious evaluations of the potential contribution that could be made by wind plants appeared in the late seventies and early eighties, partly as a result of the era's oil price shocks, which had elevated energy generation to a national priority [6–8]. At that time, large-scale wind plants had yet to be built, and probabilistic techniques such as the Weibull distribution and Markov methods were being used to model projections for wind generation variability of proposed sites. Methodologies using the loss-of-load concepts were then introduced to better assess the impending generation reliability impacts. Building on this initial research,

several studies using actual wind plants' power output data have been performed [11, 14, 16, 20, 38]. In assessing generation adequacy using loss-of-load calculations, wind plants have been modeled by means of two main approaches: negative load adjustment and multi-state representation [11, 39]. The objective of this chapter is to provide a detailed description of these approaches, along with their possible limitations. The multi-state representation approach is then applied to a case study highlighting the reliability contribution of wind plants in contrast to the contribution of conventional units equivalents [20].

3.1 Integrating Wind Plants in Loss-of-Load Calculations

3.1.1 Multi-State Approach

In this approach, a wind plant is represented with a multi-state model that is similar to calculations that incorporate conventional units with possible derated states. The wind plant is modeled with partial capacity outage states C_j and corresponding individual probabilities p_j . Given a certain resolution and using a database covering multiple years of hourly power output from the desired evaluation period, the wind plant's multi-state model can be created using the simple concept of relative frequency. For example, given a resolution of 2-MW, a wind plant with a nameplate rating C_w of 20-MW would be modeled by 11 partial capacity outage states: $C_1=0$ -MW, $C_2=2$ -MW, $C_3=4$ -MW... $C_{10}=18$ -MW, $C_{11}=C_w=20$ -MW. The individual probabilities p_j associated with the capacity outage states are computed by counting

the total number of occurrences of each partial capacity outage derived from the power output data. Since a capacity outage of C_j is equivalent to a power output of $C_w - C_j$, the individual probability p_j is calculated as:

$$p_j = \left[\frac{\# \text{ of occurrences when power output is } C_w - C_j}{\text{Total } \# \text{ of power output data points}} \right] . \quad (3.1)$$

The power output data should be rounded to the determined resolution prior to calculating the relative frequencies. When the resolution of the multi-state representation is small in comparison to the nameplate capacity of the wind plant, this rounding approximation has an insignificant impact on the final model. Table 3.1 presents an example of the multi-state representation of a 20-MW wind plant given a 2-MW resolution. As this example shows, the probability of a wind plant total outage ($C_j=20\text{-MW}$) is 2%, while a 8-MW capacity outage ($C_j=8\text{-MW}$) is the more likely, having a probability of 23%.

Using the recursive algorithm in (2.2), the wind plant's multi-state representation is convolved with all other units' reliability models to form the power system's COPT. Thus, in this integration approach, wind plants are treated no differently than any other generator. LOLP and LOLE calculations are performed on an hourly basis by directly applying (2.3) and (2.11) without any modifications.

3.1.2 Negative Load Adjustment Approach

Alternatively, wind generation can be integrated into the LOLP calculations by using the negative load adjustment approach. In this approach,

Table 3.1 Example: Multi-state model of a 20-MW wind plant given a 2-MW resolution

Capacity outage state C_j [MW]	Individual probability p_j
0	0.02
2	0.05
4	0.12
6	0.15
8	0.23
10	0.14
12	0.11
14	0.06
16	0.05
18	0.05
20	0.02

a wind plant’s power output is modeled as a negative load. The wind plant power output time-series is subtracted from the load time-series to create a net load time-series, which is then included in the LOLP and LOLE calculations. Wind generation is therefore not considered when building the COPT of the power system. The hourly LOLP is computed using the following equation:

$$LOLP = P(X > C_s - (L - W)) \quad (3.2)$$

where L is a given load demand, W is the wind plant’s power output and C_s is the system capacity available. The term $P(X > C_s - (L - W))$ is the probability of having a capacity outage greater than the margin $C_s - (L - W)$, the threshold defining when a loss of load would occur in the system.

The cumulative probability $P(X > x)$ is obtained from the system's COPT. Conversely, the modified LOLE calculation becomes

$$LOLE = \sum_{i=1}^n P_i(X > C_{s,i} - (L_i - W_i)) \times \frac{\text{time durations}}{\text{evaluation period}} . \quad (3.3)$$

When the system includes multiple wind plants, aggregated hourly power output data is used in the calculations:

$$W_{a,i} = \sum_{j=1}^k W_{k,i} \quad (3.4)$$

where $W_{a,i}$ is the aggregated power output of k wind plants' power output $W_{k,i}$ at time duration i . The load adjustment LOLE describing the aggregate wind generation is then calculated as

$$LOLE = \sum_{i=1}^n P_i(X > C_{s,i} - (L_i - W_{a,i})) \times \frac{\text{time durations}}{\text{evaluation period}} . \quad (3.5)$$

3.1.3 Concerns about Wind Integration in Loss-of-Load Calculations

Two main concerns arise when implementing the wind integration methods in loss-of-load calculations: 1) the possible wind/load correlation, and 2) the statistically-dependent unavailabilities of wind plants.

3.1.3.1 Wind/Load Correlation

Depending on its geographical location, a wind plant's power output might display some level of correlation to the power system's load demand. A wind plant would contribute more to the reliability of a power system if

it provided high output levels during peak load periods, while conversely, it would make a lesser contribution to generation reliability if its output was consistently low during high peak periods. A cross-correlation statistical analysis between the time-series of the wind plant's power output and the system load might reveal periods that are significantly cross-correlated. In this case, it would be important to demarcate time-related information in the loss-of-load calculations, whether the cross-correlation is positive or negative. In the multi-state approach, period-specific LOLE could be performed using wind and load data corresponding to the identified periods of significant and non-significant correlation. For example, the yearly LOLE for a system which displays cross-correlation during the months of June-July-August could be calculated with the following four steps:

1. Two separate multi-state representations are created for the wind plant: one for the months of June-July-August hourly wind power output data, while the other for the hourly data from the rest of the year.
2. Given these two multi-state representations, two COPTs can be created for each period: one for the summer, $COPT_{summer}$, and one for the rest of the year, $COPT$.
3. Divide the yearly typical load demand data (8760 hourly load) into two periods of interest: a 2208 hourly load data point set corresponding to the summer hours and a 6552 hourly load data point set for the rest of the year.

4. The yearly LOLE calculation is then computed as follows:

$$LOLE = \left[\sum_{i=1}^{2208} P_{Summer,i}(X > C_{s,i} - L_i) + \sum_{i=1}^{6552} P_i(X > C_{s,i} - L_i) \right] \times \frac{hours}{year} . \quad (3.6)$$

Using a similar approach as described in the steps above, any significant correlation relating the load demand to the wind diurnal effect could also be included in LOLE calculations.

In the negative load adjustment approach, the wind/load correlation can be captured in the subtraction required by the method. Because this inherent property makes the load adjustment approach simple to implement, it is often preferred over the multi-state representation. However, several years of actual time-synchronized load and wind time-series are required to make this approach statistically representative. More research is currently being conducted by the wind community to determine exactly how many years of net load data are required to make sure the negative load approach is statistically representative [21, 40].

3.1.3.2 Statistical Dependence of Wind Plants

The COPT concept presented in Section 2.1.1 assumes that the forced outages of the generating units are random events, meaning that they are independent from each other. Although this assumption can be valid for conventional generators, it may not be valid for wind plants. Indeed, wind plants

in geographical proximity which are fed by the same wind regime would display statistically-dependent unavailabilities. Ultimately, all wind plants' unavailabilities are statistically-dependent as they all have one variable in common, the sun. Since winds are caused by differential heating of the earth's surface by the sun, the sun is therefore, analytically, a common variable to all wind plants' power output. Thus, the question becomes: "Can we *reasonably assume* statistical independence between wind plant's unavailabilities?". Similar to the wind/load correlation, a cross-correlation analysis between the wind plants' power output time-series could indicate significant levels of linear dependence. One could therefore reasonably conclude that a significant linear dependence between two wind plants would render the statistical independence assumption invalid. In the multi-state representation approach, if a significant cross-correlation is present, the correlated wind plants should be aggregated and represented as one multi-state unit. On the other hand, the load adjustment approach inherently bypasses this concern, as it aggregates all wind generation as negative load. In this dissertation, the multi-state representation is used over the negative load approach as time-synchronized wind power output and load time-series are still not readily available. In summary, while using the multi-state representation, the key points associated with this wind integration method are the following five:

1. Wind generation is treated as what it is: generation. In this case, wind plants are mathematically integrated in the same manner as any other generator.

2. The system load is not altered.
3. Unavailability state convolutions between wind plants and other generators are taken into account.
4. Wind/load correlation, if present and significant, can be addressed.
5. Statistical dependence of wind plants can be addressed by aggregating correlated wind plants as one multi-state unit.

Using the multi-state representation, the next section shows how a wind plant can contribute to the generation adequacy of a power system. Furthermore, the impact of increasing wind plant penetration is evaluated and compared to the impact of capacity and energy equivalent conventional units. The study presented in this section refers to [20].

3.2 Case Study: Wind Plant Contribution to Planning Generation Adequacy

In this case study, the impact of wind plants on generation adequacy is studied through the loss-of-load expectation. Using the multi-state representation, wind plants of increasing penetration are integrated in the loss-of-load calculations. As expected with the addition of any other units of generation, the addition of wind generation increases the reliability of a power system. However, the extent to which the reliability increases varies as a function of the wind plant's penetration level. It is shown that at low wind plant penetration levels less than 5%, the reliability impact of the wind plant is comparable

to the impact of an energy equivalent conventional unit. However, for wind plant penetration levels greater than 5%, the wind plant is less efficient in reducing the LOLE than its energy equivalent unit.

We apply the LOLE under the assumptions that wind plants are integrated with the multi-state representation approach described in Section 3.1.1 and that wind/load correlation is insignificant, allowing us to use one multi-state representation for the whole year. Given this simplifying assumption, numerical results are only qualitative but the resulting trends relating the LOLE reduction to the generating unit penetration levels are representative regardless of it.

3.2.1 Generation System Reliability Model

Inspired by a realistic power system, a base case scenario involving a 2,728-MW total nameplate capacity system was created, from which we derive our subsequent analysis. This system is composed of 16 generating units ranging from 20-MW to 555-MW in nameplate capacity. All units are represented with a two-state model, which entails neglecting possible derated states. Although peaking and cycling unit unavailabilities are better represented by the four-state Markov model presented in Section 2.2.1.2, for the scope of this analysis, the two-state Markov model or forced outage rate (FOR) is used to represent all unit unavailabilities. The NERC Generating Availability Data System [37] provides relevant FOR values by generation type and size. Table 3.2 presents the units composing the base case system with their respective

FOR¹.

Table 3.2 Generating units for the 2,728-MW base case power system

Size [MW]	# of units	Description in GADS	FOR
22	1	Gas Primary; 001-099MW	0.0778
50	2	Gas Primary; 001-099MW	0.0778
102	6	Gas Primary; 100-199MW	0.0657
135	1	Gas Primary; 100-199MW	0.0657
171	1	Coal Primary; 100-199MW	0.0437
188	1	Coal Primary; 100-199MW	0.0437
195	2	Gas Primary; 100-199MW	0.0657
555	2	Coal Primary; 400-599MW	0.0522

Using (2.1), the cumulative probability of all possible capacity outage states are computed to form the COPT of the base case power system. The complete COPT consists of 1,721 possible capacity outage states.

3.2.2 Wind Plant Multi-State Representation

Three consecutive years of 1 minute resolution power output data from an actual 113-MW wind plant were used in this analysis. In order to evaluate the reliability impact of a wind plant with increasing penetration, the data was scaled by using this simple equation:

$$p_c(t) = \frac{p_{113}(t) \times C_w}{113} \quad (3.7)$$

¹From GADS 1998-2002.

where C_w is the desired nameplate capacity in megawatts of the scaled wind plant. The variables $p_{113}(t)$ and $p_c(t)$ are the power time-series in megawatts at time t in minutes for the original 113-MW wind plant and the scaled wind plant respectively. In this study, the wind plant's penetration is defined as a capacity penetration,² or in other words, it is expressed as a percentage of the power system's total nameplate capacity. Therefore, if the wind plant is 10-MW and the power system capacity is 100-MW, then the wind plant penetration level will be $10/100 \times 100\%$ or 10%. The wind plant penetration levels in this study are kept under 20% to obtain more realistic scenarios. A wind plant with a 20% penetration level could in reality represent an aggregate of smaller wind plants subject to the same wind regime in geographical proximity one with the other.

3.2.3 Load Model

In this study, time-series of hourly load data over a year is used in the LOLE calculations. If periods of wind/load correlation were present and significant, corresponding wind plant multi-state representation and load data should be used in the LOLE calculation. However, we are leaving out the wind/load correlation in this study. Nevertheless, some load chronological

²Since only one wind plant is under study at a time, the *wind plant penetration* is used and defined as the wind plant's nameplate capacity over the total capacity of the system. On the other hand, the concept of *wind generation penetration* can be defined in two ways: the capacity penetration and the energy penetration. The *wind capacity penetration* is the total wind generation nameplate capacity over the total capacity of the system. The *wind energy penetration* is usually defined as the yearly wind energy produced over the yearly energy demand. In this dissertation, penetration is always defined as a capacity penetration.

information is kept by computing monthly LOLE results indicating riskier periods. The load data used in this case study represents a summer peaking system.

3.2.4 Analytical Approach

The yearly LOLE of the power system will be computed using a variant of (2.5) so as to also compute monthly LOLE values:

$$LOLE = \left[\sum_{Jan,i=1}^{744} P_i(X > C_{s,i} - L_i) + \dots + \sum_{Dec,i=1}^{744} P_i(X > C_{s,i} - L_i) \right] \times \frac{hours}{year} \quad (3.8)$$

where only one COPT is used, leaving out of consideration any unit maintenance or variation in the wind plant multi-state representation. First, in order to evaluate the impact of a wind plant on the LOLE of a power system, a base case scenario is created by using the conventional units presented in Table 3.2. Secondly, scenarios for wind plant penetration of 2%, 5%, 10%, 15% and 20% are represented. A multi-state representation is therefore created using the scaled data from Section 3.2.2 and (3.1), resulting in corresponding wind plants with nameplate capacities of 55-MW, 135-MW, 270-MW, 410-MW, 545-MW. Each wind plant is added separately to the base case scenario and the LOLE is computed with (3.8). The wind plants are then replaced by conventional units using two approaches. The first approach replaces the wind plant with a conventional unit of equal capacity. The second approach replaces the wind plant with a conventional unit that would deliver the same total amount of energy during the year. The capacity of this *energy equivalent unit* can be determined

by finding the total wind energy supplied during the year in $\text{MW} \times \text{min}/\text{year}$ or $\text{MW} \times \text{hrs}/\text{year}$ divided by 525,600 min/year or 8,760 hrs/year. Since three years of wind data was used in our study, an average value was used to find the energy equivalent conventional unit. The resultant capacities of the energy equivalent units for each wind plant penetration level can be found in the following table.

Table 3.3 Wind plants' energy equivalent conventional units

Wind plant Nameplate cap. [MW]	Energy equivalent Conventional unit cap. [MW]
55	18
135	45
270	90
410	137
545	182

The conventional units in Table 3.3 were modeled as two-state coal generating units with corresponding FOR from NERC GADS [37]. Four scenarios were thus studied, as follows:

1. Base case scenario: Compute the LOLE of the 2,728-MW power system
2. Second scenario: Compute the LOLE of the 2,728-MW power system with the addition of a wind plant at the specified penetration levels: 55-MW (2%), 135-MW (5%), 210-MW (10%), 410-MW (15%) and 545-MW (20%).

3. Third scenario: Compute the LOLE of the 2,728-MW power system with the capacity equivalent conventional units: 55-MW, 135-MW, 270-MW, 410-MW and 545-MW.
4. Fourth scenario: Compute the LOLE of the 2,728-MW power system with the energy equivalent conventional units: 18-MW, 45-MW, 90-MW, 137-MW and 182-MW.

All LOLE calculations are performed with the same load model. The results from these scenarios are presented and discussed in the following section.

3.2.5 Case Study Results and Discussion

3.2.5.1 Base Case Scenario Results

Monthly and yearly LOLE values were computed for the 2,728-MW power system. The monthly LOLE values shown in Figure 3.1 amounted to an yearly LOLE of 2.40 hours per year³. This base case scenario includes no wind generation. Figure 3.1 demonstrates that loss-of-load events are more likely to occur during the summer months when demand peaks. The results of this base case scenario will be used as a basis for comparison in evaluating the wind plants' reliability impact.

³The load demand data was adjusted to achieve this yearly LOLE.

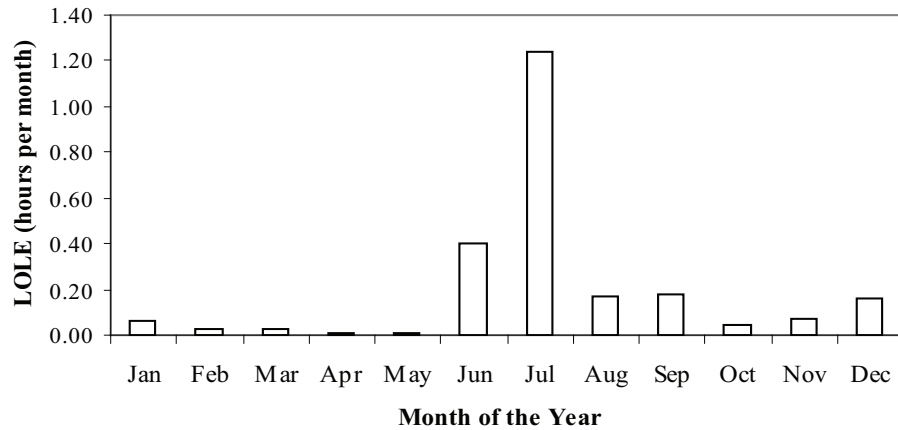


Figure 3.1 Monthly LOLE: Base case scenario

3.2.5.2 Comparing LOLE Results

Figures 3.2, 3.3 and 3.4 illustrate the monthly LOLE results obtained from these case studies, showing how the added generation reduces the monthly LOLE of the base case scenario. In all cases, the added generation contributed to significantly reduce the summer months' LOLE while slightly improving the values during the rest of the year. As their higher availability would lead one to expect, the conventional units reduce the LOLE to a greater extent. Figure 3.3 gives a quantitative view of how wind generation is compared here to conventional generation on a capacity basis. Figure 3.4 suggests a better way of comparing wind generation to conventional generation by using an energy comparative basis.

The yearly LOLE values of each case study are presented in figure

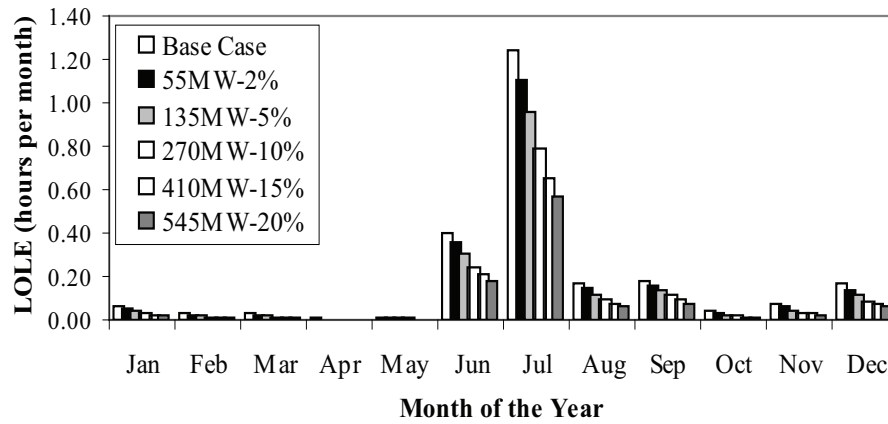


Figure 3.2 Monthly LOLE: Wind plants of various penetration levels

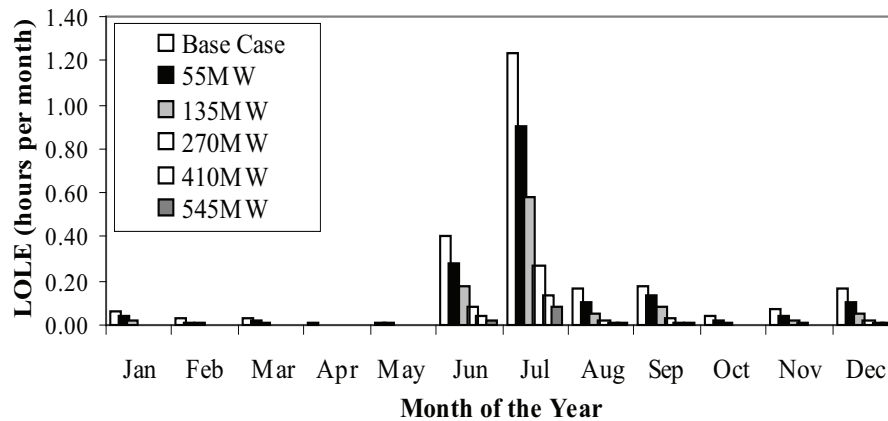


Figure 3.3 Monthly LOLE: Capacity equivalent conventional units

3.5. As previously mentioned, the results from the equivalent capacity units only give a quantitative view of how wind plants compare to conventional generating units of the same capacity, while a better metric of comparison,

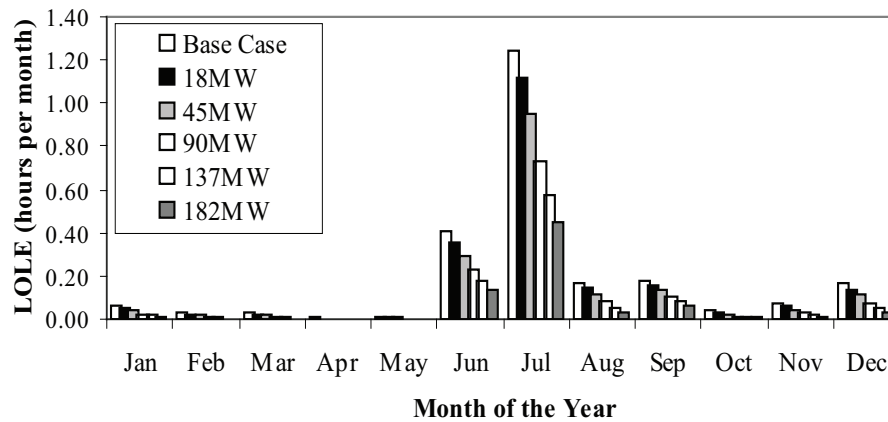


Figure 3.4 Monthly LOLE: Energy equivalent conventional units

energy equivalence, shows how the wind plants should be treated in relation to conventional generating units. In fact, the energy comparative basis is analogous to comparing the LOLE impact of a “natural” wind plant to the impact of a “steadied” wind plant producing the same amount of yearly energy.

At wind penetration levels of less than 5%, the reliability impact of the wind plants is comparable to an energy equivalent conventional unit. However, for penetration level greater than 5%, the wind plant is less efficient at reducing the LOLE, with the deficit ranging from 8% for the 10% penetration level to 28% for the 20% penetration level. Figure 3.5 appears to indicate that the percent difference will progressively increase with increasing wind plant penetration level higher than 20%. This figure also indicates that the LOLE eventually levels off so that at some point a bigger unit or more generation

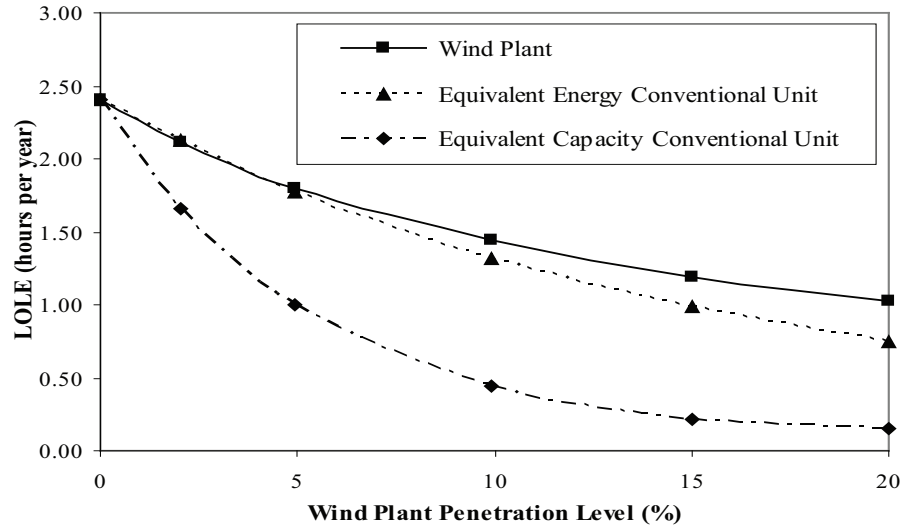


Figure 3.5 Yearly LOLE of wind plants, equivalent energy conventional units and equivalent capacity conventional units

wouldn't have much effect on reducing the LOLE further. It is important to notice that this effect is present for both wind plant and conventional units and is essentially due to the nature of the highly non-linear LOLE calculations. This point will be important when quantifying the capacity contribution of wind plant in the following chapter.

3.3 Concluding Remarks

In this chapter, we have provided a detailed description of how to integrate wind plants in loss-of-load calculations. The multi-state representation was applied to a case study to highlight the reliability contribution of wind

plants in comparison to conventional units equivalents. Methods of quantifying this reliability contributions will be presented in the following chapter.

Chapter 4

Effective Load Carrying Capability of a Wind Plant

As investigated in Chapter 3, wind plants can contribute to a power system's reliability by providing additional installed capacity and reducing the loss-of-load expectation metric. Efforts to quantify the capacity contribution of wind plants have been made through the application of various risk-based and time-period-based methods [10–12]. Several studies have promoted the effective load carrying capability (ELCC) as the most dependable metric for quantifying the reliability contribution of a wind plant [10–14, 16, 21, 38, 41]. While ELCC is certainly a thorough method based on standard probabilistic criteria, it also requires substantial reliability modeling and an iterative process that can be computationally intensive. Consequently, simpler approximations have been proposed to estimate a wind plant's ELCC using capacity factor and Garver's approximation [11, 12]. These simpler methods can be especially useful when performing a preliminary investigation of wind generation expansion in system planning studies.

A description of the ELCC concept will be presented at the outset of this chapter, followed by the illustration of the various ways it can be imple-

mented in evaluating a wind plant’s capacity contribution. To counter the concept’s inherent computational setbacks, a novel non-iterative approximation will be proposed and applied to various case studies [22, 23]. To evaluate the accuracy of the proposed approximation, we will contrast these estimates to both conventionally computed ELCC values and to the wind plant’s capacity factor.

4.1 ELCC Concept Overview

From a generation expansion perspective, when a new generating unit is to be added to an existing power system, the effective load carrying capability (ELCC) of this unit is equivalent to the amount of extra load that can be served by the system while maintaining the designated level of reliability. This designated level is usually characterized by the loss-of-load expectation (LOLE) of the system before the addition of the new generating unit. We make the preliminary assumption that the existing system is already well-planned and exhibits an acceptable LOLE relative to the system’s typical load demand. Therefore, in equating the LOLEs of the existing (E) and potential (P) systems, the concept of ELCC is classically represented by the following expressions:

$$LOLE_E = LOLE_P$$

$$\sum_{i=1}^n P_i(X_E > C_E - L_i) = \sum_{i=1}^n P_i(X_P > (C_E + C_A) - (L_i + \Delta L)) \quad (4.1)$$

where ΔL^1 is the extra load that can be served by the potential system, L_i is the load condition for the time duration i , n is the total number of time durations in the evaluation period, C_E is the total possible capacity of the existing system and C_A is the maximum possible capacity of the additional unit. $P_i(X_E > C_E - L_i)$ and $P_i(X_P > (C_E + C_A) - (L_i + \Delta L))$ are the loss-of-load probabilities (LOLP) of the existing and potential systems. As described in Chapter 2, these LOLPs represent the probabilities of having a capacity outage greater than $C_E - L_i$ and $(C_E + C_A) - (L_i + \Delta L)$ respectively. The cumulative probabilities $P_i(X_E > x)$ and $P_i(X_P > x)$ are obtained from each system's capacity outage probability table (COPT) and the i subscript is used in case maintenance schedules are considered and generation varies from one time duration to the next. The potential system's COPT includes the additional unit. The LOLE calculations of the potential system are performed by iteratively adding a load increment to all load data points of the typical load time-series until the LOLE meets the existing system's LOLE. Once (4.1) is iteratively solved for ΔL , the ELCC of the additional generator can be expressed as the percentage of the extra load over the added generator's maximum possible capacity:

$$ELCC = \frac{\Delta L}{C_A} \times 100\% \quad . \quad (4.2)$$

When applying the ELCC concept to conventional generation, the gen-

¹In the classical ELCC concept, this extra load is constant throughout the year and therefore, the same amount is added to all hourly loads. In future work, we will consider representing load growth patterns in ELCC calculations [42].

erating unit is modeled by a two-state or multi-state representation and is then integrated in the COPT as *additional generation*. In regards to adding a wind unit, the ELCC concept can be implemented differently depending on the method chosen for integrating the wind plant in the loss-of-load calculations: the multi-state representation of Section 3.1.1 or the negative load adjustment of Section 3.1.2. As we have shown, wind generation can either be handled as generation similarly to conventional generating units or, using a different approach, be handled as negative load. The following section will present the various ELCC implementations for wind generation.

4.2 Classical Computing Method using Multi-State Representation

The first way of implementing ELCC in the context of wind generation is directly in line with the original concept. The wind plants are integrated similarly to conventional generating units by being considered normal generation and being convolved in the COPT of the power system. In this classical computing method, the wind plant under study is modeled with a multi-state representation and integrated in the COPT of the potential power system as described in Section 3.1.1.

$$\sum_{i=1}^n P_i(X_E > C_E - L_i) = \sum_{i=1}^n P_i(X_P > (C_E + C_W) - (L_i + \Delta L)) \quad (4.3)$$

Because of the discrete nature of the COPTs, (4.3) is solved iteratively. Consequently, multiple LOLE calculations are performed with a series of ΔL increments until the potential system's LOLE reaches the existing system's target

LOLE. Naturally, this iterative process can turn out to be computationally-intensive. Essentially, when a wind plant of maximum capacity C_W is integrated as generation, the ELCC calculations are performed following this sequence of steps:

1. Build the existing system's COPT as described in Section 2.1.1, excluding the wind plant under study.
2. Compute the existing system's LOLE (or target LOLE) using the typical hourly load time-series for the chosen evaluation period.

$$LOLE_E = LOLE_{target} = \sum_{i=1}^n P(X_E > C_E - L_i)$$

3. Build the wind plant's multi-state representation as described in Section 3.1.1, using hourly wind data of the chosen evaluation period.
4. Build the potential system's COPT by including the wind plant's reliability model, as described in Section 2.1.1 .
5. Repeat LOLE calculations by iteratively increasing the typical hourly load time-series by adding an incremental constant ΔL to all load data points until the target LOLE is reached.

$$LOLE_P = \sum_{i=1}^n P(X_P > (C_E + C_W) - (L_i + \Delta L)) = LOLE_{target}$$

6. Express the ELCC as a percentage.

$$ELCC = \frac{\Delta L}{C_W} \times 100\% \quad (4.4)$$

4.3 Classical Computing Method using Negative Load Adjustment

When using the negative load adjustment approach to integrate a wind plant in LOLE calculations, the ELCC concept is no longer standardly implemented by adding the unit as positive generation; instead the additional unit is integrated as *negative load*. In this case, ELCC calculations are performed using a different approach summarized in these six steps:

1. Build the existing system's COPT as described in Section 2.1.1, excluding the wind plant under study.
2. Compute the existing system's LOLE (or target LOLE) using the typical hourly load time-series for the chosen evaluation period.

$$LOLE_E = LOLE_{target} = \sum_{i=1}^n P(X_E > C_E - L_i)$$

3. Subtract the wind plant's hourly power output time-series from the typical hourly load time-series, obtaining the net load time-series.
4. Compute LOLE with the existing system's COPT and the *reduced* load time-series.

$$LOLE_{wind} = \sum_{i=1}^n P(X_E > C_E - (L_i - W_i))$$

5. Repeat LOLE calculations using the typical load time-series and the potential system's COPT (including a benchmark unit of incremental

capacity C_B) until the $LOLE_{benchmark}$ is reduced to $LOLE_{wind}$.

$$LOLE_{benchmark} = \sum_{i=1}^n P(X_E > (C_E + C_B) - L_i) = LOLE_{wind}$$

6. Express the wind plant's ELCC as

$$ELCC = \frac{C_B}{C_W} \times 100\% .$$

Variants of these steps are also possible. For example, instead of adding a benchmark unit, an existing unit of increasing capacity could be removed from the COPT until the LOLE, computed with the reduced load time-series, meets the target LOLE. Another alternate approach would be to increase the net load time-series with a constant load increment until the LOLE meets the target LOLE. In this case, the ELCC would be expressed as the resulting load increment over the wind plant's nameplate capacity. In the first two negative load approaches, some subjectivity takes part in the calculations, whether it's by choosing the existing unit to remove or by defining the benchmark unit to add. Again, as explained in Chapter 3 for LOLE calculations, several years of time-synchronized load and wind power output time-series are necessary for applying this method.

4.4 Discussion on Computing Methods

Since time-synchronized wind power output and load demand time-series are not readily available, the multi-state representation will be used in this dissertation for integrating wind plants in ELCC calculations. When used

in the context of ELCC, the multi-state representation implements the metric directly in line with the original concept and treats the wind generation in the same manner as conventional generation. A wind plant is therefore integrated in terms of what it is: generation. When actual time-synchronized load and wind power output time-series become more readily available, it would be interesting to compare ELCC results obtained from all wind integration approaches.

Regardless of the integration method applied, period-specific ELCC values should be computed to capture the interannual and/or diurnal variability of a wind plant's output and also consider the possible wind/load correlation. Furthermore, when a new wind plant is added in proximity to other wind plants, their statistical dependence can be addressed. This consideration is inherently handled in the negative load adjustment approach, however in the case of the multi-state representation, as it was also described for LOLE calculations, all wind plants which display a significant cross-correlation must be aggregated into one multi-state unit. The ELCC merely has to be recalculated for the new aggregated multi-state unit, which makes the resulting value representative of the multiple wind plants. In this case, the calculations described in Section 4.2 are adjusted to account for the statistically-dependent wind plants. For example, if wind plant B is the new unit under study but it is located in close proximity to an already existing wind plant A, then a new ELCC must be calculated for the aggregated wind plant A+B. Since wind plant A must be removed from the existing system, the typical load time-series used in the first

LOLE calculation must also be recalibrated to ensure that the target LOLE is met.

Unfortunately, conventional ELCC calculations demand substantial reliability modeling and require a computationally-intensive iterative process. Hence, different methods have been proposed to estimate a wind plant's ELCC or capacity contribution [10–14]. A novel non-iterative ELCC approximation was introduced in [22] and is presented in the following section.

4.5 Non-Iterative ELCC Approximation

Various risk-based and time-period-based approximations have been proposed to estimate a wind plant's ELCC or capacity value [10–14]. Among the risk-based methods is Garver's approximation, a graphical method of estimating the ELCC of conventional generating units [43]. This approximation was mathematically derived using a two-state representation to model the additional unit. Although modeling a generating unit as being either fully on or fully off is appropriate for conventional generation, it is not well suited for variable-output generation. Therefore, the novel method presented in this section is adapted from Garver's approximation, but models the additional unit with a multi-state representation [22]. As for Garver's approximation, the proposed method uses a graphically-determined parameter and is based on the probabilistic metrics presented in Chapter 2, such as capacity outage probability table (COPT), loss-of-load probability (LOLP), and loss-of load expectation (LOLE).

4.5.1 Basis

Garver's approach proposes a way of simplifying ELCC calculations for conventional generation [43]. Indeed, the ELCC of an additional conventional unit was approximated using graphical aids and a graphically-determined parameter. This parameter characterized the existing system's loss-of-load expectation² as a function of its reserve; used along with an estimating function, it significantly reduced the amount of reliability modeling and LOLE calculations required. Although the approximation focused on the graphical aids, the most interesting aspect about Garver's method was the mathematically-derived function used to create these graphs: from a simple equation one could obtain an accurate ELCC estimate. The derivation of the estimating function was based on well-known probability concepts. Unfortunately, the function modeled the additional unit with a two-state representation, which, as we noted above, may be appropriate for conventional generation, but fails to adequately represent wind generation. Therefore, an ELCC estimating function was developed for variable-output generation using a more appropriate multi-state representation. The derived function, like Garver's expression, is based on well-known probability concepts and uses the additional unit's reliability characteristics as well as a graphically-determined parameter. This parameter characterizes the existing system's loss-of-load probability as a function of load demand. Consequently, the first step to the proposed approximation consists

²L. L. Garver interchanges the terms LOLE and LOLP in his publication but LOLE is the actual calculation performed.

of determining the graphical parameter.

4.5.2 Graphical Parameter of the Existing Power System

The graphical parameter is obtained from a plot that illustrates how the existing system's LOLE changes in response to an increase or decrease in load demand ³. Given a chosen evaluation period, different load data time-series are created as variants of the system's typical load demand by positively or negatively shifting the typical load data time-series. Consequently, each new curve has the same overall variability as the typical load data time-series (e.g. given an evaluation period of a year, each load data time-series will display the summer and winter peaks). The shift is chosen as a percentage of the typical peak load. Each load data time-series is computed using the following expression:

$$L_c = L_t \pm c \times L_{t_{pk}} \quad (4.5)$$

where L_c is a new load data time-series, L_t is the typical load data time-series with peak load $L_{t_{pk}}$ and c is a percentage. The existing system's LOLE is then computed for each new load demand. Subsequently, the resulting LOLE values are plotted as a function of both the typical and the new load data time-series. In this graph, all load data time-series are represented by their peak load, although the actual LOLE calculations are performed using the whole curves. Once these results are plotted, the data points are curve-fitted

³Load growth patterns are not yet considered in these calculation but will be part of our future research [?].

with an exponential relationship.⁴ The relationship is characterized by the following equation:

$$LOLE_{L_{pk}} = B \times e^{m \times L_{pk}} \quad (4.6)$$

where L_{pk} is the peak load of the load time-series B is the pre-exponential coefficient and m is the system's graphical parameter with units of MW^{-1} . The value of the m parameter is determined by using the exponential curve-fitting method. As the subsequent mathematical derivation will show, the B parameter becomes inconsequential in the analysis. Along with the basic probability concepts of generation adequacy presented in Chapter 2, the exponential relationship will be used to mathematically derive an ELCC estimating function for variable-output generation. The steps of this derivation are presented in the next section.

4.5.3 Mathematical Derivation of the Estimating Function

Just as we saw in (2.2) presented in Chapter 2, when an additional variable-output generator is modeled as a multi-state unit, the cumulative probabilities of the potential system after the addition of the unit $P(X_P > x)$ can be computed by:

$$P(X_P > x) = \sum_{j=1}^k p_j \times P(X_E > x - C_j) \quad (4.7)$$

⁴Garver suggested that an exponential relationship could accurately approximate how a power system's LOLE responds to a shift in load demand [43].

where $P(X_E > x - C_j)$ represents the existing system's cumulative probability of having a capacity outage greater than $(x - C_j)$. This cumulative probability can be obtained from the COPT of the existing system. Given a chosen evaluation period and corresponding load data time-series identified by its peak load L_{pk} , the LOLE of the potential system can be expressed as

$$LOLE_{P, L_{pk}} = \sum_{i=1}^n P(X_P > C_P - L_i) \quad (4.8)$$

where $P(X_P > C_P - L_i)$ ⁵ is the LOLP for the load condition L_i of time duration i and n is the number of time durations in the chosen evaluation period. Since, the term $P(X_P > C_P - L_i)$ in (4.8) is equivalent to the term $P(X_P > x)$ in (4.7) when x equals to $C_P - L_i$, it can be replaced by

$$P(X_P > C_P - L_i) = \sum_{j=1}^k p_j \times P(X_E > C_P - L_i - C_j) \quad . \quad (4.9)$$

This substitution enables the LOLE of the potential system to be expressed as a function of the existent system's COPT rather than having to be calculated in terms of its own COPT. Expanding the summation term in (4.9) and substituting in (4.8), $LOLE_{P, L_{pk}}$ becomes

$$LOLE_{P, L_{pk}} = \sum_{i=1}^n \left[p_1 \times P(X_E > C_P - L_i - C_1) \right. \\ \left. + p_2 \times P(X_E > C_P - L_i - C_2) + \dots \right. \\ \left. + p_k \times P(X_E > C_P - L_i - C_k) \right] \quad . \quad (4.10)$$

⁵The subscript i is omitted in $P_i(X > x)$ to make equations easier to read.

The total capacity of the potential system C_P is equivalent to the total capacity of the existing system C_E plus the maximum possible capacity of the added unit C_A . Consequently, (4.10) can be rewritten as

$$LOLE_{P,L_{pk}} = \sum_{i=1}^n \left[p_1 \times P(X_E > C_E + C_A - L_i - C_1) \right. \\ \left. + p_2 \times P(X_E > C_E + C_A - L_i - C_2) + \dots \right. \\ \left. + p_k \times P(X_E > C_E + C_A - L_i - C_k) \right] . \quad (4.11)$$

By rearranging and distributing the summation, (4.11) becomes

$$LOLE_{P,L_{pk}} = p_1 \times \sum_{i=1}^n [P(X_E > C_E - (L_i + C_1 - C_A))] \\ + p_2 \times \sum_{i=1}^n [P(X_E > C_E - (L_i + C_2 - C_A))] + \dots \\ + p_k \times \sum_{i=1}^n [P(X_E > C_E - (L_i + C_k - C_A))] . \quad (4.12)$$

Each one of the k summation terms in (4.12) is equivalent to the existing system's LOLE computed for a load data time-series with a peak load value of $L_{pk} + C_j - C_A$. In turn, each of these k load data time-series is equivalent to a load time-series of peak load L_{pk} , which is shifted by adding a constant $C_j - C_A$. Note that this constant is added to each hourly load data L_i . From this observation, (4.12) is rewritten as

$$LOLE_{P,L_{pk}} = p_1 \times LOLE_{E,L_{pk}+C_1-C_A} + p_2 \times LOLE_{E,L_{pk}+C_2-C_A} + \\ \dots + p_k \times LOLE_{E,L_{pk}+C_k-C_A} . \quad (4.13)$$

Because of the shifted change in the load data time-series, each $LOLE_{L_{pk}+C_j-C_A}$ term in (4.13) can be replaced by its respective exponential approximation using (4.6) and the equation becomes

$$LOLE_{P,L_{pk}} = p_1 \times B \times e^{m \times (L_{pk} + C_1 - C_A)} + p_2 \times B \times e^{m \times (L_{pk} + C_2 - C_A)} + \dots + p_k \times B \times e^{m \times (L_{pk} + C_k - C_A)} \quad . \quad (4.14)$$

Using exponential identities, $B \times e^{m \times L_{pk}}$ is isolated and replaced by (4.6) so that (4.14) can be rewritten as

$$LOLE_{P,L_{pk}} = LOLE_{E,L_{pk}} \times [p_1 \times e^{m \times (C_1 - C_A)} + p_2 \times e^{m \times (C_2 - C_A)} + \dots + p_k \times e^{m \times (C_k - C_A)}] \quad . \quad (4.15)$$

The concept of ELCC described previously now comes into play. Recall that the ELCC of an additional generator represents the extra load that can be served while keeping the designated level of reliability, usually the LOLE of the existing system calculated with its typical load data time-series. Therefore, the ELCC concept can be expressed as

$$LOLE_{P,L_{t_{pk}} + \Delta L} = LOLE_{E,L_{t_{pk}}} \quad (4.16)$$

where $L_{t_{pk}} + \Delta L$ is the typical load data time-series to which is added a constant extra load ΔL to each hourly load data. This can be seen as the typical load data time-series that has simply been positively shifted by ΔL . Contracting the $p_j \times e^{m \times (C_j - C_A)}$ terms and replacing the general load data time-series L_{pk} by the specific load data time-series $L_{t_{pk}} + \Delta L$, (4.15) is rewritten as

$$LOLE_{P,L_{t_{pk}} + \Delta L} = LOLE_{E,L_{t_{pk}} + \Delta L} \times \sum_{j=1}^k p_j \times e^{m \times (C_j - C_A)} \quad . \quad (4.17)$$

Using (4.6), (4.17) becomes

$$LOLE_{P,L_{t_{pk}}+\Delta L} = B \times e^{m \times (L_{t_{pk}} + \Delta L)} \times \sum_{j=1}^k p_j \times e^{m \times (C_j - C_A)} . \quad (4.18)$$

Once again, using exponential identities, (4.18) is rearranged as

$$LOLE_{P,L_{t_{pk}}+\Delta L} = B \times e^{m \times L_{t_{pk}}} \times e^{m \times \Delta L} \times \sum_{j=1}^k p_j \times e^{m \times (C_j - C_A)} , \quad (4.19)$$

which finally reduces to

$$LOLE_{P,L_{t_{pk}}+\Delta L} = LOLE_{E,L_{t_{pk}}} \times e^{m \times \Delta L} \times \sum_{j=1}^k p_j \times e^{m \times (C_j - C_A)} . \quad (4.20)$$

Applying the ELCC concept given by (4.16), (4.20) becomes:

$$1 = e^{m \times \Delta L} \times \sum_{j=1}^k p_j \times e^{m \times (C_j - C_A)} . \quad (4.21)$$

Finally, taking the natural logarithm on both sides of the equation to isolate ΔL , we obtain the ΔL estimating function.

$$\Delta L = \frac{1}{m} \times \left[-\ln \left[\sum_{j=1}^k p_j \times e^{m \times (C_j - C_A)} \right] \right] \quad (4.22)$$

Using (4.2) and (4.22), the ELCC of an additional multi-state unit of maximum possible capacity C_A , modeled by k possible capacity outage states C_j having corresponding individual probability p_j , can now be estimated using the existing power system's m parameter as follows:

$$ELCC = \left[-\ln \left[\sum_{j=1}^k p_j \times e^{m \times (C_j - C_A)} \right] \right] \times \frac{100\%}{m \times C_A} . \quad (4.23)$$

Note that (4.23) can also be used for two-state units. Indeed, for a two-state unit of capacity C_A there exist two possible capacity outage states C_j : fully on or fully off. If the unit's unavailability is represented by its forced outage rate (FOR) then we can replace C_1 by 0, p_1 by $(1 - FOR)$, C_2 by C_A and p_2 by FOR . Equation (4.23) is therefore reduced to

$$ELCC = \left[-\ln[(1 - FOR) \times e^{-m \times C_A} + FOR] \right] \times \frac{100\%}{m \times C_A} . \quad (4.24)$$

This expression is equivalent to Garver's approximation although the m parameter and risk basis are slightly different. One could verify that if a unit is always available and hence has an FOR of 0, the resulting ELCC obtained with(4.24) will be 100%.

The non-iterative approximation developed in this section will be applied to several case studies. The resulting estimates will be compared to ELCC values obtained from the preferred classical computing method. Before performing this comparative analysis, the essential steps of the proposed non-iterative approximation are reviewed in the next section.

4.5.4 Essential Steps of the Non-iterative Approximation

1. Choose the evaluation period (e.g. a year, peak load hours, summer months).
2. Given the chosen evaluation period, gather hourly load data, existing power system generation data and hourly wind power output data. If possible, use multiple years of relevant data.

3. Build the existing system reliability model or COPT as described in Section 2.1.1.
4. Build the wind plant multi-state representation, C_j and p_j values as explained in Section 3.1.1.
5. Determine the existing system graphical parameter, m as described in Section 4.5.2.
6. Use the estimating function in (4.23) with the values of m , C_j and p_j to obtain the wind plant's ELCC estimate.

4.6 Case Studies and Discussion

In this section, the non-iterative approximation is applied in a step-by-step fashion to estimate the capacity contribution of various wind plants. The resultant ELCC estimates are compared with the values obtained from both the preferred classical computing method and the capacity factor approximation. In each case study, an existing power system is considering wind generation expansion and the capacity value of the added wind plant is under study.

In the first case study, the existing power system (System 1) consists of 16 generating units with a 2,728-MW total capacity. Wind plants of the following penetration levels are added separately to the power system: 2%, 5%, 10%, 15% and 20%. Each wind plant is characterized by the same wind

pattern, which allows us to examine the effect of increasing wind plant penetration on the ELCC. Two sources of power output data are used in this case study.

In the second case study, the existing power system (System 2) is represented by the IEEE-RTS system⁶ [34]. System 2 is larger than System 1, both in total generating capacity (3,405-MW) and in number of generators (32 units). In this study, the capacity contribution of a 150-MW wind plant is calculated for three different evaluation periods.

Finally, the IEEE-RTS system and a 234-MW wind plant comprise the last existing power system (System 3) for the third case study. While including some already existing wind generation, this system is considering an additional 114-MW wind plant. Again, period-specific ELCCs are computed for three different evaluation periods. Case Study II and III will be presented and discussed together as they followed the same period-specific approach.

The analysis presented in Case Study I was published in [22] while Case Study II and III were presented in [23]. All LOLE calculations were performed on an hourly basis using (2.5).

4.6.1 Case Study I: ELCC and Wind Plant Penetration

The existing system used in this case study is found in Table 4.1, where it is seen to consist of 16 conventional generating units ranging from 22-MW

⁶Only the generators of the IEEE-RTS system are used, the load model used in the case study is not the IEEE-RTS load model.

to 555-MW, having a total capacity of 2,728-MW. Each generator is modeled with a two-state representation and its unavailability is expressed with the forced outage rate (FOR). The North American Electric Reliability Council “Generating Availability Data System” provided relevant FOR values by generator type and size [37].

Table 4.1 Case Study I: Generating units data of System 1

Size [MW]	# of units	Description in GADS	Unavailability; FOR
22	1	Gas Primary; 001-099MW	0.0778
50	2	Gas Primary; 001-099MW	0.0778
102	6	Gas Primary; 100-199MW	0.0657
135	1	Gas Primary; 100-199MW	0.0657
171	1	Coal Primary; 100-199MW	0.0437
188	1	Coal Primary; 100-199MW	0.0437
195	2	Gas Primary; 100-199MW	0.0657
555	2	Coal Primary; 400-599MW	0.0522

The capacity contribution of five different wind plants is evaluated with our proposed non-iterative approximation. The resultant ELCC estimates are compared to the conventionally calculated ELCC values as well as the capacity factor estimates. Given wind plants with the same wind pattern, plant penetration levels of 2%, 5%, 10%, 15% and 20% are considered. In accordance with the steps summarized in Section 4.5.4, the analysis is performed as follows.

4.6.1.1 Choosing the Evaluation Period

A typical load data time-series consisting of a full year of hourly load data points was used in the analysis. This load demand displays the usual summer and winter peaks, with an annual peak load of 1,963-MW. Using this load demand, a LOLE of 2.4 hours per year⁷ is computed for the existing power system. The wind/load correlation is not considered in this case study since the focus here is on the effect of the wind plant penetration level on ELCC.

4.6.1.2 Building the Wind Plant's Reliability Model

The additional wind plant is modeled with the multi-state representation as described in Section 3.1.1. For optimum results, multiple years of power output data from the relevant evaluation period, if available, should be used to build the multi-state representation of the studied wind plant. However, in this case study, only a full year of power output data from two different wind plants was available: WP-1 of 113-MW and WP-2 of 230-MW. In this case study, we want to demonstrate how the ELCC of a wind plant varies as its penetration level increases. To this end, various wind plant penetration levels were obtained by simply scaling the actual power output data. The following equation was used

$$p_{C_w}(t) = \frac{p_{C_o}(t) \times C_w}{C_o} \quad (4.25)$$

⁷The load demand was adjusted to obtain this LOLE.

where C_w is the desired total capacity in MW of the scaled wind plant (i.e. the eventual additional wind plant), $p_{C_o}(t)$ is the power output in MW at time t of the original wind plant (WP-1 or WP-2) of capacity C_o (113-MW or 230-MW), and $p_{C_w}(t)$ is the power output in MW at time t of the scaled wind plant. In this study, the wind plant penetration level is defined as the wind plant's capacity over the existing power system's total capacity in terms of percentage. Therefore, if the added wind plant is 10-MW and the existing power system's total capacity is 100-MW, the wind plant penetration level will be $[10 \div 100] \times 100\%$ or 10%. The levels studied are 2% (55-MW), 5% (135-MW), 10% (270-MW), 15% (410-MW) and 20% (545-MW). These levels were created using both wind data sets. This resulted in two 55-MW wind plants, two 135-MW wind plants, two 270-MW wind plant and so on. In other words, in each pair, one is created from the WP-1 data and the other is created from the WP-2 data. A multi-state representation is built for each of these 10 wind plants as described in Section 3.1.1 with a resolution of 1-MW. For example, Table 4.2 presents part of the multi-state representation for a 55-MW wind plant using the power output data of WP-1. For this wind plant, a capacity outage state C_3 of 3-MW has a probability p_3 of 0.00011416, while the probability of having all capacity on outage $C_w=C_{55}=55$ -MW is $p_{55} = 0.125$.

As explained in Section 3.1.3.1, although the evaluation period is chosen to be a full year in this case study, the interannual and/or diurnal variability of wind generation along with the possible wind/load correlation could be captured by adjusting the multi-state representation in the calculations. For

Table 4.2 Case Study I: Multi-state representation of a 55-MW wind plant using WP-1 power output data and a resolution of 1-MW

Capacity outage state C_j [MW]	Individual probability p_j
0	0
1	0
2	0
3	0.00011416
4	0.0054795
5	0.010388
6	0.013128
...	...
50	0.02911
51	0.030023
52	0.028881
53	0.032763
54	0.040868
55	0.125

example, a monthly or peak load representation could be constructed with the relevant power output data. Then, using the corresponding load data, monthly or peak load ELCC or ELCC estimates could be obtained. Such period-specific ELCCs will be investigated in the next case studies.

4.6.1.3 Building the COPT of System 1

After having established the data of the generators from Table 4.1, we use it as our base for building our existing system's COPT by means

of the recursive algorithm presented in Section 2.1.1. The resulting COPT consists of 1,721 possible capacity outage states. When classically computing a wind plant's ELCC, the multi-state representation presented in Table 4.2 would be convolved with the existing system's COPT using (2.2) to create the potential system's COPT. Table 4.3 represents part of the potential system's COPT when a 55-MW wind plant is added to System 1. The COPT of the potential system would be built on similar lines for the other nine wind plants under study. However, when using the non-iterative approximation, one must determine the m parameter instead of trying to compute the potential system's COPT. The same m parameter is used to evaluate all 10 wind plants under study.

4.6.1.4 Determining the m parameter of System 1

The existing power system's m parameter is determined graphically as described in Section 4.5.2. Using (4.5), various new load data time-series are created with shifting percentages of -20%, -17.5%, -15%, ...0%, +2.5%, ...+20%. The existent power system's LOLE is computed for the typical curve and then for the 16 new load data time-series. Table 4.4 presents the resultant LOLE values with their associated load data time-series.

Although the peak load $L_{C_{pk}}$ is used to represent the load data time-series L_c , the LOLE calculations are performed using all the relevant hourly load data points, not just the peak load. Again, the relevant load data is determined by the chosen an evaluation period; in this case study, it is a

full year. The results from Table 4.4 are graphed to obtain a relationship approximating the LOLE as a function of a shifted increase or decrease in the typical load demand. Figure 4.1 illustrates this relationship between the existing system's LOLE and each curve's annual peak load.

Using an exponential curve fitting tool on Fig. 4.1, a relationship is established which attributes a value of $7.30788 \times 10^{-03} \text{ MW}^{-1}$ to the m parameter:

$$LOLE_{L_{pk}} = B \times e^{7.30788 \times 10^{-03} \times L_{pk}} \quad . \quad (4.26)$$

Table 4.3 Case Study I: COPT for a 2,783-MW power system including a 55-MW wind plant using WP-1 power output data

Capacity outage state x [MW]	Cumulative probability $P(X_P > x)$
0	1
1	1
2	1
3	1
4	0.99996
5	0.99804
...	...
201	0.34358
202	0.34159
...	...
2781	1.1101×10^{-20}
2782	9.2703×10^{-21}
2783	6.9862×10^{-21}

Table 4.4 Case Study I: System 1's LOLE for various load data time-series

Load data time-series $L_c = L_t \pm c \times L_{t_{pk}}$ [MW]	Annual peak load $L_{C_{pk}}$ [MW]	LOLE [hrs per year]
$L_t - 20\% \times L_{t_{pk}}$	1570	0.1169
$L_t - 17.5\% \times L_{t_{pk}}$	1619	0.1839
$L_t - 15\% \times L_{t_{pk}}$	1668	0.2785
$L_t - 12.5\% \times L_{t_{pk}}$	1718	0.4226
$L_t - 10\% \times L_{t_{pk}}$	1767	0.6086
$L_t - 7.5\% \times L_{t_{pk}}$	1816	0.8546
$L_t - 5\% \times L_{t_{pk}}$	1865	1.2072
$L_t - 2.5\% \times L_{t_{pk}}$	1914	1.6996
L_t , Typical Load Data	1963	2.4000
$L_t + 2.5\% \times L_{t_{pk}}$	2012	3.4413
$L_t + 5\% \times L_{t_{pk}}$	2061	5.0314
$L_t + 7.5\% \times L_{t_{pk}}$	2110	7.2852
$L_t + 10\% \times L_{t_{pk}}$	2159	10.4796
$L_t + 12.5\% \times L_{t_{pk}}$	2208	14.7912
$L_t + 15\% \times L_{t_{pk}}$	2257	20.7699
$L_t + 17.5\% \times L_{t_{pk}}$	2306	28.0748
$L_t + 20\% \times L_{t_{pk}}$	2356	37.1675

Once the existing system's m parameter is determined, (4.23) can be applied to estimate the ELCC of the 10 different wind plants, in accordance with their respective multi-state representation (C_j and p_j values).

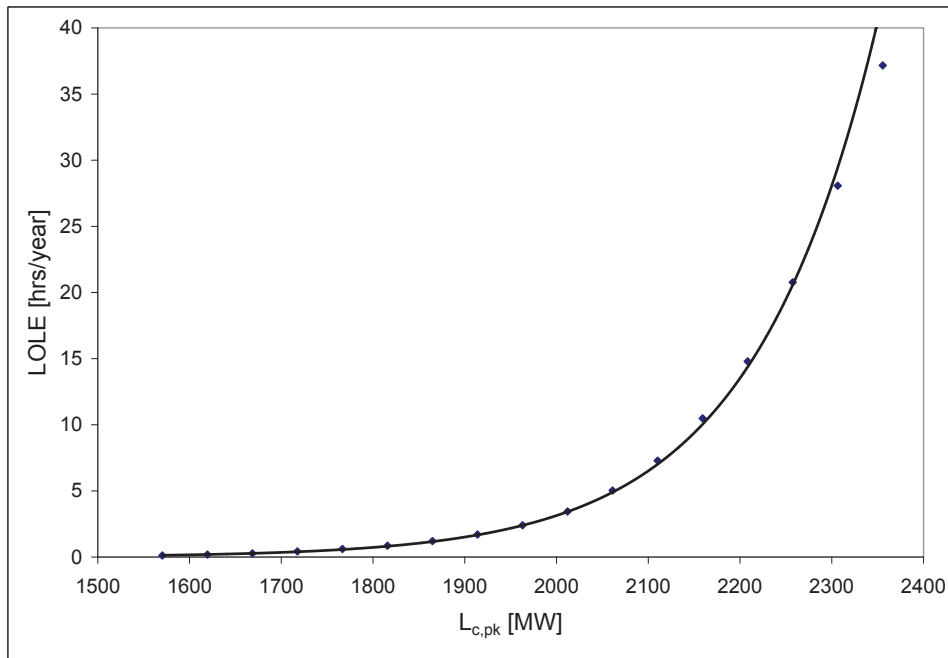


Figure 4.1 Case Study I: Exponential relationship between the existing system’s LOLE and a shifted increase or decrease in the typical load demand.

4.6.1.5 Results

The resulting ELCC estimates are then compared to the classically calculated ELCC values. As explained in Section 3.1.1, the classical ELCC computing method is applied by building a COPT for each of the 10 potential power systems, using (2.2). Next, by an iterative process, (4.3) is solved for ΔL using the typical load demand for all LOLE calculations. When the ΔL value of each wind plant is found, (4.4) is used to compute the actual ELCC value. All the ELCC results are illustrated in Figure 4.2, where the wind plant’s capacity factor is also included for comparison.

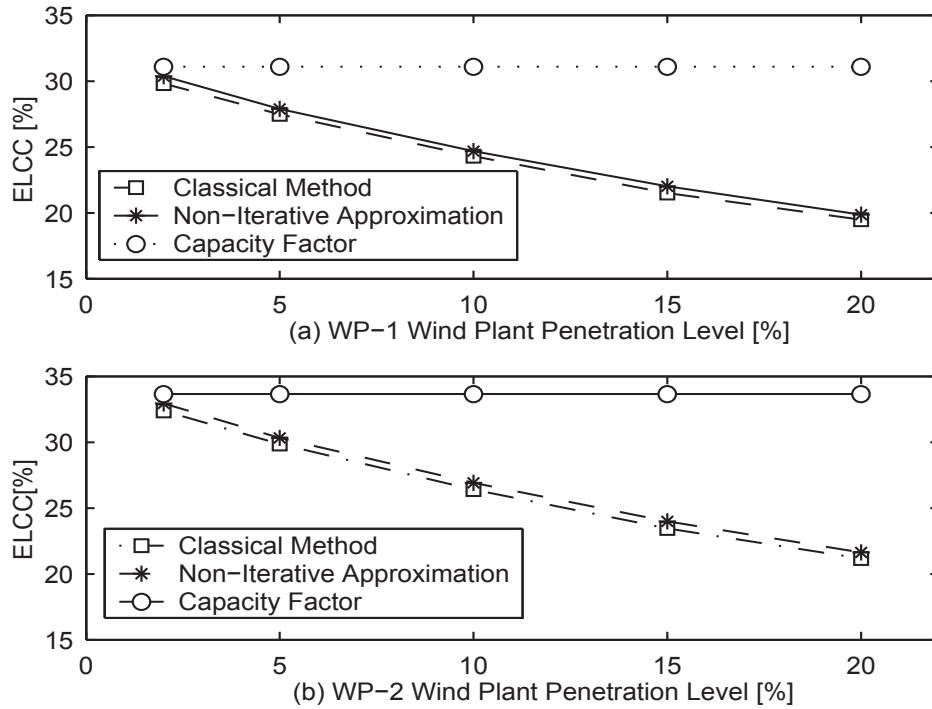


Figure 4.2 Case Study I: Comparing ELCC results from the conventional calculations, non-iterative approximation and capacity factor approximation for: (a) wind plants created from WP-1 source data, and (b) wind plants created from WP-2 source data

4.6.1.6 Discussion

Table 4.5 compares the ELCC results obtained from the case study. The non-iterative method quite accurately approximates the conventional method, only slightly overestimating the ELCC by 1.4% to 2.5%. Plus, it gives consistent results for both sources of power output data (WP-1 and WP-2). On the other hand, the capacity factor approximation is only accurate at penetration levels of 2%, with a relative error of about 4%; it becomes quite inaccurate

Table 4.5 Comparison of ELCC results for Case Study I

WP-1 (All units [%])					
Wind plant penetration level	2	5	10	15	20
ELCC Classical method	29.8	27.5	24.3	21.5	19.5
ELCC Approximate method	30.4	27.9	24.7	22.0	19.9
Percent relative error	2.0	1.4	1.6	2.3	1.9
Capacity factor	31.1	31.1	31.1	31.1	31.1
Percent relative error	4.4	13.1	28.0	44.7	59.5
WP-2 (All units [%])					
Wind plant penetration level	2	5	10	15	20
ELCC Classical method	32.4	29.9	26.4	23.4	21.2
ELCC Approximate method	32.9	30.3	26.9	24.0	21.6
Percent relative error	1.7	1.4	2.0	2.5	2.1
Capacity factor	33.6	33.6	33.6	33.6	33.6
Percent relative error	3.7	12.4	27.3	43.6	58.5

at higher penetration levels, reaching a relative error of nearly 60% for the wind plant penetration level of 20%. Therefore, although the capacity factor approximation is convenient because it does not require any reliability modeling, it is a misleading overall ELCC approximation. When system generation and load data are available, the non-iterative approximation should be used; it produces more accurate ELCC estimates for all penetration levels, while requiring minimal reliability modeling and computational efforts.

4.6.2 Case Studies II and III: Period-specific ELCCs

In the second case study, the existing power system (System 2) consists of the IEEE Reliability Test System, which has a total capacity of 3,405-MW [34]. It contains the 32 conventional generating units of Table 4.6 as well as their force outage rate (FOR), representing unit unavailability. System 2

Table 4.6 Case Study II: IEEE-RTS Generating units reliability data

Unit size [MW]	Number of units	Unavailability; FOR
12	5	0.02
20	4	0.10
50	6	0.01
76	4	0.02
100	3	0.04
155	4	0.04
197	3	0.05
350	1	0.08
400	2	0.12

serves a typical load demand with a 2,627-MW annual peak load⁸. For this typical load demand, the computed LOLE is 2.4 hours per year. Figure 4.3 illustrates the hourly load data time-series.

The addition of a 150-MW wind plant is under consideration for System 2. Only a year of power output data was available for the wind plant under study. Optimally, multiple years of data from the chosen evaluation period

⁸This is not the IEEE-RTS load demand.

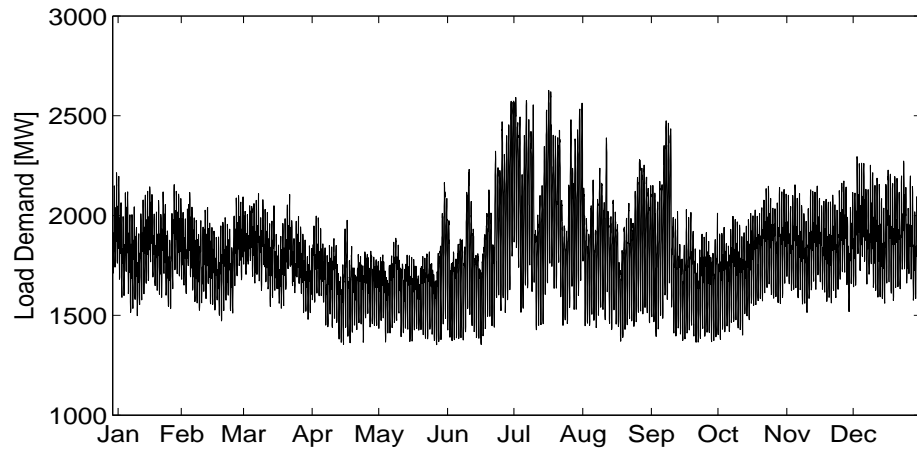


Figure 4.3 Case Study II: Hourly load data time-series for System 2 over a year long evaluation period

would be used to build the wind model. Figure 4.4 illustrates the yearly power output data of the 150-MW wind plant.

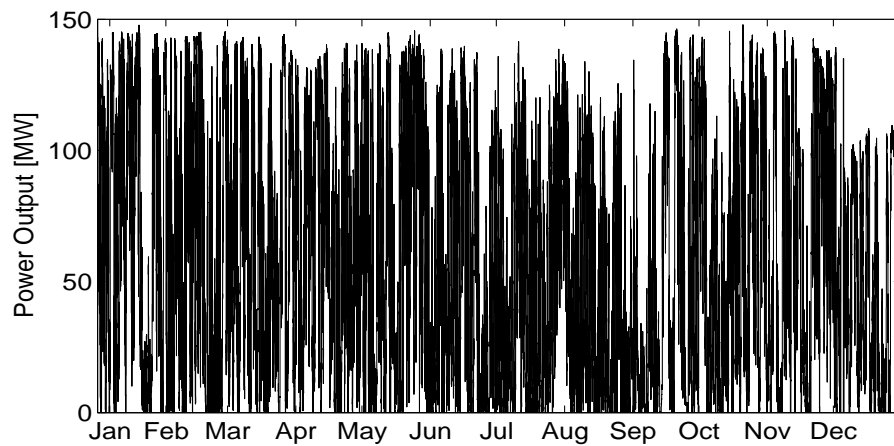


Figure 4.4 Case Study II: Power output for the 150-MW wind plant over a year long evaluation period (Note the interannual variability of the wind generation.)

In the third case study, in addition to the 32 conventional units, the existing power system (System 3) also includes a 234-MW wind plant. This 3,639-MW system serves a typical load demand of 2,682-MW annual peak load and exhibits a 2.4 hours per year LOLE. The load demand displays the same variability as the load data in Case Study II. In this case, a 114-MW wind plant is added to the generation portfolio of System 3. Figure 4.5 illustrates the yearly power output data of the 114-MW wind plant.

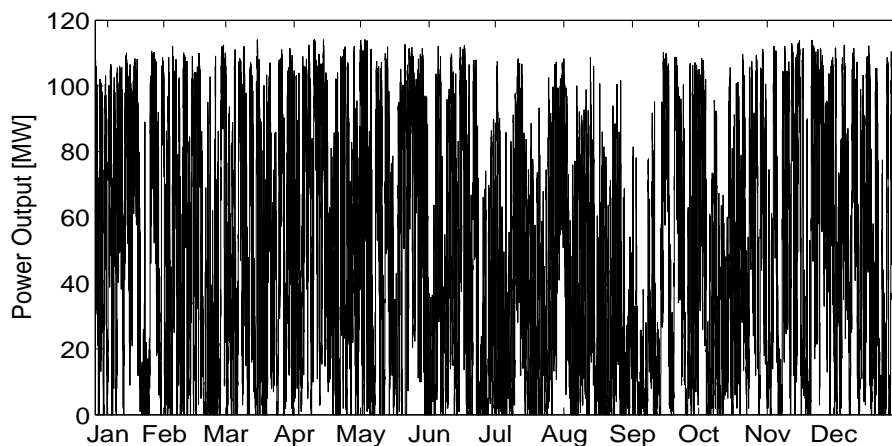


Figure 4.5 Case Study III: Power output for the 114-MW wind plant over the year long evaluation period (Note the interannual variability of the wind generation.)

4.6.2.1 Choosing the Evaluation Period

In these case studies, period-specific ELCCs are computed for three evaluation periods: yearly, monthly and peak load hours. The peak load hours period is defined as the weekdays hours from 3PM through 6PM during the months of June, July, August and September. Once the evaluation period is

chosen, the appropriate data must be used in the calculations. For example, to determine the ELCC during the month of August for the 150-MW wind plant, we use the wind power output data of August to build the wind reliability model. Furthermore, to compute the m parameter of the non-iterative method, we must also use the August load data for the LOLE calculations. Figure 4.6 illustrates System 2's load demand for the month of August while Figure 4.7 illustrates the power output data of the 150-MW wind plant during the month of August.

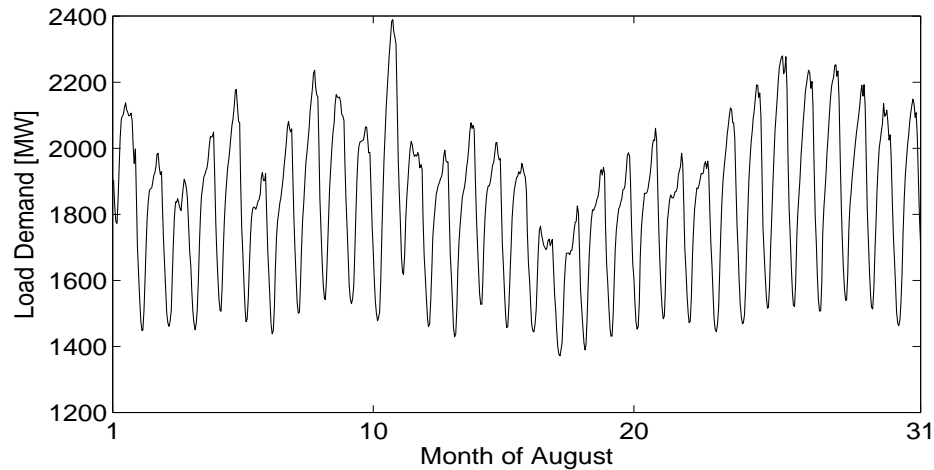


Figure 4.6 Case Study II: Hourly load data time-series for August

Although a thorough cross-correlation analysis is recommended, figures 4.8 and 4.9 give some insights on how to identify periods of significant wind/load correlation. A weak negative correlation related to diurnal effect can be identified from these figures. In further analysis, this correlation could be captured by choosing hourly evaluation periods as it is applied for the peak

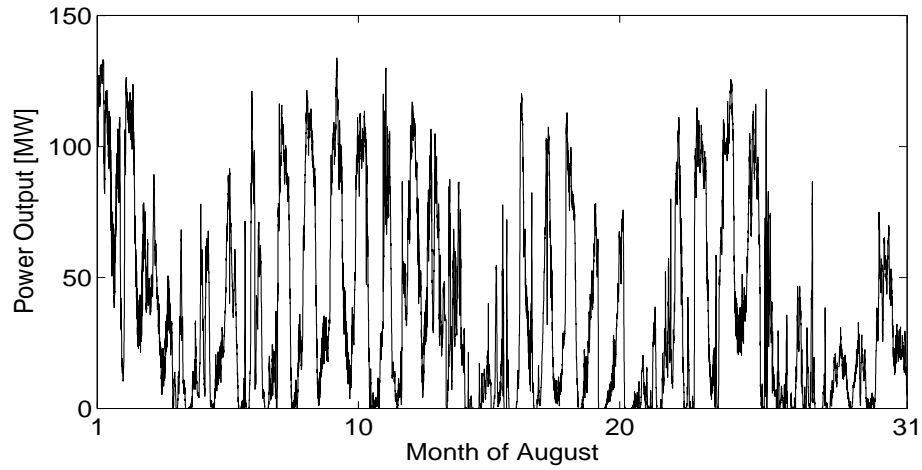


Figure 4.7 Case Study II: Power output for the 150-MW wind plant during August

load hours period. Even though correlation is not explicitly investigated in these case studies, results will show the importance of identifying periods of potential wind/load correlations. A thorough cross-correlation analysis would be more conclusive but figures 4.8 and 4.9 can still provide some insights on how to identify periods of significant wind/load correlation. A weak negative correlation related to diurnal effect can be identified from these figures. In further analysis, this correlation could be captured by choosing hourly evaluation periods as it is applied for the peak load hours period. Although correlation is not explicitly investigated in these case studies, results will show the importance of identifying periods of potential wind/load correlations.

Using the data corresponding to the relevant evaluation period, we can determine the multi-state representation of the wind plant.

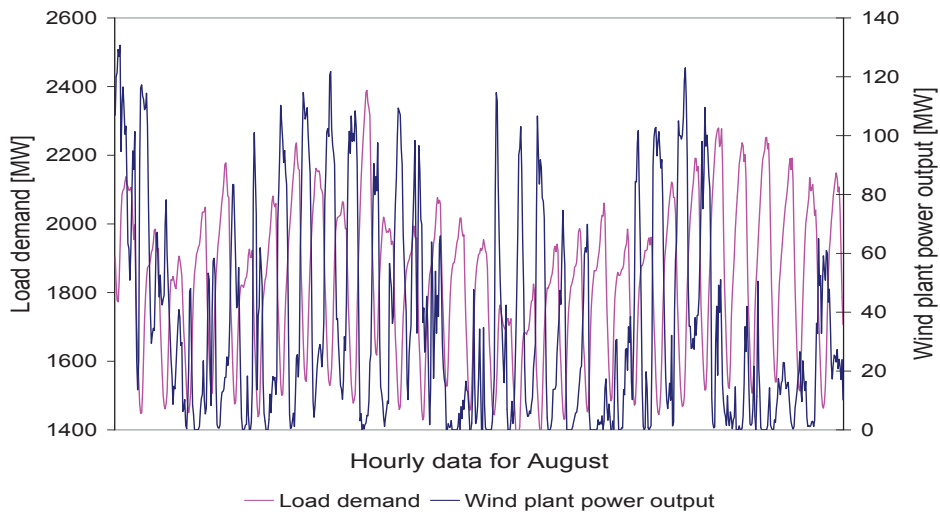


Figure 4.8 Case Study II: Superimposed load and wind power output time-series for August

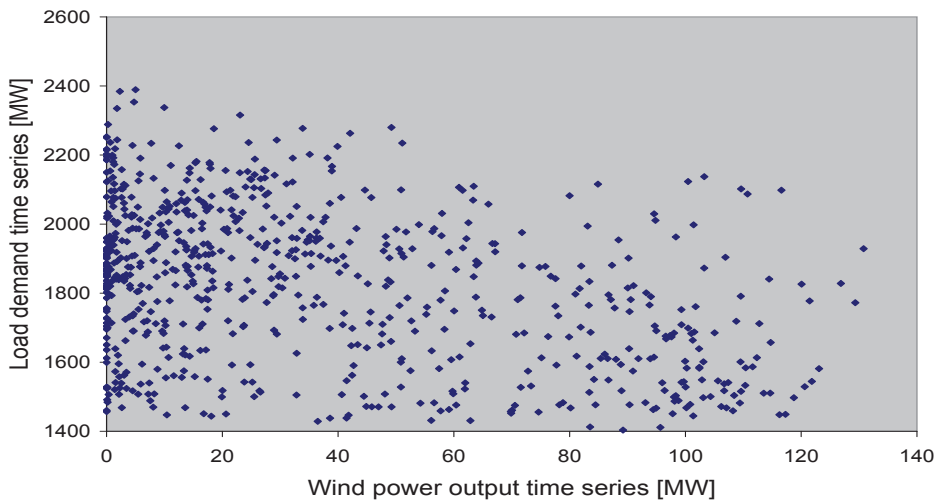


Figure 4.9 Case Study II: Correlation graph between load demand and wind power output time-series for August

4.6.2.2 Building the Wind Plant’s Reliability Model

The preferred multi-state representation as described in Section 3.1.1 is used to model the wind plant. A resolution of 1-MW is used to model

all wind plants in these case studies. For example, in the second case study, the 150-MW wind plant is modeled by 151 partial capacity outage states: $C_1=0$ -MW, $C_2=1$ -MW, ... $C_{149}=148$ -MW, $C_{150}=149$ -MW, $C_{151}=C_A=150$ -MW. Given the wind plant's power output data for the chosen evaluation period, the individual probability p_j associated with the partial capacity outage states C_j are computed using (3.1). In these calculations, when a power output data point fell between two values of $C_A - C_j$, it was rounded to the closest partial capacity outage state. For example, a power output of 142.3-MW was counted as an occurrence for the 142-MW partial capacity outage state while a power output of 65.5-MW was counted as an occurrence for the 66-MW partial capacity outage state. For low resolution, this rounding approximation has an insignificant impact on the final model. Table 4.7 represents part of the 150-MW wind plant's multi-state representation for an evaluation period of a year. Similar multi-state representations are built for the wind plants in Case Study III.

4.6.2.3 Building the COPT of System 2 and System 3

For the second case study, the generators' data from Table 4.6 is used to build the existing system's COPT using the recursive algorithm presented in Section 2.1.1. For System 3, an already existing 234-MW wind plant is also convolved in the reliability model. With the existing system's COPT, the next step is to obtain the m parameter for each case study.

Table 4.7 Case Study II: Multi-state representation for the 150-MW wind plant using a resolution of 1-MW and an evaluation period of a year

Capacity outage state C_j [MW]	Individual probability p_j
0	0
1	0
2	0.000057
3	0.000148
4	0.000272
5	0.002319
6	0.001967
...	...
145	0.013754
146	0.016739
147	0.015611
148	0.016050
149	0.018080
150	0.089935

4.6.2.4 Determining the m Parameter of System 2 and System 3

Given the chosen evaluation period's appropriate data and using (4.5), various new load data time-series are created with shifting percentages of -20%, -17.5%, -15%, ...0%, +2.5%, ...+20%. In each case study, the existent power system's LOLE is computed for these 16 new load data time-series in addition to the typical load data time-series. For example, Table 4.8 presents the resultant LOLE values with their associated load data time-series for System 2

during August. Although the peak load $L_{C_{pk}}$ is used to represent the load data

Table 4.8 Case Study II: LOLE for various load data time-series during August for System 2

Load data time-series $L_c = L_t \pm c \times L_{t_{pk}}$ [MW]	Monthly peak load $L_{C_{pk}}$ [MW]	LOLE [hrs per month]
$L_t - 20\% \times L_{t_{pk}}$	1911	0.0003254
$L_t - 17.5\% \times L_{t_{pk}}$	1971	0.0007529
$L_t - 15\% \times L_{t_{pk}}$	2031	0.001655
$L_t - 12.5\% \times L_{t_{pk}}$	2091	0.003725
$L_t - 10\% \times L_{t_{pk}}$	2150	0.007798
$L_t - 7.5\% \times L_{t_{pk}}$	2210	0.01556
$L_t - 5\% \times L_{t_{pk}}$	2270	0.03137
$L_t - 2.5\% \times L_{t_{pk}}$	2329	0.05808
L_t , Aug. Typical Load Data	2389	0.1034
$L_t + 2.5\% \times L_{t_{pk}}$	2449	0.1838
$L_t + 5\% \times L_{t_{pk}}$	2509	0.3180
$L_t + 7.5\% \times L_{t_{pk}}$	2568	0.5328
$L_t + 10\% \times L_{t_{pk}}$	2628	0.8755
$L_t + 12.5\% \times L_{t_{pk}}$	2688	1.4174
$L_t + 15\% \times L_{t_{pk}}$	2748	2.2490
$L_t + 17.5\% \times L_{t_{pk}}$	2807	3.4824
$L_t + 20\% \times L_{t_{pk}}$	2867	5.3688

time-series L_c , the LOLE calculations were performed using all the relevant hourly load data points, not only the peak load. These calculations are done for all evaluation periods in both case studies. Note that in Case Study III, period-specific COPTs are computed using the corresponding period-specific multi-state representation for the already existing wind plant. After the LOLE values have been computed for a particular evaluation period, the results are

graphed to obtain the relationship approximating the LOLE as a function of a shifted increase or decrease in load demand. Figure 4.10 illustrates the relationship between System 2's LOLE and the peak load of each curve for August. Using a curve fitting tool, the data points are curve-fitted with an

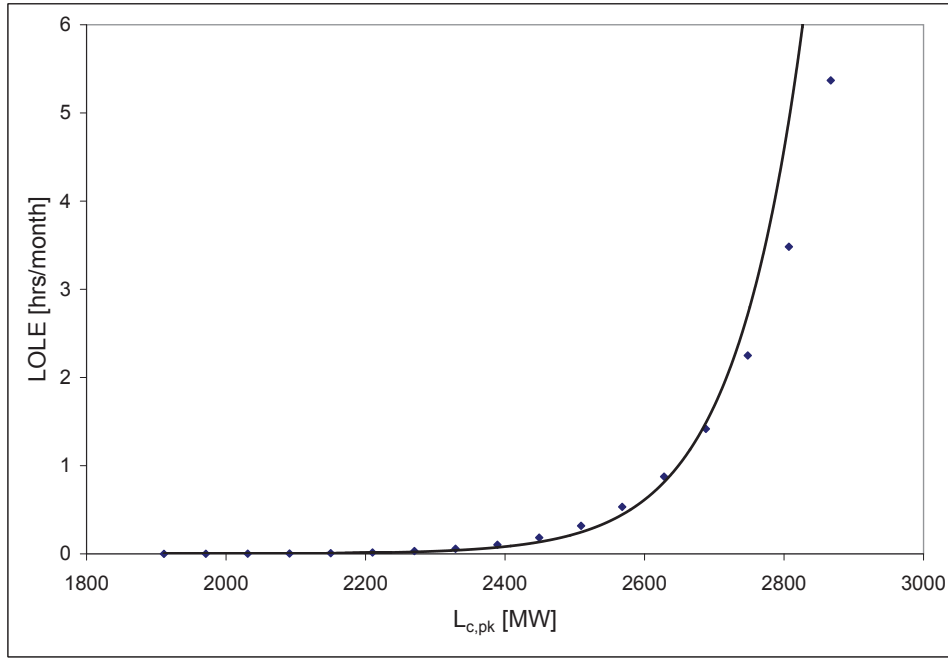


Figure 4.10 Case Study II: Exponential relationship between the existing system's LOLE and a shifted increase or decrease in the typical load demand during August

exponential relationship to determine the m parameter. The following exponential relationship was established for System 2 in August. It attributed a value of $1.0054465 \times 10^{-2} \text{ MW}^{-1}$ to the m parameter:

$$LOLE_{L_{pk}} = B \times e^{1.0054465 \times 10^{-02} \times L_{pk}} \quad . \quad (4.27)$$

Applying the same approach, the m parameters were computed for all evaluation periods in both Case Study II and III.

4.6.2.5 Results

Using the existing system's m parameter with the wind plant's multi-state model (C_j and p_j values), we applied the estimating function (4.23) to obtain the ELCC estimates. The resulting period-specific ELCC estimates were compared to the classically computed values as well as to the wind plant's capacity factor. Both the classical ELCC and the capacity factor calculations were performed using the data relevant to the evaluation period. Figures 4.11 and 4.12 illustrate these results which will be discussed in the following section.

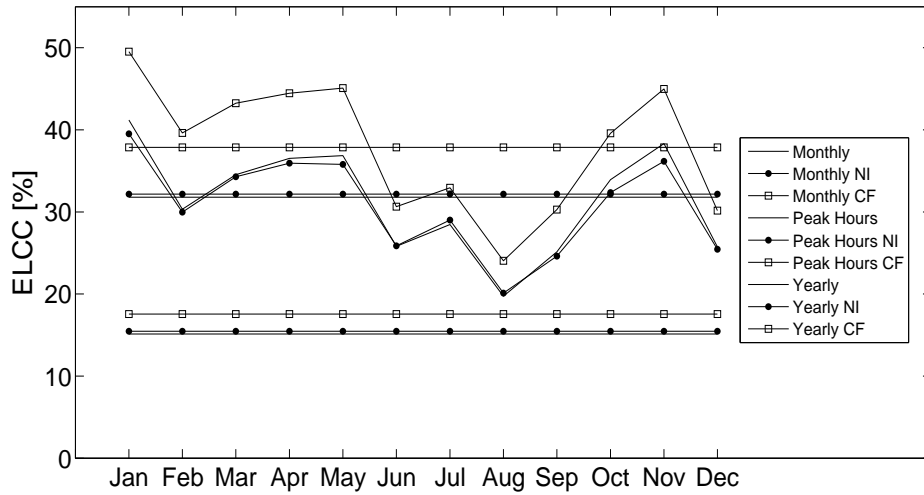


Figure 4.11 Case Study II: Comparing ELCC results obtained from the non-iterative approximation (NI), the conventional method and capacity factor approximation(CF)

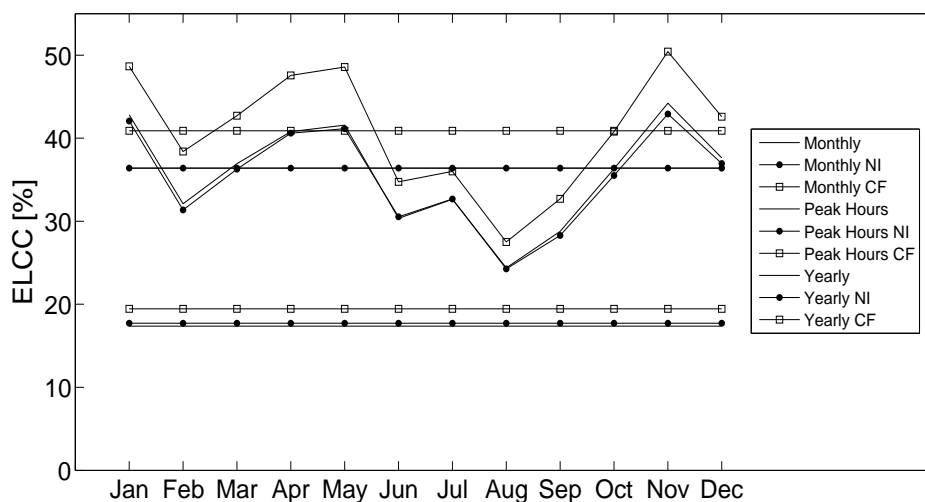


Figure 4.12 Case Study III: Comparing ELCC results obtained from the non-iterative approximation (NI), the conventional method and capacity factor approximation(CF)

4.6.2.6 Discussion

In Case Study II and III, we demonstrated that the non-iterative approximation can be applied whether or not wind generation is already present in the existing generation portfolio. Moreover, it is shown that the proposed method can be adjusted for various evaluation periods. The non-iterative approximation provides excellent ELCC estimates independent of the scenario or choice of evaluation period. Figures 4.11 and 4.12 (or tables 4.9 and 4.10) summarize and compare the ELCC results obtained in each case study. For all evaluation periods, the non-iterative method accurately approximates the conventional calculations with an average percent relative error of 2.2% for Case Study II and 1.4% for Case Study III.

Table 4.9 Case Study II: Comparison of ELCC results obtained for 150-MW wind plant (Percent relative errors in parenthesis)

Evaluation Period	Non-iterative Approx. [%]	Classical Method [%]	Capacity factor Approx. [%]
Yearly	32.2 (1.2)	31.8	37.9 (19.1)
Monthly			
January	39.5 (4.1)	41.2	49.5 (20.2)
February	30.0 (1.2)	30.3	39.6 (30.7)
March	34.3 (0.7)	34.5	43.3 (25.3)
April	35.9 (1.7)	36.5	44.5 (21.7)
May	35.8 (2.9)	36.9	45.1 (22.3)
June	25.9 (0.3)	25.8	30.6 (18.8)
July	29.0 (1.9)	28.5	32.9 (15.7)
August	20.1 (1.9)	19.7	24.0 (21.8)
September	24.6 (2.0)	25.1	30.3 (20.5)
October	32.3 (4.7)	33.9	39.6 (16.6)
November	36.2 (5.6)	38.3	45.0 (17.3)
December	25.4 (1.1)	25.7	30.1 (17.2)
Peak Hours	15.5 (2.2)	15.1	17.6 (16.0)
Average % Rel. Error	(2.2)	—	(20.2)

On the other hand, the capacity factor approximation offers less accurate ELCC estimates with average percent relative error of 20.2% for Case Study II and 14.1% for Case Study III. The capacity factor method is also less consistent between the two case studies. As we pointed out in Case Study I, the greater the size of the wind plant in comparison with the total system's capacity (wind plant penetration level), the less accurate are the capacity fac-

Table 4.10 Case Study III: Comparison of ELCC results for 114-MW wind plant (Percent relative errors in parenthesis)

Evaluation Period	Non-iterative Approx. [%]	Classical Method [%]	Capacity factor Approx. [%]
Yearly	36.4 (0.1)	36.4	40.9 (12.4)
Monthly			
January	42.1 (1.7)	42.8	48.6 (13.6)
February	31.3 (2.4)	32.1	38.4 (19.6)
March	36.3 (1.8)	36.9	42.7 (15.7)
April	40.6 (0.5)	40.8	47.6 (16.6)
May	41.1 (1.1)	41.6	48.6 (16.8)
June	30.5 (0.6)	30.4	34.7 (14.5)
July	32.7 (0.1)	32.6	36.0 (10.4)
August	24.3 (0.5)	24.4	27.5 (12.7)
September	28.3 (1.7)	28.8	32.7 (13.6)
October	35.5 (2.2)	36.3	40.8 (12.3)
November	42.9 (2.9)	44.2	50.4 (14.1)
December	37.0 (1.8)	37.6	42.6 (13.2)
Peak Hours	17.7 (2.0)	17.4	19.4 (11.9)
Average % Rel. Error	(1.4)	N/A	(14.1)

tor estimates. Here, the non-iterative approximation offers more consistent estimates between the two case studies, with 0.8% difference between the average errors. Again, although the capacity factor approximation is convenient because it does not require any reliability modeling, it is not a good method for obtaining an overall ELCC approximation. When system generation and load data are available, the non-iterative approximation is more appropriate;

it produces more accurate ELCC estimates for any chosen evaluation period while requiring minimal reliability modeling and computational efforts. In summary, there are four advantages to using the non-iterative approximation over the conventional calculations:

1. The only LOLE calculations needed are the ones performed to determine the m parameter.
2. There is no need to build a generation reliability model, or COPT, to represent the potential power system including the additional wind plant. Consequently, alternate wind expansion scenarios can easily be studied.
3. There is no computationally-intensive iterative process to solve for ΔL .
4. Only a simple function using basic operations is needed to compute an accurate ELCC estimate.

Furthermore, if the actual ELCC value is needed, one could use the resulting ΔL estimate as a starting point to reduce the number of iterations required by the conventional calculations.

Finally, results in Case Study II and III show that there can be a significant difference between the capacity values computed for different evaluation periods. In Case Study II, the estimated capacity value of the 150-MW wind plant varies from a minimum of 15.5% during the peak hours period to a maximum of 39.5% during the month of January, a 24% difference between

the two values. In Case Study III, the estimated capacity value of the 114-MW wind plant varies from a minimum of 17.7% for the peak hours period to a maximum of 42.9% during the month of November, a 25.2% difference. These findings suggests the importance of period-specific ELCC calculations to qualify a wind plant's *variable* reliability contribution.

4.7 Concluding Remarks

In this chapter, a wind plant's capacity contribution was quantified by using the metric of effective load carrying capability. In addition to applying conventional ELCC calculations to several case studies, a novel non-iterative approximation was introduced and yielded accurate ELCC estimates. Case study findings suggested the importance of period-specific ELCC calculations to better evaluate the *variable* reliability contribution of wind plants. Relevant evaluation periods should be system and wind plant dependent while also reflecting interannual variability and possible wind/load correlation.

Thus far, the reliability contribution of wind plants has been studied from a system planning perspective. The findings and methods presented in this chapter should prove useful in generation expansion studies or generation adequacy assessment when determining system planning reserves. Even when considering a well-planned system where wind generation has been appropriately integrated in the adequacy assessment, wind plants do create significant challenges to maintaining reliability on an operational level. The following chapter will address these challenges while proposing an operational adequacy

assessment method for power systems with significant wind generation.

Chapter 5

Operational Generation Adequacy Assessment for Power Systems with Wind Generation

System operators are responsible for maintaining adequate system reliability while constantly monitoring and matching the system generation to the load demand. Ancillary services are procured to maintain security and reliability during system disturbances and to account for load forecasting deviations. The increasing presence of wind generation, with its inherent variability, makes it more challenging for system operators to maintain the desired system reliability. Adequate monthly or annual ancillary service requirements are usually determined based on engineering experience and historical system performance. Since these requirements may or may not capture wind generation's uncertainties, being able to assess the system reliability status would be beneficial for system operators.

As we have shown in previous chapters, generation adequacy assessments using loss-of-load calculations are not usually made from an operational perspective but are instead based on planning cases to determine planning reserve margins. In this chapter, we propose an approach that would allow system operators to assess whether enough capacity is available to cover for

potential generator forced outages, load forecasting deviations and, most importantly, wind forecasting deviations. Our purpose with this assessment tool is to equip system operators with a quantitative evaluation method to assess the reliability risk levels on day-ahead and hour-ahead basis, and consequently enable them to identify high risk periods and make the necessary adjustments to ensure acceptable levels of system reliability.

5.1 Concept Description

While most commonly used in generation adequacy assessment studies for system planning purposes, the loss-of-load probability (LOLP) has been adapted in the past to provide useful operational information such as spinning reserve requirements [44]. In this chapter, a novel application of the LOLP is presented while proposing to use the metric as an operational reliability assessment tool in the context where wind capacity is a significant part of the generation portfolio. As described in Chapter 3, in planning generation adequacy studies, loss-of-load calculations are usually performed while integrating wind plants using one of two main approaches: negative load adjustment or multi-state representation. In each approach, preferably a year or more of actual power output data is used to create the wind plant's reliability model. Given an acceptable yearly risk level, loss-of-load calculations are then performed to ensure that enough generating capacity is present in the system to meet the projected load demands. Unlike system planning applications, the proposed operational assessment tool performs hourly LOLP calculations to ensure that

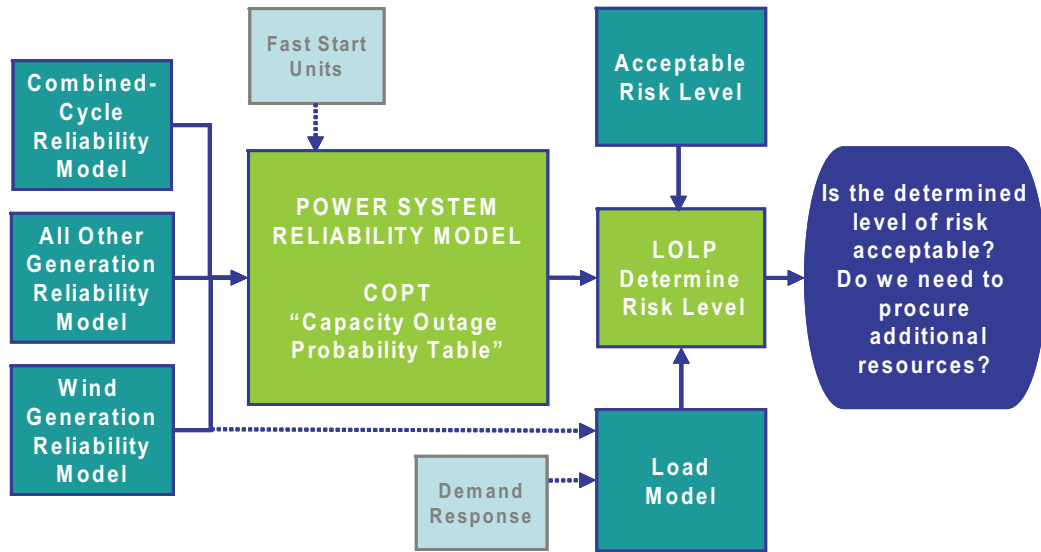


Figure 5.1 Conceptual diagram of the operational reliability assessment tool reflecting hourly operational LOLP calculations

enough generators have been scheduled to reliably meet the hourly forecasted load demand. The hourly LOLP reflects not only the possible generator forced outages but also the load and wind power forecasting deviations. Figure 5.1 summarizes the proposed operational reliability assessment tool. As shown in this figure, each scheduled generating unit is represented with a reliability model specific to the type of generation: conventional¹, combined-cycle and wind. When all generating units have been modeled, the system’s COPT is created using the recursive probabilistic algorithm of Section 2.1.1. Similar to

¹In this case, conventional generation means all generation except combined-cycle and wind.

planning applications, wind plants can be modeled either as generation in the COPT or as negative load. Incorporating an hourly load model which considers forecasting deviations, the loss-of-load probability is then computed for the hour under study. This hourly assessment can be performed on a day-ahead or hour-ahead time horizon given that appropriate forecasting deviations are used in the calculations. The calculated hourly risk or the compounded daily risk is then compared to a pre-determined acceptable risk criterion. If the scheduled generation turns out to be inadequate to meet the criterion, demand response and additional fast start units can then be included in the risk assessment.

The proposed operational LOLP calculations are performed much like the planning LOLP calculations, with the main difference being how the wind generation and load demand are represented and handled in the calculations. Note that wind and load forecasting deviations are assumed to be statistically independent while performing the hourly LOLP calculations, an assumption which will be discussed later in this chapter. The following sections will present the generation and load reliability models used in the proposed tool.

5.2 Conventional Unit and Combined-cycle Plant Reliability Model

Conventional units and combined-cycle plants are modeled as described in Section 2.2.1 and Appendix A by using a two-state and multi-state representations respectively. Since short term statistics are not readily available, long term steady-state statistics can be used to approximate a unit's unavailability

in an operational time frame. When unit-specific statistics are unavailable, the NERC GADS database can provide the necessary information to compute a unit's unavailability probability according to its type and size [37].

5.3 Proposed Operational Load Reliability Model

The operational load model is created using the hourly forecasted system load and expected forecasting deviations. Optimally, these forecasting deviations would be obtained from the load forecasting provider and be dependent on the number of hours-ahead for which the forecast is being performed. Meanwhile, we proposed that a reasonable approximation of the forecasting deviations could be determined using multiple years of historical load forecasts and actual load demands. These approximate forecasting deviations could also be period-specific such as on a seasonally, monthly and/or peak/off-peak hourly bases. The following simple example suggests how these forecasting deviations can be approximated using historical forecasts and actual load demands for the period of interest. For a particular hourly load forecast, the conditional probability that the actual load demand will take a certain historically possible value is simply computed as follows:

$$P_l(L_a|L_f) = \frac{\# \text{ of actual load equal to } L_a \text{ when the forecasted load is } L_f}{\# \text{ of load forecast } L_f} . \quad (5.1)$$

Note that we only use the historical load forecast and actual load demand for the period of interest in the calculations. For example, if we have a year of historical load data, but we want to build a forecasting deviations distribution

for the month of July, we will only use the hourly load data of that month. Given the simple load history shown in Table 5.1, a forecast L_f of 10-MW can take actual values L_a of 5-MW, 10-MW and 15-MW with probabilities $P_l(L_a|L_f)$ of $P_l(5|10) = 1/5 = 0.20$, $P_l(10|10) = 3/5 = 0.60$ and $P_l(15|10) = 1/5 = 0.20$. Similarly, a 20-MW forecast can take actual values of 10-MW, 15-MW and 20-MW, with probabilities of $P_l(10|20) = 1/5 = 0.20$, $P_l(15|20) = 2/5 = 0.40$ and $P_l(20|20) = 2/5 = 0.40$.

Table 5.1 Example: Simple history of forecasts and actual load demands for estimating forecasting deviations (Note that the load history is specific to the period of interest.)

Load forecast L_f [MW]	Actual load L_a [MW]
10	5
10	10
10	10
10	10
10	15
20	10
20	15
20	15
20	20
20	20

The forecasting deviations distribution associated with a particular forecast L_f is then represented with the n possible actual values $L_{a,i}$ and corresponding probabilities $P_l(L_{a,i}|L_f)$. Table 5.2 represents the resulting distributions for our simple example.

Table 5.2 Example: Estimated load forecasting deviations distribution by load forecast

Load forecast L_f of 10-MW	
Possible actual load $L_{a,i}$ [MW]	Probability $P_l(L_{a,i} L_f)$
5	0.20
10	0.60
15	0.20
Load forecast L_f of 20-MW	
Possible actual load $L_{a,i}$ [MW]	Probability $P_l(L_{a,i} L_f)$
10	0.20
15	0.40
20	0.40

The load forecasting deviations distribution associated with a particular load forecast embodies the operational load model used in the hourly LOLP calculation. As we will show in subsequent sections, we mathematically incorporate this load model in the LOLP by applying the law of total probability. Firstly, though, the wind plant reliability model must be developed.

5.4 Proposed Operational Wind Plant Reliability Model

As was shown in regard to planning LOLP calculations, wind plants can also be integrated in the operational calculations as either generation or negative load. In both cases, the wind plant's hourly power output forecast and associated forecasting deviations are used to create the reliability model. The following sections describe the two integration approaches.

5.4.1 Integrating Wind Plant as Generation

In this approach, the proposed wind plant's hourly operational reliability model is essentially a multi-state representation. As for the planning model, the operational multi-state representation consists of partial outage states and corresponding individual probabilities which is then convolved as generation in the system's COPT. The operational model differs from the planning model in that hourly forecasted power output and associated forecasting deviations are used instead of the power output times series. Ideally, the forecasting deviations would be obtained from the wind forecasting provider and depend on the number of hours-ahead the forecast is being performed. Usually, one would expect an hour-ahead forecast to be more accurate than a day-ahead forecast. In addition, forecasting deviations could also reflect other aspects, such as particular weather patterns or extreme weather conditions. It is recognized that wind forecasting is still a developing area and accurate forecasting deviations are still limited at this time.

Meanwhile, analogously to the method used to construct the load model, reasonable forecasting deviations can be approximated given enough historical forecasted power output data and corresponding actual values. A wind plant's forecasting deviations distribution would be created along lines similar to the load distribution described in the previous section. To each power output forecast would be associated a distribution of possible actual values and corresponding probabilities. Using this distribution, the wind plant's operational multi-state representation would be determined and then convolved

in the COPT of the system. Table 5.3 provides the forecasting deviations distribution associated with a 100-MW wind plant and a 70-MW forecast.

Table 5.3 Example: Forecasting deviations distribution associated with a 70-MW forecast of a 100-MW wind plant

Wind power forecast W_f of 70-MW	
Possible actual wind power $W_{a,k}$ [MW]	Probability $P_w(W_{a,k} W_f)$
90	0.125
80	0.50
70	0.25
60	0.10
50	0.025

In this case, the distribution indicates that a 70-MW forecast has historically taken actual values $W_{a,k}$ of 50-MW, 60-MW, 70-MW, 80-MW and 90-MW with corresponding individual probabilities $P_w(W_{a,k}|W_f)$ of 0.025, 0.10, 0.25, 0.50, 0.125. Again, analogous to the probabilities $P_l(L_{a,i}|L_f)$ for the load model, the probability $P_w(W_{a,k}|W_f)$ of having a power output of $W_{a,k}$ given a forecasted power output of W_f can be obtained as follows:

$$P_w(W_a|W_f) = \frac{\# \text{ of actual power output equal to } W_{a,k} \text{ when forecast is } W_f}{\# \text{ of forecasts } W_f} . \quad (5.2)$$

For the purpose of building the system's COPT and given the 70-MW forecast's distribution in Table 5.3, the 100-MW wind plant is seen as a multi-state unit with maximum possible capacity of 90-MW that can exist in 4 partial capacity outage states. The maximum possible capacity C_w of the multi-state unit is therefore defined as the maximum possible actual power output

$\max(W_{a,k})$. Table 5.4 presents the multi-state representation with all possible capacity outage states and corresponding individual probability. The possible capacity outage states C_j are simply obtained from $C_w - W_{a,k}$.

Table 5.4 Example: Operational multi-state representation of a 100-MW wind plant given a 70-MW forecast

Capacity outage C_j [MW]	Individual probability p_j
0	0.125
10	0.50
20	0.25
30	0.10
40	0.025
90	0

Only the capacity outage states with non-zero probabilities will actually have an impact on the system's COPT. However, when calculating the LOLP, the margin $C_s - L$ must take into account a multi-state unit of 90-MW in the maximum possible capacity C_s of the system, which is the reason it is included in the model.

Since the COPT concept requires that all generator unavailabilities be independent random events, wind plants in geographical proximity which are subject to the same wind regime must be aggregated into one multi-state unit. In this case, forecasting deviations would be determined for the aggregated wind plants. As previously mentioned, it is assumed that wind forecasts and forecasting deviations are uncorrelated and statistically independent from load

forecasts and forecasting deviations. It may be possible to formulate the negative load approach without this assumption, but we will initially consider that forecasting deviations are statistical independent.

5.4.2 Wind Plants Integrated as Negative Load

The negative load approach also models wind plants by incorporating hourly power output forecasts and forecasting deviations. However, in this case, the forecasts of all wind plants are aggregated into one forecast with its associated aggregated forecasting deviations. The aggregated forecasting deviations distribution can be estimated from the history of aggregated forecasts and aggregated actual power output, as it was done for load or individual wind plants. Since the wind generation is considered as negative load, it is not integrated in the COPT but, instead, is subtracted from the load. In this case, the aggregated wind power forecasting deviations distribution directly represents the wind generation model since power output levels are needed instead of capacity outages. The following section will provide a detailed description of computing the LOLP considering both wind plant integration methods.

5.5 Operational LOLP Calculations

The operational LOLP is computed hourly given the generation scheduled, the wind plants' power output forecast and the load forecast. The wind power output and load forecasting deviations which are chosen depend upon the assessment's time horizon and perhaps even the season, month and/or time

of day. The load model is integrated in the LOLP calculations using the law of total probability. Given that the load forecast L_f can take n possible actual values $L_{a,i}$ with corresponding probabilities $P_l(L_f|L_a)$, the hourly LOLP is calculated with the following equation

$$LOLP_{L_f} = \sum_{i=1}^n LOLP_{L_{a,i}} \times P_l(L_{a,i}|L_f) \quad (5.3)$$

where $L_{a,i}$ and $P_l(L_{a,i}|L_f)$ are provided from the load forecasting deviations distribution. The $LOLP_{L_{a,i}}$ is computed using the basic LOLP equation for a load level $L_{a,i}$

$$LOLP_{L_{a,i}} = P(X > C_s - L_{a,i}) \quad (5.4)$$

where C_s is the total possible system capacity and $P(X > C_s - L_{a,i})$ is the cumulative probability of having a system capacity outage greater than $C_s - L_{a,i}$, which is obtained from the COPT. When wind plants are integrated as generation, this operational LOLP calculation doesn't need to be modified, as the wind plants' multi-state representations are integrated in the COPT. However, if wind plants are integrated as negative load, then the calculations must be modified. Given that an aggregated wind forecast of W_f can take m actual values $W_{a,k}$ with corresponding probabilities $P_w(W_{a,k}|W_f)$, there exists n times m possible combinations of net load $L_{a,i} - W_{a,k}$. The probability of the net load is simply the multiplication of $P_l(L_{a,i}|L_f)$ and $P_w(W_{a,k}|W_f)$ - in this case, it is assumed that the likelihood of a certain actual load $L_{a,i}$ happening is independent of the likelihood of a certain aggregated wind power output $W_{a,k}$ happening. When wind plants are integrated as negative load, the LOLP can

be computed with the following equation:

$$LOLP_{L_f, W_f} = \sum_{i=1}^n \sum_{k=1}^m \left[P(X > C_s - (L_{a,i} - W_{a,k})) \times P_l(L_{a,i} | L_f) \times P_w(W_{a,k} | W_f) \right]. \quad (5.5)$$

However, suppose that during certain periods of the year or during certain weather conditions, almost each time the load is overforecasted, the aggregated wind power output is also underforecasted. In this case, the two distributions would display some correlation and we can't assume independence. The only wind integration method that could mathematically consider the potential statistical dependence would be the negative load approach by using the joint probability of $P_{l,w}(L_{a,i}, W_{a,k} | L_f, W_f)$. However, even building an estimate of this system-specific joint probability would require access to several years of synchronized forecasted and actual values for both load and aggregated wind power output. Future research considering hidden Markov chains could possibly address this issue [45]. At this point, from a practical point of view, if certain weather patterns seem to indicate a significant correlation, and if these events threaten the system reliability, they should be handled separately by procuring additional capacity. Note that the study presented in [19] reports that, for the system under study, an “extremely weak correlation” exists between the load forecast deviations and the wind forecast deviations²

In summary, an hourly operational LOLP can now be computed while integrating wind plants as either generation or negative load. However, in

²Note that we are not referring to the wind/load correlation mentioned in planning calculations but rather to the correlation between the *forecast deviations*.

this dissertation, the operational assessment tool will integrate wind plants as generation in the system's COPT. Prior to applying the proposed method to a simple case study, the risk criterion used in the assessment must be discussed.

5.5.1 Operational LOLP Risk Criterion

A risk criterion is essential in the operational generation adequacy assessment: it determines whether the risk concurred by the system is acceptable. Ideally, this risk criterion would be system specific and based on socio-economic studies which outline what level of reliability consumers are willing to pay for. However, in practice, as it was discussed for the planning LOLE criteria, acceptable risk levels are usually based on engineering judgment and system historical performance. Therefore, by studying a history of operational hourly LOLPs or compounded daily LOLEs, a system specific criterion could be designed specific to seasons, months and/or peak/off peak periods. Furthermore, by looking at the historical operational LOLPs before wind generation became a significant part of the system, one could determine what has been considered an acceptable level of operational reliability.

There might be some interest in relating the planning LOLE standard of "1 day in 10 years" to an hourly or daily operational criterion. However, since the planning LOLE and operational LOLP concepts are derived from different system conditions and apply different mathematics, they can't be readily related. One might say that a conservative hourly or daily criterion could be determined from the LOLE standard by computing an "average"

hourly LOLP or an “average” daily LOLE. In this case, the “1 day in 10 years” would reduce to a “average” hourly LOLP of 2.74×10^{-4} or an “average” daily LOLE of 6.58×10^{-3} hours/day. By using such criteria in an operational assessment, there would be some peak load periods when the criterion wouldn’t be reachable. Keep in mind that the “1 day in 10 years” standard is obtained from a planning LOLE calculation that basically compounds LOLP values, some higher and some lower than the “average” LOLP value. Therefore if the average LOLP is not reachable from a planning perspective when all system generation is considered, it won’t be more reachable from an operational one.

5.6 Feasibility Study

The purpose of this simple study is to provide a reproducible scenario to test the feasibility of the proposed concept and help the reader understand its application. Consequently, the results obtained do not refer to any specific real world system.

In the presented case study, a day-ahead and hour-ahead assessment will be performed for two different days: a summer day with high load and low wind penetration and a winter day with low load and high wind penetration³. Prior to applying the operational assessment, hourly generation schedules will be created given three parameters: the system’s generation, the forecasted load demand and the wind plant power forecast. To this end, a

³Wind penetration is defined as the wind forecast divided by the load forecast.

simple offer-based economic dispatch will be used [46]. We will assume the same forecasted values for both the day-ahead and hour-ahead assessment. However, the forecasting deviations will be different to reflect the forecasting time horizons. The assessment will be based on an hourly risk criterion of 2%. A step-by-step application will be presented and followed by a discussion of the outcome.

5.6.1 Test System

The test system's conventional generation consists of the 23 units presented in Table 5.5, totaling 2760-MW of capacity. The capacity, number, fuel type, marginal cost, unavailability probability and start up time are defined for each type of generator. No combined-cycle plants are present and the system includes a demand response program of 150-MW.

In addition to the conventional generation, the test system also includes a 525-MW wind plant, which will be scheduled in every dispatch. The hourly load and wind power forecasts for the two-days under study are listed in Table 5.6; the same forecasts will be used for both day-ahead and hour-ahead assessment.

For simplicity's sake, a discrete seven-step approximation of the normal distribution [25] is chosen to model both the wind and load forecasting deviations. The resulting discrete distribution is found in Table 5.7. In practice, the forecasting deviations would either be obtained from the forecasting provider or approximated as described in Sections 5.3 and 5.4.1.

Table 5.5 Feasibility Study: Conventional generating units data

Cap.[MW]	# Units	Fuel	Marg. cost[\$/MWh]	P _{down}	Start up[hrs]
20	1	Gas	105	0.0778	0.25
30	2	Gas	100	0.0778	0.25
50	3	Gas	90	0.0778	0.25
60	2	Gas	85	0.0778	0.30
100	4	Gas	80	0.657	0.8
120	5	Coal	40	0.0437	2
130	1	Gas	65	0.0657	1
170	1	Coal	35	0.0437	4
180	1	Coal	30	0.0437	4
190	2	Gas	50	0.0657	2
550	1	Coal	20	0.0522	8

The standard deviations are defined as 10% of the load forecast for the day-ahead assessment and 2% for the hour-ahead assessment. For the wind power forecasting deviations distribution, a standard deviation of 50% of the forecast will be used for day-ahead and 20% for hour-ahead. It is assumed that the day-ahead forecasting deviations distribution is the same throughout the day, even though in reality it would depend on the number of hours ahead the forecast is being performed. As an example, Table 5.8 represents the hour-ahead wind forecasting deviations for a 200-MW wind power forecast and the resulting 0.20×200 -MW or 40-MW standard deviation. The load forecasting deviations are also determined in this manner.

Table 5.6 Feasibility Study: Two days of 24 hourly load forecasts (L_f) and wind plant power output forecasts (W_f)

Hour	Day 1: Summer day forecasts		Day 2: Winter day forecasts	
	L_f [MW]	W_f [MW]	L_f [MW]	W_f [MW]
12AM	1235	120	960	210
1AM	1140	135	960	195
2AM	1140	135	960	195
3AM	1045	120	880	195
4AM	1045	135	960	195
5AM	1140	135	1040	180
6AM	1235	120	1120	180
7AM	1425	105	1360	180
8AM	1615	90	1520	165
9AM	1710	90	1600	150
10AM	1805	90	1600	150
11AM	1900	90	1520	135
12PM	1805	60	1440	150
1PM	1900	60	1440	150
2PM	1900	90	1440	150
3PM	1805	90	1360	165
4PM	1710	105	1440	165
5PM	1615	105	1440	180
6PM	1615	105	1520	180
7PM	1615	120	1520	195
8PM	1615	120	1440	195
9PM	1520	135	1440	210
10PM	1425	135	1280	210
11PM	1330	120	1120	210

Table 5.7 Discrete seven-step approximation of the normal distribution

# of st. dev. from the mean	Probability
-3	0.006
-2	0.061
-1	0.242
0	0.382
1	0.242
2	0.061
3	0.006

Table 5.8 Hour-ahead wind power forecasting deviations for a 200-MW forecast using the discrete seven-step approximation of the normal distribution

Possible actual wind power $W_{a,k}$ [MW]	Probability $P_w(W_{a,k} W_f)$
80	0.006
120	0.061
160	0.242
200	0.382
240	0.242
280	0.061
320	0.006

5.6.2 Creating Hourly Generation Schedules

The hourly generation schedules are created using a simplified offer-based economic dispatch [46]. The first step is to sort all generators in ascending order of marginal cost. Then, generators (each of which commits 80% of its total output to meet the demand and 20% as reserve) are procured un-

til the forecasted demand is met. Maximum and minimum generating limits are ignored. The wind power is always procured in the generation schedule. The simplified offer-based economic dispatch is therefore performed with the following steps:

1. Sort the n conventional units of the system by marginal cost (MC) in ascending order.

$$MC(P_{G,1}) \leq MC(P_{G,2}) \leq \dots \leq MC(P_{G,n}) \quad (5.6)$$

2. Add one unit at a time and find $\min(y)$ that satisfies

$$\sum_{i=1}^y 0.80 \times P_{G,i} \geq (L_f - W_f) . \quad (5.7)$$

All 23 generators of the test system in Table 5.5 are considered available and participants in the dispatch. Transmission constraints are ignored.

5.6.3 Step-by-step Application of the Operational Assessment

A step-by-step application of the operational assessment will be presented with intermediate results for the day-ahead summer system conditions at 11PM. Although the presented steps are applied to the day-ahead assessment, the hour-ahead assessment follows the same approach.

Firstly, generation schedules must be created for the 11PM summer day conditions, that is a 120-MW wind power forecast and a 1330-MW load forecast. The simplified, offer-based economic dispatch described in Section

Table 5.9 Summer Day at 11PM: Conventional generators scheduled given a 120-MW wind power forecast and a 1330-MW load forecast

Capacity C [MW]	Unavailability prob. p_{down}
550	0.0522
180	0.0437
170	0.0437
120	0.0437
120	0.0437
120	0.0437
120	0.0437
120	0.0437
120	0.0437
190	0.0657

5.6.2 is applied according to the generator’s marginal cost of Table 5.5. The resulting generation schedule is found in Table 5.9.

The scheduled generators will be integrated in the COPT of the system using a two-state representation. In practice, the day-ahead or hour-ahead resource plans would provide the hourly generation scheduled.

5.6.3.1 Step 1: Build the wind plant’s operational reliability model

Before building the COPT of the system, the wind plant must also be modeled with its multi-state representation. For a 120-MW wind forecast and a day-ahead assessment, the standard deviation will be 0.50×120 -MW or 60-MW. In this case, when using the seven-step approximation of Table 5.7, the possible wind power outputs are -60-MW, 0-MW, 60-MW, 120-MW, 180-MW, 240-MW and 300-MW. When negative values of possible output arise,

they are grouped with the 0-MW level. When using actual or even estimated forecasting deviations, this approximate grouping won't be necessary. Thus, for the example hour, the resulting possible wind power outputs and respective probabilities are presented in Table 5.10.

Table 5.10 Summer Day at 11PM: Day-ahead wind power forecasting deviations for a 120-MW forecast

Possible actual wind power $W_{a,k}$ [MW]	Probability $P_w(W_{a,k} W_f)$
0	0.067
60	0.242
120	0.382
180	0.242
240	0.061
300	0.006

As explained in Section 5.4.1, when a wind plant is integrated as generation, the multi-state model is used to represent the wind plant. This model consists of the possible capacity outage states and is integrated in the COPT of the system. Given the possible power output levels in Table 5.10, the wind plant is seen as a multi-state unit with maximum possible capacity C_w of 300-MW. Consequently, the possible power output states must be converted to possible capacity outage states. Table 5.11 represents the resulting operational multi-state representation for the 120-MW forecast.

Along with the two-state representation of the conventional generators, the wind plant multi-state representation can now be integrated in the COPT calculations.

Table 5.11 Summer Day at 11PM: Day-ahead wind plant operational multi-state representation for a 120-MW forecast

Capacity outage C_j [MW]	Individual probability p_j
300	0.067
240	0.242
180	0.382
120	0.242
60	0.061
0	0.006

5.6.3.2 Step 2: Build the system’s hourly COPT

The system’s COPT is built as described in Section 2.1.1, using a two-state model for each conventional generator of Table 5.9 and the multi-state wind plant model of Table 5.11. The resulting COPT consists of 100 possible capacity outage states, a sample of which is represented in the following table.

5.6.3.3 Step 3: Determine the operational load model

The load model consists of the load forecasting deviations distribution. Given a 1330-MW forecast and a day-ahead assessment, the standard deviation will be 0.10×1330 -MW or 133-MW. The resulting load reliability model is found in Table 5.13.

Table 5.12 Summer Day at 11PM: Day-ahead hourly COPT

Capacity outage states x [MW]	$P(X \geq x)$
0	1.000000
60	0.996114
120	0.956605
170	0.798978
180	0.798801
190	0.542181
230	0.541908
...	...
530	0.068388
540	0.066066
550	0.062312
590	0.058525
...	...
1810	3.93242×10^{-11}
1820	9.90340×10^{-12}
1870	8.37304×10^{-12}
1930	3.22526×10^{-13}
1990	6.99328×10^{-14}

Table 5.13 Summer Day at 11PM: Day-ahead load reliability model for 1330-MW forecast

Possible actual load $L_{a,i}$ [MW]	Probability $P_l(L_{a,i} 1330)$
931	0.006
1064	0.061
1197	0.242
1330	0.382
1463	0.242
1596	0.061
1729	0.006

5.6.3.4 Step 4: Compute the hourly operational LOLP

The hourly operational LOLP is computed using (5.3). For the example hour, the calculations are performed as follows.

1. Using (5.3), the law of total probability is applied as:

$$LOLP_{1330} = \sum_{i=1}^7 LOLP_{L_{a,i}} \times P_l(L_{a,i}|1330) \ .$$

2. Expanding the previous equation, it becomes:

$$\begin{aligned} LOLP_{1330} &= LOLP_{931} \times P_l(931|1330) + LOLP_{1064} \times P_l(1064|1330) \\ &+ LOLP_{1197} \times P_l(1197|1330) + LOLP_{1330} \times P_l(1330|1330) \\ &+ LOLP_{1463} \times P_l(1463|1330) + LOLP_{1596} \times P_l(1596|1330) \\ &+ LOLP_{1729} \times P_l(1729|1330) \ . \end{aligned}$$

3. Considering the total possible capacity C_s of 1990-MW and replacing the $LOLP_{L_{a,i}}$ terms by (5.4), the equation is as follows:

$$\begin{aligned} LOLP_{1330} &= P(X > 1990 - 931) \times P_l(931|1330) \\ &+ P(X > 1990 - 1064) \times P_l(1064|1330) \\ &+ P(X > 1990 - 1197) \times P_l(1197|1330) \\ &+ P(X > 1990 - 1330) \times P_l(1330|1330) \\ &+ P(X > 1990 - 1463) \times P_l(1463|1330) \\ &+ P(X > 1990 - 1596) \times P_l(1596|1330) \\ &+ P(X > 1990 - 1729) \times P_l(1729|1330) \end{aligned}$$

or

$$\begin{aligned}
LOLP_{1330} = & P(X > 1059) \times P_l(931|1330) \\
& + P(X > 926) \times P_l(1064|1330) \\
& + P(X > 793) \times P_l(1197|1330) \\
& + P(X > 660) \times P_l(1330|1330) \\
& + P(X > 527) \times P_l(1463|1330) \\
& + P(X > 394) \times P_l(1596|1330) \\
& + P(X > 261) \times P_l(1729|1330) .
\end{aligned}$$

4. Reading the $P(X > x)$ from the system's COPT and replacing all $P_l(L_{a,i}|1330)$ with the corresponding probabilities from the load reliability model in Table 5.11, the equation becomes:

$$\begin{aligned}
LOLP_{1330} = & 8.91789 \times 10^{-04} \times 0.006 + 4.62301 \times 10^{-03} \times 0.061 \\
& + 0.016235 \times 0.242 + 0.051188 \times 0.382 \\
& + 0.068388 \times 0.242 + 0.136053 \times 0.061 \\
& + 0.342886 \times 0.006 .
\end{aligned}$$

The day-ahead hourly LOLP for the 1330-MW load forecast amounts to 0.050677.

5.6.3.5 Step 5: Compare hourly LOLP to the criterion

In this case study, the hourly criterion or acceptable level of loss-of-load probability is 0.02. For the hours which displayed hourly LOLP higher

than the hourly criterion, demand response and additional fast start units were considered to reduce the level of risk. For 11PM on the summer day, the day-ahead hourly LOLP is around 0.051, which is higher than our 0.02 hourly criterion. The following section will demonstrate how demand response and fast start units can be included in the operational reliability assessment.

5.6.3.6 Step 6: Consider demand response and fast start units

The test system includes a 150-MW demand response program that is assumed to be fully available upon request. This demand response (DR) was integrated in the assessment and the resulting hourly LOLPs were compared once more to the hourly criterion. To consider demand response, (5.4) must be modified as follows. Note that this modification requires no change to the system COPT.

$$LOLP_{L_{a,i}, DR} = P(X > C_s - (L_{a,i} - DR)) \quad (5.8)$$

For the example hour, the LOLP calculations are adjusted as follows:

$$\begin{aligned} LOLP_{1330} &= P(X > 1990 - (931 - 150)) \times P_l(931|1330) \\ &+ P(X > 1990 - (1064 - 150)) \times P_l(1064|1330) \\ &+ P(X > 1990 - (1197 - 150)) \times P_l(1197|1330) \\ &+ P(X > 1990 - (1330 - 150)) \times P_l(1330|1330) \\ &+ P(X > 1990 - (1463 - 150)) \times P_l(1463|1330) \\ &+ P(X > 1990 - (1596 - 150)) \times P_l(1596|1330) \\ &+ P(X > 1990 - (1729 - 150)) \times P_l(1729|1330) \end{aligned}$$

or

$$\begin{aligned}
LOLP_{1330} &= P(X > 1209) \times P_l(931|1330) \\
&+ P(X > 1076) \times P_l(1064|1330) \\
&+ P(X > 943) \times P_l(1197|1330) \\
&+ P(X > 810) \times P_l(1330|1330) \\
&+ P(X > 677) \times P_l(1463|1330) \\
&+ P(X > 544) \times P_l(1596|1330) \\
&+ P(X > 411) \times P_l(1729|1330) \ .
\end{aligned}$$

The next step is to obtain the $P(X > x)$ from the system's COPT and replace the $P_l(L_{a,i}|1330)$ with the corresponding values in Table 5.13.

$$\begin{aligned}
LOLP_{1330,DR} &= 1.06215 \times 10^{-04} \times 0.006 + 8.91782 \times 10^{-04} \times 0.061 \\
&+ 4.62301 \times 10^{-03} \times 0.242 + 0.016082 \times 0.382 \\
&+ 0.041943 \times 0.242 + 0.062312 \times 0.061 \\
&+ 0.127167 \times 0.006 \ .
\end{aligned}$$

When considering the 150-MW of demand response, the resulting hourly LOLP becomes 0.022031. This hourly LOLP is still higher than the hourly criterion that is our benchmark for the acceptable level of risk, which tells us that additional capacity must be procured.

In this case study, generators are identified as fast start units when they are not scheduled and they have a start up time equal to or less than 30

minutes. These fast start units are used for both time horizons although units with longer start up time could be considered in the day-ahead assessment. For the hour under study, the available fast start units are found in Table 5.14.

Table 5.14 Summer Day at 11PM: Day-ahead available fast start generators

Cap.[MW]	# Units	Fuel	Marg. cost[\$/MWh]	p _{down}	Start up[hrs]
20	1	Gas	105	0.0778	0.25
30	2	Gas	100	0.0778	0.25
50	3	Gas	90	0.0778	0.25
60	2	Gas	85	0.0778	0.30

For the purpose of this study, fast start units were chosen based on the lowest marginal cost. One fast start unit is added at a time as a two-state unit in the system's COPT until the LOLP (considering demand response) meet the hourly criterion. For the hour under study, only one 60-MW fast start unit was needed to reduce the hourly LOLP below the criterion. With this additional 60-MW unit, the new COPT consists of 104 possible capacity outage states with a maximum possible capacity C_s of 2050-MW. Part of the new COPT is found in Table 5.15.

The LOLP calculations are adjusted as follows when adding a 60-MW

Table 5.15 Summer Day at 11PM: Day-ahead COPT including additional fast start unit

Capacity outage states x [MW]	$P(X \geq x)$
0	1.000000
60	0.996416
120	0.959679
170	0.811242
180	0.811078
190	0.562160
...	...
530	0.070026
540	0.067501
550	0.063376
590	0.059293
...	...
1860	1.08584×10^{-11}
1870	1.07810×10^{-11}
1880	1.06792×10^{-12}
1930	9.48856×10^{-13}
1990	8.95845×10^{-14}
2050	5.44077×10^{-15}

fast start unit and still considering the 150-MW of demand response.

$$\begin{aligned}
 LOLP_{1330} &= P(X > 2050 - (931 - 150)) \times P_l(931|1330) \\
 &+ P(X > 2050 - (1064 - 150)) \times P_l(1064|1330) \\
 &+ P(X > 2050 - (1197 - 150)) \times P_l(1197|1330) \\
 &+ P(X > 2050 - (1330 - 150)) \times P_l(1330|1330) \\
 &+ P(X > 2050 - (1463 - 150)) \times P_l(1463|1330) \\
 &+ P(X > 2050 - (1596 - 150)) \times P_l(1596|1330) \\
 &+ P(X > 2050 - (1729 - 150)) \times P_l(1729|1330)
 \end{aligned}$$

or

$$\begin{aligned}
LOLP_{1330} &= P(X > 1269) \times P_l(931|1330) \\
&+ P(X > 1136) \times P_l(1064|1330) \\
&+ P(X > 1003) \times P_l(1197|1330) \\
&+ P(X > 870) \times P_l(1330|1330) \\
&+ P(X > 737) \times P_l(1463|1330) \\
&+ P(X > 604) \times P_l(1596|1330) \\
&+ P(X > 471) \times P_l(1729|1330) .
\end{aligned}$$

Then, obtain the $P(X > x)$ from the system's new COPT and replace the $P_l(L_{a,i}|1330)$ terms with the corresponding values in Table 5.13.

$$\begin{aligned}
LOLP_{1330,DR} &= 4.28070 \times 10^{-5} \times 0.006 + 4.01551 \times 10^{-4} \times 0.061 \\
&+ 2.25243 \times 10^{-3} \times 0.242 + 9.62261 \times 10^{-3} \times 0.382 \\
&+ 0.028385 \times 0.242 + 0.056457 \times 0.061 \\
&+ 0.087831 \times 0.006 .
\end{aligned}$$

When considering demand response and the additional fast start unit of 60-MW, the hourly LOLP is reduced to 0.015086, which is now below the hourly criterion of 0.02. The step-by-step approach described in this section was applied for both days and both time-horizons. The obtained results are presented and discussed in the following section.

5.6.4 Case Study Results

Following the step-by-step approach described in the previous section, day-ahead and hour-ahead operational assessments were performed for the daily system conditions presented in Table 5.6. For the summer day, we observe higher load forecasts with lower wind power forecasts, while we observe lower load forecasts with higher wind power forecasts for the winter day. Results are gathered in Figures 5.2, 5.3, 5.4 and 5.5, and will be discussed in the following sections.

5.6.5 Discussion

First and foremost, system operators equipped with the proposed reliability assessment tool would have a direct and quick means to track the system's operational generation adequacy status. This tool would enable operators to identify high risk periods in both day-ahead and hour-ahead time frames. As a complement to ancillary services requirements, the proposed assessment could ensure that enough total capacity is available to account for potential capacity outages, load forecasting deviations and wind power forecasting deviations. When necessary, adequate adjustments such as procuring additional generation could be made to maintain the acceptable level of risk. The actual amount of additional generation needed can also be determined with the proposed assessment tool. The main objective of the case study was to demonstrate these capabilities but also help the reader understand how to apply the method. Although the obtained results don't represent an ac-

Summer Day: Day-ahead Assessment												
Hour	Load forecast [MW]	Wind plant power output [MW]	Wind penetration [%]	Total conv. gen. scheduled [MW]	Total possible capacity [MW]	Margin [MW]	Total possible capacity with FS units [MW]	Margin FS [MW]	Additional fast start capacity [MW]	Day-ahead LOLP	Day-ahead LOLP with demand response	Day-ahead LOLP with demand response & fast start units
12:00 AM	1235	120	9.72	1500	1800	565	1970	735	170	0.0636	0.0375	0.0142
1:00 AM	1140	135	11.8	1260	1598	458	1868	728	270	0.1114	0.0572	0.0153
2:00 AM	1140	135	11.8	1260	1598	458	1868	728	270	0.1114	0.0572	0.0153
3:00 AM	1045	120	11.5	1260	1560	515	1730	685	170	0.0689	0.0427	0.0160
4:00 AM	1045	135	12.9	1140	1478	433	1748	703	270	0.1287	0.0564	0.0193
5:00 AM	1140	135	11.8	1260	1598	458	1868	728	270	0.1114	0.0572	0.0153
6:00 AM	1235	120	9.72	1500	1800	565	1970	735	170	0.0636	0.0375	0.0142
7:00 AM	1425	105	7.37	1690	1953	528	2123	698	170	0.0890	0.0425	0.0193
8:00 AM	1615	90	5.57	2010	2235	620	2355	740	120	0.0664	0.0292	0.0157
9:00 AM	1710	90	5.26	2110	2335	625	2455	745	120	0.0706	0.0307	0.0166
10:00 AM	1805	90	4.99	2210	2435	630	2555	750	120	0.0762	0.0331	0.0179
11:00 AM	1900	90	4.74	2310	2535	635	2655	755	120	0.0802	0.0347	0.0189
12:00 PM	1805	60	3.32	2210	2360	555	2480	675	120	0.0877	0.0371	0.0200
1:00 PM	1900	60	3.16	2310	2460	560	2630	730	170	0.0930	0.0396	0.0163
2:00 PM	1900	90	4.74	2310	2535	635	2655	755	120	0.0802	0.0347	0.0189
3:00 PM	1805	90	4.99	2210	2435	630	2555	750	120	0.0762	0.0331	0.0179
4:00 PM	1710	105	6.14	2010	2273	563	2443	733	170	0.1047	0.0453	0.0192
5:00 PM	1615	105	6.5	2010	2273	658	2393	778	120	0.0600	0.0284	0.0138
6:00 PM	1615	105	6.5	2010	2273	658	2393	778	120	0.0600	0.0284	0.0138
7:00 PM	1615	120	7.43	1880	2180	565	2400	785	220	0.1043	0.0485	0.0157
8:00 PM	1615	120	7.43	1880	2180	565	2400	785	220	0.1043	0.0485	0.0157
9:00 PM	1520	135	8.88	1880	2218	698	2278	758	60	0.0541	0.0251	0.0174
10:00 PM	1425	135	9.47	1690	2028	603	2198	773	170	0.0793	0.0340	0.0155
11:00 PM	1330	120	9.02	1690	1990	660	2050	720	60	0.0507	0.0220	0.0151

Figure 5.2 Summer Day: Day-ahead assessment results

Summer Day: Hour-ahead Assessment												
Hour	Load forecast [MW]	Wind plant power output [MW]	Wind penetration [%]	Total conv. gen. scheduled [MW]	Total possible capacity [MW]	Margin [MW]	Total possible capacity with FS units [MW]	Margin FS [MW]	Additional fast start capacity [MW]	Hour-ahead LOLP	Hour-ahead LOLP with demand response	Hour-ahead LOLP with demand response & fast start units
12:00 AM	1235	120	9.7	1500	1692	457	1812	577	120	0.0542	0.0384	0.0122
1:00 AM	1140	135	11.8	1260	1476	336	1696	556	220	0.0654	0.0528	0.0149
2:00 AM	1140	135	11.8	1260	1476	336	1696	556	220	0.0654	0.0528	0.0149
3:00 AM	1045	120	11.5	1260	1452	407	1572	527	120	0.0550	0.0507	0.0158
4:00 AM	1045	135	12.9	1140	1356	311	1576	531	220	0.0656	0.0528	0.0176
5:00 AM	1140	135	11.8	1260	1476	336	1696	556	220	0.0654	0.0528	0.0149
6:00 AM	1235	120	9.7	1500	1692	457	1812	577	120	0.0542	0.0384	0.0122
7:00 AM	1425	105	7.4	1690	1858	433	1978	553	120	0.0590	0.0468	0.0167
8:00 AM	1615	90	5.6	2010	2154	539	2214	599	60	0.0545	0.0202	0.0138
9:00 AM	1710	90	5.3	2110	2254	544	2314	604	60	0.0542	0.0208	0.0143
10:00 AM	1805	90	5.0	2210	2354	549	2414	609	60	0.0549	0.0219	0.0143
11:00 AM	1900	90	4.7	2310	2454	554	2514	614	60	0.0535	0.0219	0.0143
12:00 PM	1805	60	3.3	2210	2306	501	2366	561	60	0.0588	0.0255	0.0181
1:00 PM	1900	60	3.2	2310	2406	506	2466	566	60	0.0589	0.0266	0.0187
2:00 PM	1900	90	4.7	2310	2454	554	2514	614	60	0.0535	0.0219	0.0143
3:00 PM	1805	90	5.0	2210	2354	549	2414	609	60	0.0549	0.0219	0.0143
4:00 PM	1710	105	6.1	2010	2178	468	2298	588	120	0.0630	0.0355	0.0167
5:00 PM	1615	105	6.5	2010	2178	563	2178	563	0	0.0511	0.0183	0.0183
6:00 PM	1615	105	6.5	2010	2178	563	2178	563	0	0.0511	0.0183	0.0183
7:00 PM	1615	120	7.4	1880	2072	457	2192	577	120	0.0634	0.0411	0.0174
8:00 PM	1615	120	7.4	1880	2072	457	2192	577	120	0.0634	0.0411	0.0174
9:00 PM	1520	135	8.9	1880	2096	576	2096	576	0	0.0503	0.0165	0.0165
10:00 PM	1425	135	9.5	1690	1906	481	1966	541	60	0.0564	0.0320	0.0189
11:00 PM	1330	120	9.0	1690	1882	552	1882	552	0	0.0518	0.0156	0.0156

Figure 5.3 Summer Day: Hour-ahead assessment results

Winter Day: Day-ahead Assessment												
Hour	Load forecast [MW]	Wind plant power output [MW]	Wind penetration [%]	Total conv. gen. scheduled [MW]	Total possible capacity [MW]	Margin [MW]	Total possible capacity with FS units [MW]	Margin FS [MW]	Additional fast start capacity [MW]	Day-ahead LOLP	Day-ahead LOLP with demand response	Day-ahead LOLP with demand response & fast start units
12:00 AM	960	210	21.9	1020	1545	585	1815	855	270	0.1147	0.0506	0.0140
1:00 AM	960	195	20.3	1020	1508	548	1778	818	270	0.1209	0.0512	0.0143
2:00 AM	960	195	20.3	1020	1508	548	1778	818	270	0.1209	0.0512	0.0143
3:00 AM	880	195	22.2	900	1388	508	1688	808	300	0.1162	0.0549	0.0145
4:00 AM	960	195	20.3	1020	1508	548	1778	818	270	0.1209	0.0512	0.0143
5:00 AM	1040	180	17.3	1140	1590	550	1810	770	220	0.1133	0.0511	0.0188
6:00 AM	1120	180	16.1	1260	1710	590	1880	760	170	0.0866	0.0418	0.0194
7:00 AM	1360	180	13.2	1500	1950	590	2170	810	220	0.1089	0.0492	0.0163
8:00 AM	1520	165	10.9	1880	2293	773	2353	833	60	0.0504	0.0221	0.0160
9:00 AM	1600	150	9.4	1880	2255	655	2425	825	170	0.0831	0.0383	0.0156
10:00 AM	1600	150	9.4	1880	2255	655	2425	825	170	0.0831	0.0383	0.0156
11:00 AM	1520	135	8.9	1880	2218	698	2278	758	60	0.0541	0.0251	0.0174
12:00 PM	1440	150	10.4	1690	2065	625	2235	795	170	0.0837	0.0357	0.0156
1:00 PM	1440	150	10.4	1690	2065	625	2235	795	170	0.0837	0.0357	0.0156
2:00 PM	1440	150	10.4	1690	2065	625	2235	795	170	0.0837	0.0357	0.0156
3:00 PM	1360	165	12.1	1500	1913	553	2133	773	220	0.1184	0.0537	0.0196
4:00 PM	1440	165	11.5	1690	2103	663	2273	833	170	0.0758	0.0342	0.0146
5:00 PM	1440	180	12.5	1690	2140	700	2260	820	120	0.0724	0.0329	0.0168
6:00 PM	1520	180	11.8	1690	2140	620	2360	840	220	0.1164	0.0514	0.0171
7:00 PM	1520	195	12.8	1690	2178	658	2398	878	220	0.1127	0.0503	0.0161
8:00 PM	1440	195	13.5	1690	2178	738	2298	858	120	0.0688	0.0324	0.0165
9:00 PM	1440	210	14.6	1690	2215	775	2335	895	120	0.0632	0.0294	0.0153
10:00 PM	1280	210	16.4	1380	1905	625	2125	845	220	0.1187	0.0508	0.0165
11:00 PM	1120	210	18.8	1140	1665	545	1965	845	300	0.1346	0.0663	0.0154

Figure 5.4 Winter Day: Day-ahead assessment results

Winter Day: Hour-ahead Assessment												
Hour	Load forecast [MW]	Wind plant power output [MW]	Wind penetration [%]	Total conv. gen. scheduled [MW]	Total possible capacity [MW]	Margin [MW]	Total possible capacity with FS units [MW]	Margin FS [MW]	Additional fast start capacity [MW]	Hour-ahead LOLP	Hour-ahead LOLP with demand response	Hour-ahead LOLP with demand response & fast start units
12:00 AM	960	210	21.9	1020	1545	585	1815	855	270	0.0583	0.0523	0.0106
1:00 AM	960	195	20.3	1020	1508	548	1778	818	270	0.0602	0.0525	0.0133
2:00 AM	960	195	20.3	1020	1508	548	1778	818	270	0.0602	0.0525	0.0133
3:00 AM	880	195	22.2	900	1388	508	1688	808	300	0.0698	0.0529	0.0105
4:00 AM	960	195	20.3	1020	1508	548	1778	818	270	0.0602	0.0525	0.0133
5:00 AM	1040	180	17.3	1140	1590	550	1810	770	220	0.0589	0.0523	0.0185
6:00 AM	1120	180	16.1	1260	1710	590	1880	760	170	0.0572	0.0507	0.0123
7:00 AM	1360	180	13.2	1500	1950	590	2170	810	220	0.0606	0.0510	0.0154
8:00 AM	1520	165	10.9	1880	2293	773	2353	833	60	0.0414	0.0136	0.0136
9:00 AM	1600	150	9.4	1880	2255	655	2425	825	170	0.0579	0.0276	0.0183
10:00 AM	1600	150	9.4	1880	2255	655	2425	825	170	0.0579	0.0276	0.0183
11:00 AM	1520	135	8.9	1880	2218	698	2278	758	60	0.0503	0.0165	0.0165
12:00 PM	1440	150	10.4	1690	2065	625	2235	795	170	0.0564	0.0320	0.0187
1:00 PM	1440	150	10.4	1690	2065	625	2235	795	170	0.0564	0.0320	0.0187
2:00 PM	1440	150	10.4	1690	2065	625	2235	795	170	0.0564	0.0320	0.0187
3:00 PM	1360	165	12.1	1500	1913	553	2133	773	220	0.0625	0.0524	0.0175
4:00 PM	1440	165	11.5	1690	2103	663	2273	833	170	0.0559	0.0297	0.0178
5:00 PM	1440	180	12.5	1690	2140	700	2260	820	120	0.0548	0.0256	0.0165
6:00 PM	1520	180	11.8	1690	2140	620	2360	840	220	0.0633	0.0478	0.0196
7:00 PM	1520	195	12.8	1690	2178	658	2398	878	220	0.0615	0.0437	0.0179
8:00 PM	1440	195	13.5	1690	2178	738	2298	858	120	0.0537	0.0220	0.0146
9:00 PM	1440	210	14.6	1690	2215	775	2335	895	120	0.0526	0.0200	0.0121
10:00 PM	1280	210	16.4	1380	1905	625	2125	845	220	0.0602	0.0510	0.0158
11:00 PM	1120	210	18.8	1140	1665	545	1965	845	300	0.0718	0.0532	0.0194

Figure 5.5 Winter Day: Hour-ahead assessment results

tual power system with real forecasting deviations, we can still discuss certain observations. However, keep in mind that LOLP calculations are highly non-linear and absolute conclusions shouldn't be drawn. It will be shown that results are not necessarily intuitive but are highly dependent on the actual system conditions used in the calculations. Intuitions don't cope well with non-linearity - consequently one should always rely on the calculations.

5.6.5.1 Effect of Demand Response and Fast Start Units on LOLP

Figures 5.6, 5.7, 5.8 and 5.9 present the effect of demand response and fast start units on the hourly LOLP. For both days and both time horizons, demand response effectively reduces the hourly LOLP. The margin $C_s - (L_{a,i} - DR)$ is greater in the presence of demand response and therefore more generators would have to be on simultaneous capacity outage for a loss of load to occur. The likelihood of having more generators on forced outage all at the same time is less probable and consequently considering demand response will lower the LOLP. Adding fast start units also has the effect of increasing the margin and therefore reducing the LOLP. In this case study, fast start units were added only if the LOLP with demand response was higher than the hourly criterion. In all hours under study, the hourly LOLP was effectively reduced when additional fast start units were included in the assessment. The exact amount of fast start capacity can be found in the overall tabulated results given in Section 5.6.4.

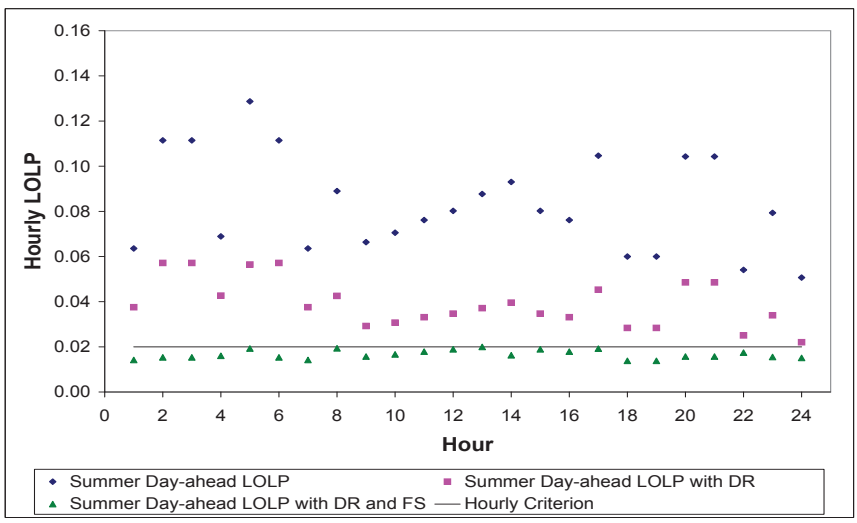


Figure 5.6 Summer Day Day-ahead Assessment: Effects of demand response (DR) and fast start units (FS) on LOLP

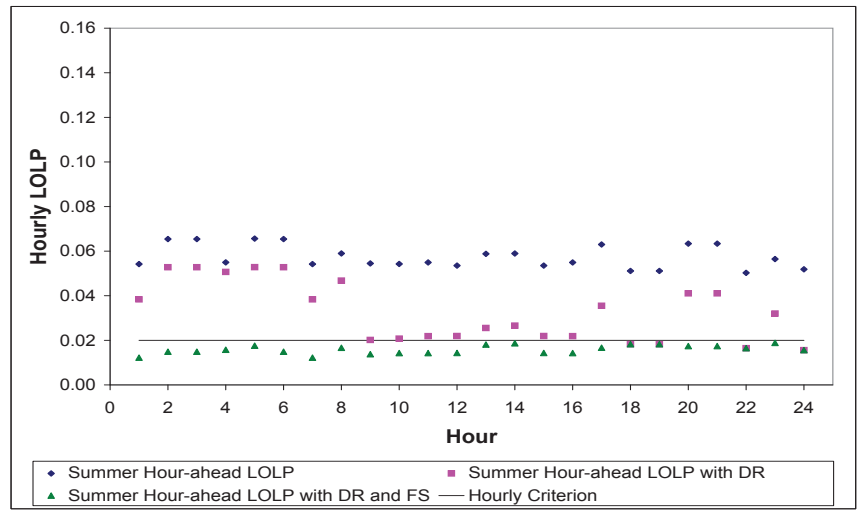


Figure 5.7 Summer Day Hour-ahead Assessment: Effects of demand response (DR) and fast start units (FS) on LOLP

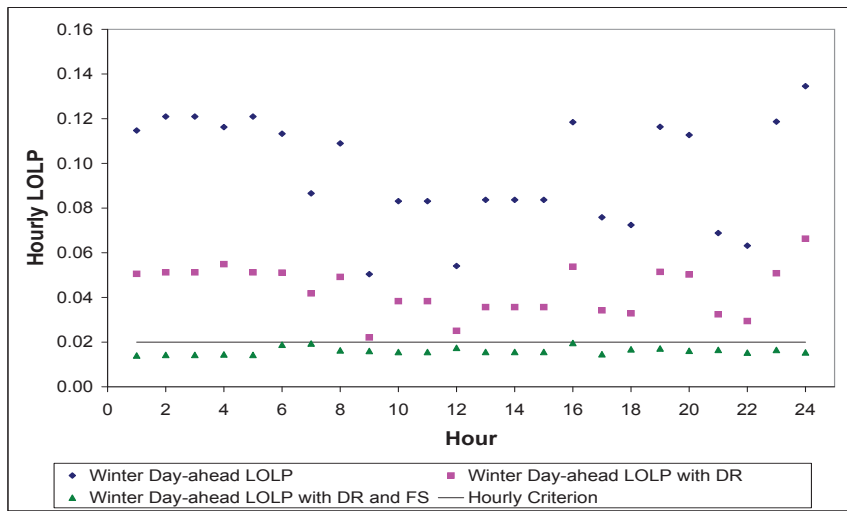


Figure 5.8 Winter Day Day-ahead Assessment: Effects of demand response (DR) and fast start units (FS) on LOLP

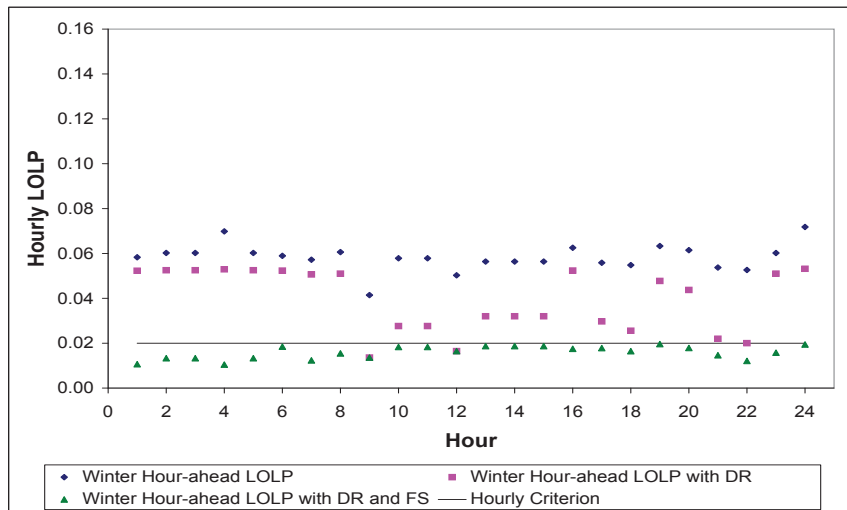


Figure 5.9 Winter Day Hour-ahead Assessment: Effects of demand response (DR) and fast start units (FS) on LOLP

5.6.5.2 Comparing Hour-ahead vs. Day-ahead Results

The forecasting deviations used in this case study are defined such that hour-ahead forecasts are more likely to be accurate than day-ahead forecasts. In this case, since system conditions and generation schedules were the same in both time-horizons, one would intuitively expect the hour-ahead LOLP results to be lower than the day-ahead LOLP results; yet it turns out that this is not necessarily always the case. Indeed, it is true that for the summer day results in Tables 5.3 and 5.2, all hour-ahead LOLPs are lower than day-ahead LOLPs except at 11PM. Even if the generation scheduled are the same for both time horizons, the respective COPTs will be different since wind power forecasting deviations and corresponding resulting wind power multi-state representations are not the same. The different load forecasting deviations will also affect the LOLP calculations. The day-ahead calculations for the summer day at 11PM were presented in the step-by-step section and resulted in a hourly LOLP of 0.050677; let's look at the hour-ahead calculations for comparison.

For a forecast of 120-MW, the hour-ahead wind power forecasting deviations distribution will present a standard deviation of 20% instead of 50% and can be found in Table 5.16. For the purpose of building the COPT, the wind plant can be seen as a multi-state unit with maximum possible capacity of 192-MW and the multi-state representation of Table 5.17.

Given this new wind power multi-state representation but the same generation schedule shown on Table 5.9, the hour-ahead COPT for the summer day at 11PM is represented with a new set of possible capacity outage states

Table 5.16 Summer Day at 11PM: Hour-ahead wind power forecasting deviations for a 120-MW forecast

Possible actual wind power $W_{a,k}$ [MW]	Probability $P_w(W_{a,k} W_f)$
48	0.006
72	0.061
96	0.242
120	0.382
144	0.242
168	0.061
192	0.006

Table 5.17 Summer Day at 11PM: Hour-ahead wind plant multi-state representation for a 120-MW forecast (Note that the capacity outage state of 192-MW has no impact on the whole system's COPT. However, it must be considered in the maximum possible capacity of the system C_s when computing the LOLP.)

Capacity outage C_j [MW]	Individual probability p_j
192	0
144	0.006
120	0.061
96	0.242
72	0.382
48	0.242
24	0.061
0	0.006

and cumulative probabilities. The complete COPT consists of 384 possible capacity outage states and is partly represented in Table 5.18. Note that the maximum possible *capacity outage state* is 1834-MW, even though the maximum possible system *capacity* is 1882-MW. Indeed, since the wind plant is being represented as a multi-state unit with a maximum possible capacity

of 192-MW but minimal power output of 48-MW, it is impossible to have all 1882-MW on forced outage.

Table 5.18 Summer Day at 11PM: Hour-ahead hourly COPT

Capacity outage states x [MW]	$P(X \geq x)$
0	1.000000
24	0.996114
48	0.956605
72	0.799866
96	0.552451
120	0.395712
...	...
530	0.053684
538	0.053646
540	0.053531
542	0.053493
...	...
1714	1.72275E-12
1738	9.73840E-13
1762	7.21247E-13
1786	3.22526E-13
1810	6.99328E-14
1834	6.26264E-15

The hour-ahead load forecast's distribution found in Table 5.19 considers a standard deviation of 2% the forecasted load.

Table 5.19 Summer Day at 11PM: Hour-ahead load reliability model for 1330-MW forecast

Possible actual load $L_{a,i}$ [MW]	Probability $P_l(L_{a,i} 1330)$
1250.2	0.006
1276.8	0.061
1303.4	0.242
1330	0.382
1356.6	0.242
1383.2	0.061
1409.8	0.006

Finally, the hour-ahead LOLP calculations are performed as follows:

$$\begin{aligned}
 LOLP_{1330} = & P(X > 1834 - 1250.2) \times P_l(1250.2|1330) \\
 & + P(X > 1834 - 1276.8) \times P_l(1276.8|1330) \\
 & + P(X > 1834 - 1303.4) \times P_l(1303.4|1330) \\
 & + P(X > 1834 - 1330) \times P_l(1330|1330) \\
 & + P(X > 1834 - 1356.6) \times P_l(1356.6|1330) \\
 & + P(X > 1834 - 1383.2) \times P_l(1383.2|1330) \\
 & + P(X > 1834 - 1409.8) \times P_l(1409.8|1330)
 \end{aligned}$$

$$\begin{aligned}
LOLP_{1330} &= P(X > 631.8) \times P_l(1250.2|1330) \\
&+ P(X > 605.2) \times P_l(1276.8|1330) \\
&+ P(X > 578.6) \times P_l(1303.4|1330) \\
&+ P(X > 552) \times P_l(1330|1330) \\
&+ P(X > 525.4) \times P_l(1356.6|1330) \\
&+ P(X > 498.8) \times P_l(1383.2|1330) \\
&+ P(X > 472.2) \times P_l(1409.8|1330) \ .
\end{aligned}$$

Reading the $P(X > x)$ from the system's COPT and replacing the $P_l(L_{a,i}|1330)$ with the corresponding probability from the load model in Table 5.19, the final LOLP is obtained from the following calculations:

$$\begin{aligned}
LOLP_{1330} &= 0.027749 \times 0.006 + 0.041485 \times 0.061 \\
&+ 0.050332 \times 0.242 + 0.052915 \times 0.382 \\
&+ 0.054033 \times 0.242 + 0.054857 \times 0.061 \\
&+ 0.055884 \times 0.006 \ .
\end{aligned}$$

The resulting hour-ahead LOLP amounts to 0.051849, which is higher than the day-ahead results of 0.050677. These results, as we pointed out above, go against what would intuitively be expected: a better hour-ahead LOLP since forecasting deviations are more accurate. But because LOLP calculations are highly non-linear, when system conditions or even only forecasting deviations change, it is hard to predict what effect it will have on the calculated risk. When a set of generator models are convolved together it will

create a certain set of possible capacity outage states and corresponding cumulative probabilities; when we change one of the generator's models, as in the case of the wind plant, a whole new set of possible outage states and corresponding cumulative probabilities will be created. Furthermore, depending on the total possible capacity of the system and the load distribution, conditional LOLPs will also vary. The bottom line is that one should always rely on the calculations to determine the operational risk level. Figure 5.11 and 5.10 compare hour-ahead and day-ahead results for both days. For the winter day, all hour-ahead LOLPs happen to be lower than day-ahead LOLPs. In the next section, it will be shown that the effect of wind penetration level can produce results that also seem counterintuitive.

5.6.5.3 Effect of Wind Penetration Level on Hourly LOLP

If wind penetration is described as the forecasted wind power output divided by the forecasted load, one might expect to see higher risk levels when wind penetration is high. However, this is not necessarily the case. As seen in Figure 5.12, high LOLPs are not necessarily tied to high wind penetration levels; rather, the calculated LOLP depends on multiple variables and how they merge together in the calculations. Not only does wind forecast and forecasting deviations come into play, but also the load forecast and forecasting deviations, the total capacity available and the mix of generators and their unavailabilities. Furthermore, in the case of a symmetric wind power forecasting deviations distribution, wind power output can take higher values leading

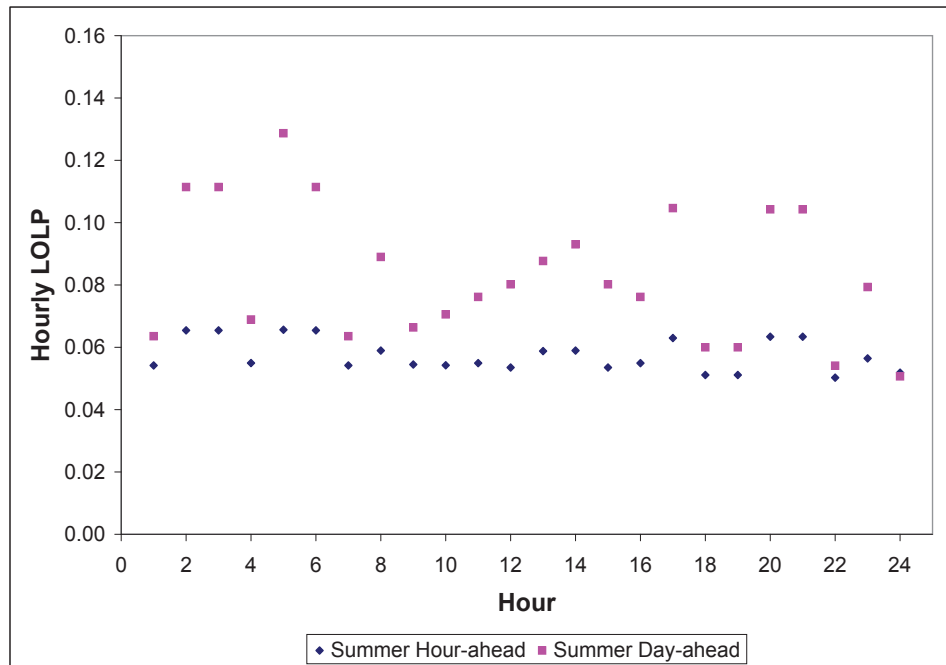


Figure 5.10 Summer Day: Day-ahead against hour-ahead hourly LOLP results

to the possibility of more capacity in the system. Perhaps if high wind levels were constantly overforecasted, one might see riskier periods with high wind penetration levels. However, a system characteristic that is more likely to be related to high LOLPs is the capacity margin $C_s - L_f$, which will be discussed in the next section.

5.6.5.4 Effect of Capacity Margin on Hourly LOLP

Figure 5.13 presents the relationship between the hourly capacity margin $C_s - L_f$ and the hourly LOLP for both days and both time horizons. It can

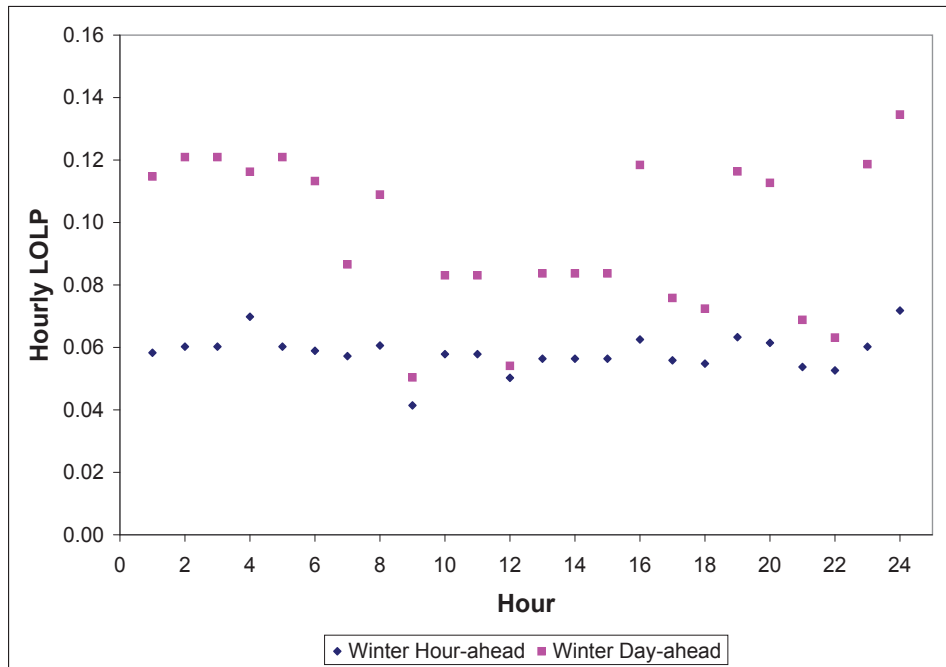


Figure 5.11 Winter Day: Day-ahead against hour-ahead hourly LOLP results

be seen from the figure that LOLPs are more likely to be lower when margins are higher. Keep in mind however, that system conditions are different from hour to hour; the load, the wind, the scheduled generation all vary, and the system is essentially a different one every hour. Again, because of the nature of the calculations, even if there is a general tendency to have lower LOLPs for higher margins, this relationship is not linear. Furthermore, the results suggest that using a fixed capacity margin reliability criteria, such as the loss of the largest unit reserve, could actually result in high levels of risk. For example, margins of around 550-MW results in LOLPs between 0.05 to 0.13.

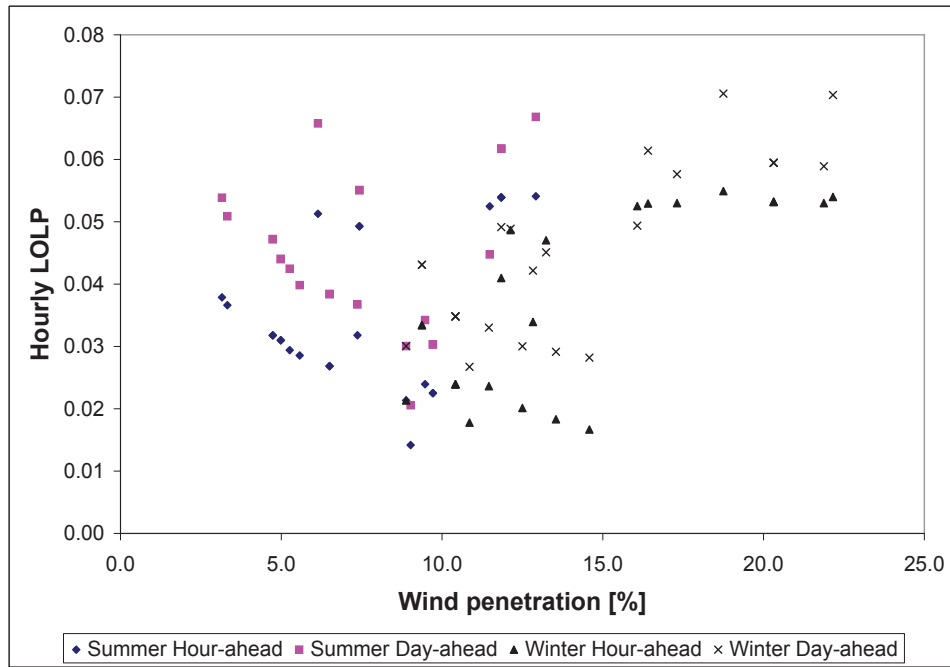


Figure 5.12 Effect of wind penetration on hourly LOLP

Again, expecting the system to behave a certain way corresponding to changes in the system conditions could turn out to be erroneous; one should always rely on the calculations.

5.6.5.5 Effect of Large Units on the LOLP

Finally, when a relatively large unit is scheduled relative to the scheduled maximum possible capacity, it will have a significant effect on the calculated hourly LOLP. Indeed, in the test system, the 550-MW baseload generator has a significant effect on the risk level. When this unit's unavailability was changed from 0.0522 to 0.02 and all other variables were kept constant, the

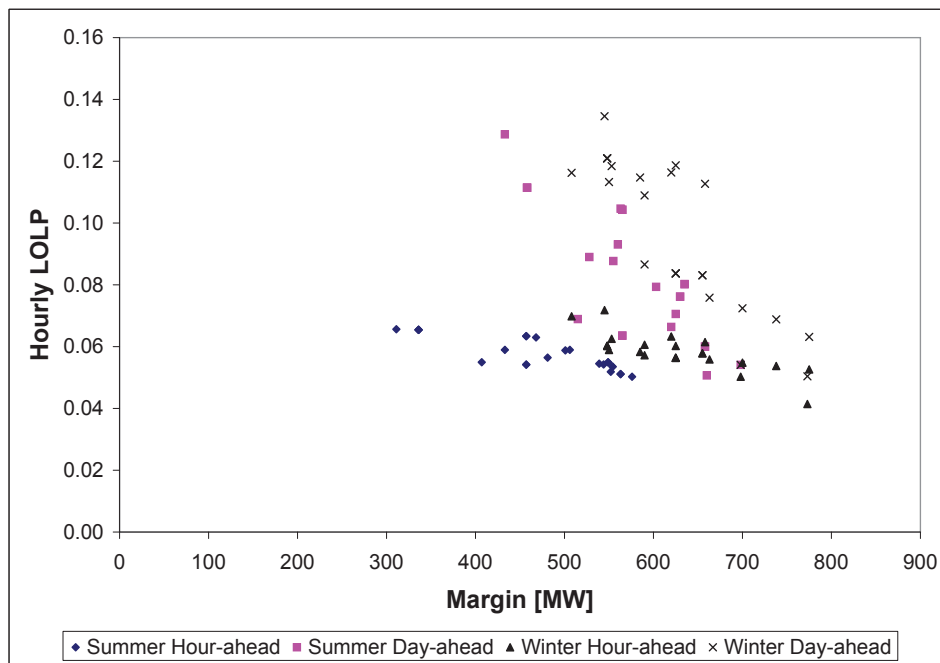


Figure 5.13 Effect of capacity margin on hourly LOLP

resulting hourly LOLPs were significantly reduced. Figure 5.14 depicts this effect for the summer day day-ahead assessment. In this case study, the 550-MW unit was modeled with a two-state representation for simplicity, but since a large unit has such a large impact on the LOLP result, the best practice would be to model it as accurately as possible. Consequently, if derated states are possible, they should be taken into account by modeling the unit with a multi-state representation. The larger the unit in comparison with the maximum possible capacity scheduled, the more weight it will have on the LOLP results.

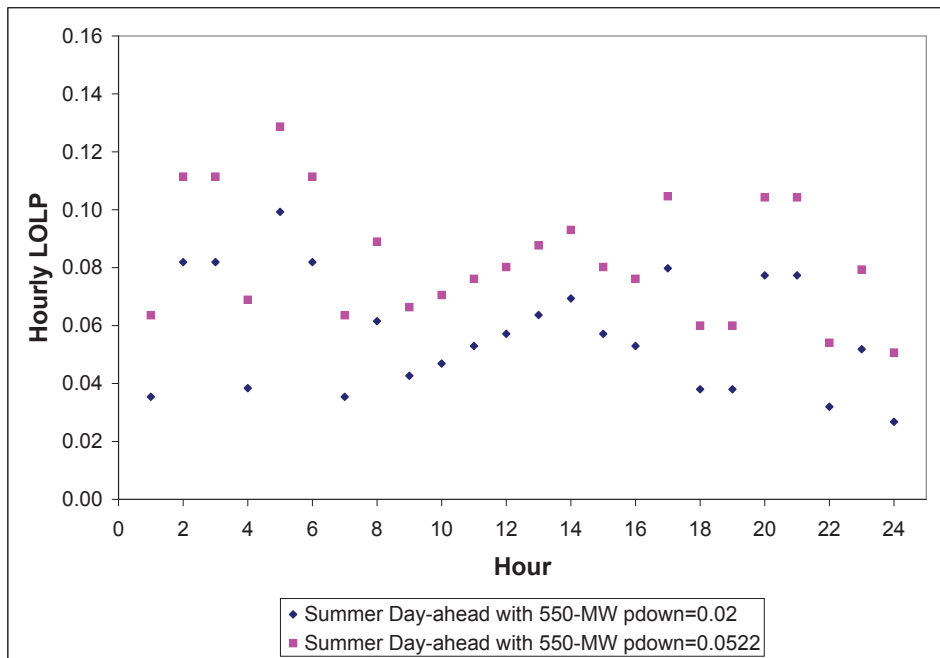


Figure 5.14 Summer Day Day-ahead Assessment: Effect of large units on LOLP

5.6.6 Concluding Remarks

In this chapter, an operational reliability assessment tool has been proposed to assist operators in quantitatively evaluating the system’s operational generation adequacy while considering generator forced outages, load and wind power forecasts and forecasting deviations. Using the loss-of-load probability metric from an operational perspective, operators will be able to identify high risk periods both on a day-ahead and hour-ahead horizon. When the scheduled generation doesn’t ensure an acceptable risk level, the risk assessment can include demand response and even determine the fast start generation to

meet the risk criterion. Since LOLP calculations are highly non-linear and dependent on various variables, resulting hourly LOLPs should be carefully interpreted. If system conditions or forecasting deviations change, one should always rely on the calculations to determine the operational risk level. The success of the proposed concept is contingent on having accurate system-specific load and wind forecasting deviations as well as on determining an acceptable hourly risk criterion.

Chapter 6

Summary and Conclusion

Although new wind plants are now capable of offering low-voltage ride-through, voltage control and reactive power capabilities just like conventional generation, they remain a variable, uncertain and non-dispatchable source of electric power. When wind generation formed only an insignificant portion of generation portfolios, existing system capabilities and operations processes were capable of handling its variable and uncertain nature. However, the increasing presence of wind generation is creating new challenges for both system planners and system operators. Among these challenges is the need to ensure generation adequacy. Obviously, when it comes to maintaining power system reliability, the primary objective must be to avoid falling short of generating capacity. In this dissertation, we investigated and assessed the planning and operational generation adequacy of power systems with significant wind generation.

In Chapter 2, we reviewed the key metrics determining a power system's generation adequacy assessment based on loss-of-load analytical methods. The concepts of loss-of-load probability, loss-of-load expectation, and the capacity outage probability table, along with conventional generating unit's reliability

modeling were all presented to obtain a framework for assessing generation adequacy. With these key metrics understood, we moved on, in Chapter 3, to clearly describe how to integrate wind plants in term of these assessments methods. Indeed, in this chapter, we provided a detailed methodology for appropriately integrating wind plants in system planning-based loss-of-load calculations. Through the examination of a case study, we demonstrated that wind generation can indeed contribute to the generation adequacy of power systems. Results from this case study suggested that at penetration levels of 5%, a wind plant could reduce the loss-of-load expectation metric to the same extent as an energy equivalent conventional unit [20]. However, at higher penetration levels the wind plants were less efficient at improving the risk metric.

In Chapter 4, a wind plant's capacity contribution was quantified using the concept of effective load carrying capability. In addition to providing a detailed methodology and applying the conventional ELCC calculations to several case studies, a novel non-iterative approximation was introduced and yielded accurate¹ ELCC estimates while requiring less reliability modeling and being less computationally-intensive. Case study findings suggested the importance of period-specific ELCC calculations as a means to better evaluate the *variable* reliability contribution of wind plants [22, 23]. Furthermore, relevant evaluation periods should be system and wind plant dependent and reflect

¹Percent relative errors between the non-iterative method estimates and the classically-computed ELCC values averaged around 2%.

interannual variability and possible wind/load correlation.

Chapter 2 to 4 provided the necessary concepts and methodologies to ensure that wind plants are adequately integrated in the generation adequacy assessment from a system planning perspective. Even in well planned systems, system operators are responsible for constantly monitoring and matching the system generation to the load demand and from this operational perspective, the variable and uncertain nature of wind generation still presents significant challenges. To maintain security and reliability of supply, monthly or annual ancillary service requirements are determined usually based on a system's historical performance. Since these requirements may or may not capture the wind generation's uncertainty in the operational time frame, being able to assess the operational generation adequacy would be very beneficial for system operators. To address this need, Chapter 5 proposes an operational reliability assessment tool to assist operators in quantitatively evaluating the system's operational generation adequacy, while considering generator forced outages, load and wind power forecasts and forecasting deviations [24]. The core of the reliability assessment tool was to apply the loss-of-load probability metric from a operational perspective by considering hourly forecasted load and wind power information and comparing the resulting computed risk to an acceptable criterion. The feasibility of the proposed concept was examined through a reproducible case study. We concluded that if system operators were equipped with the proposed tool, they would be able to identify high risk periods in both day-ahead and hour-ahead horizons and make the necessary adjustments to

ensure acceptable levels of operational system reliability. Since LOLP calculations are highly non-linear and dependent on various variables, resulting hourly LOLPs need to be carefully interpreted. It was noted that if system conditions or forecasting deviations change, one should always rely on the calculations, rather than intuitions, to determine the operational risk level. Foremost, we pointed out that the success of the proposed operational assessment tool is not only contingent on having accurate system-specific load and wind forecasting deviations, but also on the determination of an acceptable risk criterion.

Appendices

Appendix A

Combined-Cycle Plant Reliability Modeling

Reference [35] addresses the importance of representing the operating characteristics of combined-cycle plants when performing generation adequacy assessment with loss-of-load analytical methods. Instead of assuming that the steam and gas units of a combined-cycle plant function independently, a model based on dispatch patterns is proposed to consider the joint operating characteristics. As is shown in [35], neglecting these operating characteristics may lead to over-optimistic LOLP results for power systems with significant combined-cycle generation. Furthermore, when plant-specific dispatch patterns are unavailable, a generic model is proposed to accurately estimate the actual LOLP of the system. This appendix summarizes the key concepts of the proposed combined-cycle plant reliability models.

A.1 Combined-Cycle Plants

Combined-cycle plants (CC plant) are usually composed of one or more high-temperature gas turbines (GTs) that are combined with a low-temperature steam turbine (ST). Combined-cycle plants usually fall in two categories: single-shaft and multi-shaft plants. Single-shaft plants consist of

one GT and one ST while multi-shaft plants usually consist of multiple GTs combined with one ST. The ST uses the energy from the GTs' exhaust gas. Therefore, the ST's power output is dependent on the availability of the GTs. When a GT in a multi-shaft plant becomes unavailable due to some forced outage, the ST's power output may be reduced or even shut down. Considering that the units of a combined cycle plant act separately when we are building the system's reliability model will not reflect this operating characteristic. For example, Table A.1 represents the unavailability probability of the units of a 3GT-1ST combined-cycle plant.

Table A.1 Example: Combined-cycle units unavailability

	Size [MW]	p_{down}
GT 1	50	0.0864
GT 2	50	0.0864
GT 3	50	0.0864
ST	150	0.0697

Again, each generating unit could be added separately to the COPT with a two-state reliability model by ignoring the combined-cycle operation of the plant. However, [35] shows us why this may yield over-optimistic LOLP results. Therefore, two different models are proposed to account for the operating characteristics of CC plants: a plant-specific dispatch model and a generic dispatch model. In addition to the separate unit unavailability information, further logic must be considered to build the representative CC plant models. The first approach uses the plant's actual dispatch pattern while the

other applies a generic dispatch and can be used when plant-specific dispatch patterns are unavailable. The generic approach provides decent estimates of the actual LOLP.

A.2 Plant-Specific Dispatch Model

First, the availability matrix of the combined-cycle plant is built without any combined-cycle operations. This matrix consists of the possible power output states with their corresponding probability, which is computed by multiplying the appropriate p_{down} and p_{up} (or $1 - p_{down}$) values. Table A.2 represents the availability matrix for our example in Table A.1, where 1 means the unit is available and 0 means the unit is on forced outage and therefore unavailable. In order to accurately determine the combined-cycle plant's unknown capacity outputs (Cap. In and Cap. Out¹) in Table A.2, the plant's dispatch patterns must be known. In some cases, the plant might have a minimum number of GTs required to allow any output on the ST. In other cases, when a reduced number of GTs are present, the associated reduction in the ST's output might not be proportional to the GTs' reduced total output. Table A.3 presents the dispatch patterns of our example.

From Table A.3, we note that this particular plant requires a minimum of two GTs for the ST to have an output. Furthermore, when the number

¹Cap. In refers to the actual capacity outputs and Cap. Out refers to the capacity outages calculated by subtracting the Cap. In from the total possible capacity of the combined-cycle plant

Table A.2 Example: Initial combined-cycle plant availability matrix

GT1 50-MW	GT2 50-MW	GT3 50-MW	ST 150-MW	Cap. In [MW]	Cap. Out [MW]	Individual probability
1	1	1	1	300	0	0.7094
0	1	1	1	?	?	0.06709
1	0	1	1	?	?	0.06709
0	0	1	1	?	?	0.006345
1	1	0	1	?	?	0.06709
0	1	0	1	?	?	0.006345
1	0	0	1	?	?	0.006345
0	0	0	1	?	?	0.0006000
1	1	1	0	150	150	0.05315
0	1	1	0	100	200	0.005026
1	0	1	0	100	200	0.005026
0	0	1	0	50	250	0.0004754
1	1	0	0	50	250	0.005026
0	1	0	0	50	250	0.0004754
1	0	0	0	50	250	0.0004754
0	0	0	0	0	300	0.00004495

of GTs is less than the original three units, the ST's output is not reduced in proportion; the pattern displays a particular reduction ratio. Using the information provided by the dispatch pattern, we can complete the unknown capacity values in the availability matrix of Table A.2. The complete availability matrix is presented in Table A.4. Note that because of the minimum requirement of 2 GTs for the ST to function, when only one GT is available, the ST will not produce any output even if it is available. Although the ST's power output is dependent on the GTs, the GTs can function independently from the ST.

Table A.3 Example: Plant-specific dispatch patterns for the 3GT-1ST combined-cycle plant

Dispatch Block	GT1 Gross MW	GT2 Gross MW	GT3 Gross MW	ST Gross MW
DB-1	50	50	50	150
DB-2	50	0	50	80
DB-3	50	50	0	80
DB-4	0	50	50	80
DB-5	50	50	50	0
DB-6	50	50	0	0
DB-7	50	0	50	0
DB-8	0	50	50	0
DB-9	50	0	0	0
DB-10	0	50	0	0
DB-11	0	0	50	0

The availability matrix in Table A.4 can be reduced to a multi-state representation with corresponding partial capacity outage states and individual probabilities. If a particular capacity outage state can occur from different unit combinations, the probabilities are simply given by being summed up. For example, a capacity outage of 300-MW can occur two different ways: if all units are unavailable or if all GTs are unavailable. Therefore, the probability of a capacity outage of 300-MW is equal to $0.0006000+0.0000450=0.0006450$. Table A.5 represents the multi-state model of our CC plant.

A.3 Generic Dispatch Model

When plant-specific dispatch patterns are not available, the generic dispatch model can be used to estimate the ST's derated states. In this model

Table A.4 Example: Complete combined-cycle availability matrix
(The symbol * indicates when the minimum requirement of 2 GT is not met)

GT1 50-MW	GT2 50-MW	GT3 50-MW	ST 150-MW	Cap. In [MW]	Cap. Out [MW]	Individual probability
1	1	1	1	300	0	0.7094
0	1	1	1	180	120	0.06709
1	0	1	1	180	120	0.06709
0	0	1	1	50*	250	0.006345
1	1	0	1	180	120	0.06709
0	1	0	1	50*	250	0.006345
1	0	0	1	50*	250	0.006345
0	0	0	1	0	300	0.0006000
1	1	1	0	150	150	0.05315
0	1	1	0	100	200	0.005026
1	0	1	0	100	200	0.005026
0	0	1	0	50	250	0.0004754
1	1	0	0	50	250	0.005026
0	1	0	0	50	250	0.0004754
1	0	0	0	50	250	0.0004754
0	0	0	0	0	300	0.00004495

Table A.5 Example: Combined-cycle plant multi-state representation using the plant-specific dispatch model

Capacity outage states C_j [MW]	Individual prob. p_j
0	0.7094
120	0.2013
150	0.05315
200	0.01508
250	0.02046
300	0.0006450

the ST's output is reduced proportionally to the GTs' power output reduction. For example, when GTs are reduced from 150-MW (or 50+50+50-MW) to 100-MW (or 50+50-MW), the ST's output is reduced to 100-MW (or $100/150 \times 150$ -MW). The generic dispatch pattern for the example unit is presented in Table A.6. Using the same approach, the generic dispatch model can be reduced to

Table A.6 Example: Generic dispatch patterns for the 3GT-1ST combined-cycle plant

Dispatch Block	GT1 Gross [MW]	GT2 Gross [MW]	GT3 Gross [MW]	ST Gross [MW]
DB-1	50	50	50	150
DB-2	50	0	50	100
DB-3	50	50	0	100
DB-4	0	50	50	100
DB-5	50	50	50	0
DB-6	50	50	0	0
DB-7	50	0	50	0
DB-8	0	50	50	0
DB-9	50	0	0	50
DB-10	0	50	0	50
DB-11	0	0	50	50
DB-12	50	0	0	0
DB-13	0	50	0	0
DB-14	0	0	50	0

the multi-state representation of Table A.7, which is slightly different than the plant-specific dispatch representation.

Table A.7 Example: Combined-cycle plant multi-state representation using the generic dispatch model

Capacity outage states C_j [MW]	Individual prob. p_j
0	0.7094
100	0.2013
150	0.05315
200	0.03411
250	0.001426
300	0.0006450

A.4 Concluding Remarks

In contradistinction from the cases we have been presenting, building a multi-state representation while considering all units independent from each other would result in a significantly different representation as seen in Table A.8.

Table A.8 Example: Combined-cycle plant multi-state representation considering independent units

Capacity outage states C_j [MW]	Individual prob. p_j
0	0.7094
50	0.2013
100	0.01903
150	0.05375
200	0.01508
250	0.001426
300	0.00004495

Combined-cycle plants must be adequately represented in LOLP cal-

culations, especially when they represent a significant portion of a generation portfolio. More details on the proposed combined-cycle models are presented in [35], where the concept is applied to a case study.

Bibliography

- [1] American Wind Energy Association. Installed U.S. wind power capacity surged 45% in 2007, January 2008.
[Online] <http://www.awea.org/newsroom/releases/>.
- [2] R. Thresher et al. To capture the wind. *IEEE Power & Energy Magazine*, 5(6):34–46, November/December 2007.
- [3] 20% Wind Energy by 2030: Increasing wind energy’s contribution to U.S. electricity supply, July 2008.
[Online] <http://www1.eere.energy.gov/windandhydro/pdfs/41869.pdf>.
- [4] K.S. Cory and B.G. Swezey. Renewable portfolio standards in the states: Balancing goals and implementation strategies. Technical report, National Renewable Energy Laboratory, Golden, CO, December 2007. NREL/TP-670-41409.
- [5] R. Zavadil et al. Queuing up. *IEEE Power & Energy Magazine*, 5(6):47–58, November/December 2007.
- [6] R. Deshmukh and R. Ramakumar. Reliability analysis of combined wind-electric and conventional generation systems. *Solar Energy*, 28(4):345–352, 1982.

- [7] W. Melton. Loss of load probability and capacity credit calculations for wecs. In *Proceedings of the Third Biennial Conference and Workshop on Wind Energy Conversion Systems*, number CONF-770921, pages 728–741, September 1977.
- [8] K. Schenk and S. Chan. Incorporation and impact of a wind energy conversion system in generation expansion planning. *IEEE Transactions on Power Apparatus and Systems*, PAS-100(12):4710–4718, 1981.
- [9] PJM rule change supports wind power: wind turbines to receive capacity credits. PJM Interconnection. News Release April 24 2003.
- [10] M. Milligan and B. Parsons. A comparison and case study of capacity credit algorithms for intermittent generators. National Renewable Energy Laboratory, April 1997. NREL/CP-440-22591.
- [11] M. Milligan and K. Porter. Determining the capacity value of wind: A survey of methods and implementation. National Renewable Energy Laboratory, May 2005. NREL/CP-500-38062.
- [12] M. Milligan and K. Porter. Determining the capacity value of wind: A updated survey of methods and implementation. National Renewable Energy Laboratory, June 2008. NREL/CP-500-43433.
- [13] M. Milligan. Modeling utility-scale wind power plants, part 2: Capacity credits. *Wind Energy*, (3):167–206, 2000.

- [14] California Wind Energy Collaborative. California renewables portfolio standard renewable generation integration cost analysis, phase III: Recommendations for implementation. Technical Report 500-04-054, California Energy Commission, Sacramento, CA, July 2004.
[Online] <http://www.energy.ca.gov/reports/500-04-054.PDF>.
- [15] E. DeMeo et al. Accomodating wind's natural behavior. *IEEE Power & Energy Magazine*, 5(6):59–67, November/December 2007.
- [16] Enernex Corporation with the Collaboration of The Midwest Independent System Operator. Final report-2006 Minnesota wind integration study. Technical report, for The Minnesota Public Utilities Commission, Saint Paul, MN, Novemeber 2006. [Online] <http://www.uwig.org>.
- [17] Enernex Corporation. Avista corporation wind integration study. Technical report, for for Avista Corporation, Spokane, WA, March 2007.
[Online] <http://www.uwig.org/AvistaWindIntegrationStudy.pdf>.
- [18] GE Electric International, inc. Analysis of wind generation impact on ERCOT ancillary services requirements. Technical report, prepared for the Electric Reliability Council of Texas, Schenectady, NY, March 2008.
[Online] <http://www.uwig.org>.
- [19] GE Energy. Analysis of wind generation impact on ERCOT ancillary services requirements. Technical report, for The Electric Reliability Council of Texas, Schenectady, NY, March 2008. [Online] <http://www.uwig.org>.

- [20] C. D'Annunzio and S. Santoso. Wind power generation reliability analysis and modeling. In *Proceedings of the 2005 IEEE Power Engineering Society General Meeting*, volume 1, pages 35–39, 2005.
- [21] IEEE Power Task Force on the Capacity Credit of Wind Power and Energy Society (A. Keane, M. Milligan, C. D'Annunzio, C. Dent, K. Dragoon, B. Hasche, N. Samaan, L. Söder and M. O'Malley). Capacity credit of wind power. *to be submitted to IEEE Transactions on Power Systems*.
- [22] C. D'Annunzio and S. Santoso. Noniterative method to approximate the effective load carrying capability of a wind plant. *IEEE Transactions on Energy Conversion*, 23(2):544–550, June 2008.
- [23] C. D'Annunzio and S. Santoso. Analysis of a wind farm's capacity value using a non-iterative method. In *Proceedings of the 2008 IEEE Power and Energy Society General Meeting*, pages 1–8, 20-24 July 2008.
- [24] C. D'Annunzio et al. Generation adequacy assessment of power systems with wind generation: A system operations perspective. In *Proceedings of the 2009 IEEE Power and Energy Society General Meeting*, pages 1–7, July 2009.
- [25] R. Billinton and R. N. Allan. *Reliability evaluation of power systems*. Plenum Press, New York and London, 2nd edition, 1996.
- [26] G. J. Anders. *Probability concepts in electric power systems*. Wiley-Interscience Publications, New York, 1990.

- [27] R. Billinton and R. N. Allan. Probabilistic assessment of power systems. In *Proceedings of the IEEE*, volume 88, pages 140–162, February 2000.
- [28] G. Calabrese. Generating reserve capacity determined by the probability method. *AIEE Transactions*, 66:1439–1450, 1947.
- [29] G. Calabrese. Determination of reserve capacity by probability method. *AIEE Transactions*, 69(part II):1681–1687, 1950.
- [30] C. Watchorn. Probability methods applied to generating capacity problems of combined hydro and steam system. *AIEE Transactions*, 66:1645–1654, 1947.
- [31] C. Watchorn. The determination and allocation of capacity benefits resulting from interconnecting two or more generating systems. *AIEE Transactions*, 69(part II):1180–1186, 1950.
- [32] C. Watchorn. Elements of system capacity requirements. *IEEE Transactions on Power Apparatus and Systems*, PAS-70(part II):1163–1180, 1951.
- [33] L. Garver. Reserve planning using outage probabilities and load uncertainties. *IEEE Transactions on Power Apparatus and Systems*, PAS-89(4):514–512, 1970.
- [34] IEEE Task Force. IEEE-Reliability Test System. *IEEE Transactions on Power Apparatus and Systems*, PAS-98(6):2047–2054, 1979.

- [35] C. D’Annunzio and S. Huang. Impact of combined-cycle plant reliability modeling in generation adequacy loss-of-load calculations. *to be submitted for publication to IEEE Transactions on Energy Conversion*.
- [36] Application of Probability Methods Subcommittee IEEE Task Group on Models for Peaking Service Units. A four-state model for estimation of outage risk for units in peaking service. *IEEE Transactions on Power Apparatus and Systems*, PAS-91(2):618–627, 1972.
- [37] Generating Availability Data System. Electronic GADS publications for windows. North American Electric Reliability Council.
[Online] www.nerc.com/gads/.
- [38] GE Energy Consulting. The effects of integrating wind power on transmission system planning, reliability, and operations. Technical report, for The New York State Energy Research and Development Authority, Albany, NY, March 2005. [Online] <http://www.nyserda.org/>.
- [39] R. Billinton and A. A. Chowdhury. Incorporation of wind energy conversion systems in conventional generating capacity adequacy assessment. In *IEE Proceedings-C*, volume 139, pages 47–56, January 1992.
- [40] Discussion with Dr. Marc O’Malley, November 2008.
- [41] C. Ensslin et al. Current methods to calculate capacity credit of wind power, IEA. In *Proceedings of the 2008 IEEE Power and Energy Society General Meeting*, pages 1–3, 20–24 July 2008.

- [42] Discussion with Dr. Ross Baldick, April 2009.
- [43] L. Garver. Effective load carrying capability of generating units. *IEEE Transactions on Power Apparatus and Systems*, PAS-85(8):910–916, 1966.
- [44] L. T. Anstine et al. Application of probability methods to the determination of spinning reserve requirements for the Pennsylvania-New Jersey-Maryland Interconnection. *IEEE Transactions on Power Apparatus and Systems*, PAS-82(68):726–735, October 1963.
- [45] Discussion with Dr. Aristotle Arapostathis, December 2008.
- [46] R. Baldick. Course notes for EE394V restructured electricity markets: Market power, 2007. [Online] <http://users.ece.utexas.edu/~baldick>.
- [47] PJM Manual 21: PJM rules and procedures for determination of generating capability. PJM Interconnection.
[Online] <http://www.pjm.com/documents/manuals.aspx>.
- [48] J. Smith et al. Utility wind integration and operating impact state of the art. *IEEE Transactions on Power Systems*, 22(3):900–908, 2007.

Vita

Claudine D'Annunzio graduated with honors from The University of Texas at Austin with a Bachelor of Science in Electrical Engineering in 2001 and continued to complete a Master of Science in Electrical Engineering in 2004. As a doctoral candidate, Ms. D'Annunzio was a graduate research assistant funded by the National Science Foundation and published in IEEE journals and conference proceedings. Her research interests include the power system integration of renewable electric generation.

Permanent address: 75 rue Grignon
St-Eustache, QC, Canada J7P 4J2

This dissertation was typeset with L^AT_EX[†] by the author.

[†]L^AT_EX is a document preparation system developed by Leslie Lamport as a special version of Donald Knuth's T_EX Program.